NEURAL MECHANISMS OF SPATIAL CODING: A MULTIMODAL IMAGING STUDY

DERBIE, ABIOT YENEALEM

PhD

The Hong Kong Polytechnic University

2021

The Hong Kong Polytechnic University

Department of Rehabilitation Sciences

Neural Mechanisms of Spatial Coding: A Multimodal Imaging Study

Derbie, Abiot Yenealem

A thesis submitted in partial fulfilment of the requirements for the degree of Doctor of Philosophy

March 2021

CERTIFICATE OF ORIGINALITY

I hereby declare that this thesis is my own work and that, to the best of my knowledge and belief, it reproduces no material previously published or written, nor material that has been accepted for the award of any other degree or diploma, except where due acknowledgement has been made in the text.

Derbie, Abiot Yenealem

Abstract

Allocentric and egocentric spatial coding has been revealed involving similar processes of the parieto-frontal attention network. Because of the difference in nature and conceptual underpinnings of experimental paradigm used, the neural mechanisms subserving allocentric (aSC) and egocentric spatial coding (eSC) has been controversial. In this thesis, using multimodal neuroimaging methods, series of studies aimed at enhancing and integrating the model of spatial representations in human, were carried out.

The aim of the first study was to give a synopsis of converging evidence about the present state of these two types of spatial coding. By using activation likelihood estimation (ALE) (N = 28; Subjects = 447, voxel height $p < 0.001$, cluster $p < 0.05$ FWE-corrected)), both common and differentiated clusters of convergence for eSC and aSC were revealed. The common clusters were the right precuneus and the right superior frontal gyrus indicating attention selection/maintenance and response mapping are required in both types. The differences were the clusters in the superior occipital gyrus for aSC and in the middle occipital gyrus for eSC. They suggested visualizing and maintaining spatial relationships of objects in space were prevailed in aSC. Task-specific designs, i.e. spatial judgment and virtual environment were found to bias the convergent results of aSC but not eSC. The findings enable better understanding of the construct of spatial coding as well as the design of experimental tasks for assessing their neural underpinnings.

The second study was aimed to use fine-grained cue-to-target paradigm, required to allocate top-down attention control, for characterizing the neural processes associated with aSC and eSC. Twenty-two participants completed a custom visuospatial task, and changes in the concentration of oxygenated haemoglobin (O_2-Hb) were recorded using functional near-infrared spectroscopy (fNIRS). The least absolute shrinkage and selection operator-regularized principal component (LASSO-RPC) algorithm was used to identify cortical sites that predicted the aSC and eSC conditions' reaction times. Significant changes in the O_2-Hb concentration in the right superior frontal gyrus (SFG) and in the post-central gyrus (PoG) were common in both conditions. In contrast, the O_2-Hb concentration changes unique to aSC were in the left precentral gyrus (PG) and intraparietal sulcus (IPS); those changes unique to eSC were in the right posterior inferior parietal lobule (IPL). The fNIRS results suggest that top-down attention, encoding visual representation, and response-mapping processes were common to both spatial

coding types. When compared with egocentric coding, allocentric spatial coding demands more orienting attention and updating of spatial information. A future study will use other visuospatial tasks to further inform the task-specificity in spatial coding processes.

The aim of the third study was, using diffusion tensor imaging (DTI) and functional magnetic resonance imaging (fMRI), to investigate how age-related changes in white-mater integrity, as indexed by the fractional anisotropy (FA), could be accounted for age-related changes of neural processes associated to aSC and eSC. In this study, older (n = 24) and younger (n = 27) participants completed the DTI and fMRI scans during which they engaged in a cue-to-target task to elicit aSC or eSC processes. To define white matter ROI's, the FA seed regions were correlated with the task-related blood-oxygen-level dependent (BOLD) signal changes. The relationships between the white matter and functional ROI's were tested by with hierarchical multiple regression. The significant structural ROIs were then used to construct functional connectivity models using generalized psychophysiological interaction analyses (gPPI). The results revealed that white-matter tract of the posterior corona radiata (PCR) facilitated aSC- and eSC-modulated connectivity of the frontal eye fields (FEF) with other neural substrates in the parieto-occipital circuits. White-matter tract of the superior longitudinal fasciculus (SLF) exerted positive influences on the aSC-modulated connectivity of the FEF with neural substrates in the parieto-frontal circuits (involving precuneus, anterior supramarginal gyrus, and somatosensory association cortex) and with the neural substrates in the dorsal and ventral streams (inferior and superior temporal gyrus). It is noteworthy that the connectivity with the middle frontal gyrus (MFG), which plays a gate control role for signals projected from the dorsal attention network (DAN) and the ventral attention network (VAN) during aSC and from the DAN during eSC. The white-matter tract of the superior corona radiata (SCR) facilitated the aSC and eSC-modulated connectivity of the posterior parietal cortex (PPC) with neural substrates in its sub-regions. Disregarding of ageing, effect modulation of spatial coding in FEF requires structure-function interaction and connected to dorsal and ventral attention systems equally. FEF were a critical node for feedforward and feedbackward loops for the resource demanding aSC (involving iLOC, ITG, MFG). The aSC functional efficiency were associated to the function-structure interaction mediated by WM tract in PCR for parieto-occipital gray matter (GM) functions, SLF for near and far neural areas along the fronto-parietal attention network, and SCR for PPC GM functions.

Publications arising from the thesis

Articles under revision/review/preparation

Derbie AY, Chau B, Lam B, Fang YH, Ting KH, Wong CYH, Tao J, Chen LD, Chan CCH (2021). Cortical Hemodynamic Response Associated with Spatial Coding: A Near-Infrared Spectroscopy Study. *Brain Topogr*, *34*(2), 207-220. doi: https://doi.org/10.1007/s10548-021-00821-9. PMID: 33484379.

Derbie, A.Y., Chau, B.K.H., Chetwyn C. H. Chan (under review). Common and distinct nueral trends in allocentric and egocentric spatial coding: An ALE meta-analysis.

Derbie, A.Y., Chau, B.K.H., Chetwyn C. H. Chan (under preparation). Functional and structural architectures of allocentric and egocentric spatial coding: a combined DTI and fMRI study.

Derbie, A.Y., Chau, B.K.H., Chetwyn C. H. Chan (under preparation). Dynamic interaction in the fronto-parietal attention network during stimulus-response mapping in egocentric and allocentric spatial coding.

Abstract and Poster Presentations

Derbie, A. Y., Chau, B.K.H. & Chetwyn C. H. Chan (2020, February). Modulation of allocentric spatial coding in inferior parietal lobule and frontal eye-fields are associated to changes in white-matter integrity: a combined DTI-fMRI study. Poster session presented at the Annual Convention of the International Neuropsychological Society, Denver, CO., USA.

Derbie, A. Y., Chau, B.K.H & Chetwyn C. H. Chan (2020, February). Cortical hemodynamic response associated with spatial coding: a near-infrared spectroscopy study. Poster

session presented at the Annual Convention of the International Neuropsychological Society, Denver, CO., USA.

Derbie, A. Y., Chau, B.K.H & Chetwyn C. H. Chan (2018, November). Egocentric and Allocentric Spatial Coding in Supporting Endogenous Orienting Signals. A Functional Near-infrared Spectroscopy Study. Abstract presented at the 11th Pan Pacific Conference on Rehabilitation (PPCR) (p. 55), Hong Kong, Hong Kong.

Co-author

Chan, S., Chan, C., Derbie, A. Y., Hui, I., Tan, D., Pang, M., Lau, S., & Fong, K. (2017). Chinese Calligraphy Writing for Augmenting Attentional Control and Working Memory of Older Adults at Risk of Mild Cognitive Impairment: A Randomized Controlled Trial. Journal of Alzheimer's disease, 58(3), 735–746. doi: https://doi.org/10.3233/JAD-170024.

Chan, C. C., Derbie, A. Y., Hui, I., Pang, M. Y., Fong, K. N., & Chan, S. C. (2018). Chinese calligraphic writing to enhance cognitive performance and emotional calmness in older adults with mild cognitive impairment. Hong Kong Medical Journal, 24 Suppl 2(1), 4–7.

Acknowledgements

First, I would like to express my heart-felt gratitude to my chief supervisor, Prof. Chetwyn C.H. Chan, for his patience, encouragement to see the other dimension of inquiry and unreserved support over the years. I have gained a lot from Professor Chan advices and modelling on shaping my academic career and personal pursuits. I am also indebted to have Dr. Bolton Chau as my co-supervisor who particularly enlightens me to neuroimaging methodologies. I am thankful for staff and members of the University Research Facilities in Systems and Behavioural Neuroscience (UBSN) and Applied Cognitive Neuroscience Laboratory. Special thanks to Dr. Clive Wong for his insightful help in MRI data management and Dr. Yun-hua Fang of Fujian University of Traditional Chinese Medicine for her assistance in designing and planning of the study protocol and data collection of the MRI data.

ለዓተ እና ለዓባ

Table of Contents

List of Tables

List of Figures

CHAPTER 1

1.1. General Introduction

Our sensory organs receive multibillion bits of information in one second. Approximately one third of the human brain is involved in processing visual signals (Van Essen, Anderson, & Felleman, 1992). An efficient visual system is to attend to relevant stimuli and ignore the irrelevant signals from the environment (Kastner & Ungerleider, 2000). Decoding visual information for processing involves orienting of attention on the object in space (Chun, Golomb, & Turk-Browne, 2011; Desimone & Duncan, 1995). Human navigation is a special process. To capture the world far beyond our unaided locomotion, the brain would need a cognitive map which relies heavily on how one captures and utilize the cues embedded in the external environment.

This project is on spatial coding – an important attentional process in spatial navigation. Spatial navigation involves individuals using spatial strategies for selecting useful cues for manoeuvring within a space (Chun et al., 2011; Colby, 1998; Kanwisher & Wojciulik, 2000). The common spatial coding strategies are relative to the viewer (bodily coordinates) or relative to the visual cue(s) related to the object or the object itself in space (object-centred). The former is known as allocentric spatial coding (aSC) and the latter is egocentric spatial coding (eSC).

1.1.1. Theoretical Frameworks of Spatial Coding

Neural Networks associated to aSC and eSC

Review of brain imaging literature suggests three different views on the neural processes involved in the two spatial coding. The first view stipulated that the cognitive processes underlying the two spatial representations are different, which are sub-served by

distinct neural substrates distributed along the dorsal and ventral visual attention pathways (Chen, Weidner, Weiss, Marshall, & Fink, 2012; Fox, Corbetta, Snyder, Vincent, & Raichle, 2006; Vossel, Geng, & Fink, 2014). This view is in line with the perception–action model proposed by Goodale and Milner (1992) suggesting functional specializations along the neuroanatomical division of the ventral and dorsal steams of the brain. The dorsal pathway was found to mediate spatial relationships between visual objects in space (Ungerleider, 1982; Ungerleider, 1994). The ventral pathway was reported to mediate memory-guided identification and enduring features of objects (Ungerleider, 1982; Ungerleider, 1994). The ventral stream was proposed to mediate aSC whilst the dorsal stream mediate eSC (Burgess, 2006; Milner & Goodale, 2008). Previous functional imaging study identified activations of the posterior parietal cortex (part of the dorsal stream) were associated with eSC (Committeri et al., 2004; Stein, 1992). In contrast, activations of the medial temporal lobe (MTL; part of the ventral stream) was associated with aSC. The major controversy of the proposed two pathway hypothesis is the unclear role played by the dorsal stream in spatial coding (Kravitz, Saleem, Baker, & Mishkin, 2011; Kravitz, Saleem, Baker, Ungerleider, & Mishkin, 2013). Szczepanski, Pinsk, Douglas, Kastner, and Saalmann (2013) argued that the dorsal pathway is likely to be involved in both the egocentric and allocentric types.

Kravitz et al. (2011) argued against the two pathway (or stream) hypothesis on spatial coding on the basis of the unclear role played by the dorsal stream. The main reason rest with the notion that the dorsal stream has three separate sub-pathways: the parieto-prefrontal (supports spatial working memory), parieto-premotor (supports visual-guided behaviour), and parieto-medial temporal pathways (supports navigation). These three pathways mediate different aspects of visuospatial attention (see below), which are functionally integrated by the

occipito-parietal circuit for generating egocentric map. Kravitz et al. (2011) further explained the occipito-parietal circuit's role in encoding incoming visual information egocentrically. The parieto-premotor pathway associates body position with motor action (Milner & Goodale, 2008) of which the eSC information held is projected from extrastriate cortex (Goodale, 2014). The parieto-medial pathway is less clear cut however as it has been implicated to mediate spatial representation in an allocentric map (Byrne, Becker, & Burgess, 2007; Ekstrom, Arnold, & Iaria, 2014). In other words, the dorsal pathway would have supported both eSC and aSC, with each of them involves a subset of the dorsal visual stream (Galati et al., 2000; Zaehle et al., 2007). These are a few examples of the challenges of the notion that eSC and aSC are mediated by distinctive neural systems, which will be addressed in this study.

The second view supports the notion that eSC and aSC are mediated by a unified neural system. Byrne et al. (2007), for example, argued that encoding information from visual field requires translation between allocentric and egocentric spatial coding. The posterior parietal cortex (PPC) (Castiello, 2005; Culham & Valyear, 2006) and the retrosplenial cortex (RSC) as projected from the PPC (Burgess, 2008; Epstein, 2008; Iaria, Chen, Guariglia, Ptito, & Petrides, 2007) have been reported to be the core neural substrates for mediating the related interactive translational processes. Later studies further illustrated that the crucial role played by the posterior parietal cortex in registering different types of spatial representations regardless of egocentric or allocentric spatial coding (Bernier & Grafton, 2010; Pertzov, Avidan, & Zohary, 2011; Szczepanski et al., 2013). Spatial coding, under this view, inevitably would involve integration of the dorsal and ventral visual attention pathways. The integrative neural activities of the two pathways are further differentiated into two directional activities. Dorsal-to-ventral activities are for capturing and transferring the incoming visual information, whereas the

ventral-to-dorsal activities are for translating the input information into context for producing meaningful actions (Goodale, 2014; Kravitz et al., 2013; Milner, 2017). The eSC and aSC representations from dorsal-to-ventral or vice-versa are suggested to associate with activities of RSC and PCC (Burgess, 2008; Epstein, 2008). A recent review further strengthens this view and explained that the findings on the differences between the two types of spatial coding were likely to be due to the nature and cognitive resource demands of the spatial tasks employed across the studies (critical review: Ekstrom et al., 2014).

The third view supports the notion that neural substrates mediating eSC are subsumed under those mediating aSC (Zaehle et al., 2007). This view implicates aSC involving additional neural processes to the eSC. eSC is primarily transitory in nature which updates representations of the object in space (Wang & Spelke, 2000), which is mediated by the dorsal visual attention pathway (Mou, McNamara, Valiquette, & Rump, 2004). aSC in contrast is more enduring than eSC by incorporating "cognitive map" into the representations (Wang & Spelke, 2002). The additional features are the involvement of visual working memory (Cooper & Humphreys, 2000) and greater cognitive resources (for critical review: Ekstrom et al., 2014; Filimon, 2015). These additional neural processes were reported to be mediated by the parietal cortex particularly the precuneus (Ekstrom et al., 2014; Zaehle et al., 2007; Zhang & Ekstrom, 2013). Other core neural substrates associated with aSC but not eSC are the MT which connects with the precuneus (Byrne et al., 2007) and the retrosplenial cortex (RSC) and IPS involved in translating egocentrically encoded information into allocentric maps or vice versa (e.g: Gomez, Rousset, & Baciu, 2009; Lambrey, Doeller, Berthoz, & Burgess, 2012; Schindler & Bartels, 2013; Zhang & Ekstrom, 2013).

Underlying Behavioural and Cognitive Processes in aSC and eSC

Allocentric and egocentric representations of space could be driven by either bottom-up or top-down, or a mixture of both (Byrne et al., 2007). In both top-down and bottom-up attention processing, information processes sequentially, where top-down might give the perceiver much opportunity to operate while bottom up is mainly operated by the properties of the task being encoded and the encoder is relatively passive. Barrett, Bradshaw, Rose, Everatt, and Simpson (2001) for example, suggested that visual target selection uses eSC, which associates with a reflexive shift of attention centred to the retina, whereas aSC operates based on endogenous covert shifts of attention which involves higher cognitive processing.

The nature of the spatial task may determine the type of encoding strategy to be recruited. It has been proposed that the utilization of either type of spatial coding depends upon the timescale of the visuospatial task. Sensory information requiring transient coding of object in space is likely to be eSC (Mou et al., 2004). An object in space involving maintenance of the object image and top-down orienting tends to involve aSC. These prompt the propositions that eSC is to the fronto-parietal attention network while aSC is to temporo-parietal circuit. Comprising SPL, PreCG, FEF, and DLPFC, the dorsal frontoparietal attention network maintains top-down attention control (Corbetta, Patel, & Shulman, 2008). In the real world, the demarcation between eSC and aSC does not seem to be possible. When viewing an object against another, one would need to first transform the coordinates of oneself to the objects and then locating them in space. In other words, eSC could be a part of the aSC process (for critical reviews see: Ekstrom et al., 2014; Filimon, 2015).

Types of spatial coding has been found to associate with different timescale and orienting attention of the visuospatial task. For instance, two distinctive tasks and their associated processes are simple spatial judgment (SSJ) or virtual environment (VE) tasks. For former involves exogenous orienting attention and the spatial decision is based on rules associated with the priori cue to the location of the target stimuli (example: Galati et al., 2000). The latter involves attention bases on the imagined or given landmarks (fixed or moving) and spatial decision is to make with reference to these those landmarks (example: Committeri et al., 2004). SSJ task process would demand less cognitive resource allocation (Barrett et al., 2001). whereas VE task process tends to demand relatively intense maintenance in the visual working memory (Barra, Laou, Poline, Lebihan, & Berthoz, 2012; Committeri et al., 2004; Frings et al., 2006; Gomez, Cerles, Rousset, Le Bas, & Baciu, 2013; Gomez, Cerles, Rousset, Remy, & Baciu, 2014; Gomez et al., 2009; Gramann, Muller, Schonebeck, & Debus, 2006; Parslow et al., 2004; Weniger et al., 2010; Zhang & Ekstrom, 2013).

1.1.2. Knowledge Gap

The mainstream proposition on the cognitive processes between allocentric and egocentric spatial coding is that they are not unified. The major controversy however rests with the differences in the neural substrates and networks mediating these cognitive processes. Previous experiments implicated that egocentric processes would subsume under the allocentric processes. Egocentric spatial coding may require only the sub-system and resources of the allocentric one (e.g. Zaehle et al., 2007). The task processes employed in previous studies could have confounded the results of the studies stipulated along the two-stream hypothesis and that both spatial coding types are mediated by the same group of neural substrates. Analyses of the tasks employed in the studies revealed that they lack top-down attention allocation. The main difference between tasks of bottom-up and top-down attention allocation

is on the cue-to-target effects acting on the visual processing during the target phase (Botta, Santangelo, Raffone, Lupianez, & Belardinelli, 2010; Corbetta & Shulman, 2002). Cues processed with bottom-up attention facilitate temporal effects on the target (Chica, Bartolomeo, & Lupianez, 2013) whereas cues processed with top-down attention facilitate spatial orientating effects on the target (Awh & Jonides, 2001). By simultaneously recording neurons in the frontal area (FEF) and superior parietal cortices, Buschman and Miller (2007), for example, showed that the firing rates of these two key visual attention areas are different across different task paradigms. They showed that FEF neurons encoded target stimulus earlier than parietal neurons during voluntarily shift of attention and inversely for salient stimulus. Such encoding variability may confound the stimulus-response mapping processes (Clark, Squire, Merrikhi, & Noudoost, 2015). In fMRI studies, these neural fluctuations are usually averaged out and treated as task-irrelevant noise when converging across trials to the whole brain (Mitchell, Sundberg, & Reynolds, 2009). The question then becomes whether such latency and intra-regional encoding difference accounts for the extensive overlap of aSC and eSC signals.

The cue-to-target processes involving both bottom-up and top-down attention would need to mediate by a common (for bottom-up) as well as a task-specific networks (top-down). Over-emphasizing bottom-up attention processes in the task design henceforth could have generated results biased toward that both the allocentric and egocentric spatial coding processes associated with similar neural networks.

Generalization to the common and district neural areas associated to both types of spatial coding is challenged due to the lack of network level analysis of function-structure interactions in the previous studies. Understanding the structure of connections within the feed-forward and

feed-backward loops of those separate functional networks underlying spatial coding is a powerful way to reveal the function of brain regions at the nodes of the networks associated to aSc and eSC. The feed-forward and feed-backward loops of those separate functional networks were implicated to be influenced by distinct longitudinal or non-longitudinal WM tracts (Madden et al., 2010; Niogi, Mukherjee, Ghajar, & McCandliss, 2010). In addition, even though, functional dissociations along the key nodes of FPAN (cIPL, IPS, FEF, and LPFC) are observed for aSC and eSC, whether age-related changes in FA could be accounted for age-related differences in aSC and eSC are yet to be determined. The mechanisms how the changes in structural integrity and the interaction of it with the function nodes sub-serving aSC is unclear, of which in-turn helps to fill age-related gap of knowledge in the model of spatial coding.

1.1.3. Study Aims

Aim 1

Using neuroimaging meta-analysis, this part of the study is to test the similarity and distinctiveness of activations of neural substrates associated with eSC and aSC. The results will help construct preliminary functional connectivity models for eSC and aSC for further testing for their robustness in Aims 2 and 3. Besides, this part of the study is to examine the potential effects of task designs on confounding activations of neural substrates associated with the spatial coding types. It's hypothesised that;

i. the involvements of the FEF and SPL would be common to both egocentric and allocentric spatial coding and the neural substrates may not be allocentric or egocentric strategy specific.

ii. egocentric spatial coding would be unique to activations in the superior occipital gyrus and lateral/ventral intraparietal sulcus. Allocentric spatial coding in contrast would be unique to activations in the IPL, superior temporal gyrus and perhaps TPJ.

iii. allocentric-related processes involve retrieval of spatial representations from memory which is not the case in the egocentric spatial coding, and thus there would be differences in the activations in the temporal region particularly in MTL.

iv. for both spatial coding types, task-specific difference will underlie in occipito-parietal circuit and temporo-parietal circuit.

Aim 2

Using custom-designed spatial attention tasks, this part of the study is to further explore the dissociative roles of the fronto-parietal-attention network (FPAN) in eSC and aSC. The results of this study, based on functional near-infrared spectroscopy, will inform the extent to which task-specific processes would confound the overlaps in neural substrates and hence the neural processes between aSC and eSC. It's hypothesised that.

i. using visuospatial paradigms maintained by top-down orienting, the neural substrates corresponding to the dorsal attention network (which contains the juncture of the precentral and superior frontal sulcus) would be common to aSC and eSC conditions.

ii. the eCS condition would involve the SPL, and the aCS condition would involve the inferior parietal lobule (IPL).

Aim 3

This part of the study is to explore how the degeneration of structural integrity in the spatial coding related network due to aging effect would modulate the connectivity of the

functional networks mediating eSC and aSC. Its results will test the robustness of the neural networks constructed for eSC and aSC. They will also inform plausible neural models of spatial coding for older adults. It's hypothesised that.

i. There would be differences in the structural integrity and connectivity associated with the neural activations mediating the feedforward and feed-backward loop between aSC and eSC spatial coding. It is anticipated that eSC would recruit the WM tracts in the parieto-frontal regions (i.e. IPS-FEF), while aSC would extend the WM tracts to those located in the LPFC and superior temporal regions. The integrity and connectivity of the involved WM tracts would differentially relate to the functional connectivity associated with aSC or eSC.

ii. Functional connectivity among PCC, MT and LPFC in the older group would be different from that in the younger group. The decline in the aSC-related functional connectivity in the older group would be relate to the decrease in the structural integrity of the ILF, SLF, ACR and SPN. The structure-function relationships observed in aSC however would not occur in eSC in the older group.

CHAPTER 2

2. Common and Distinct Neural Trends of Allocentric and Egocentric Spatial Coding: An ALE Meta-Analysis

2.1. Introduction

Spatial navigation is a complex cognitive process that relies heavily on how one dynamically selects and utilizes the cues embedded in the external environment. To enhance the signal-to-noise ratio in visuospatial attention, individuals need to use spatial strategies for selecting useful cues and ignoring less useful ones. The common strategies are egocentric and allocentric spatial coding, the former encoding relative to the viewer and the latter encoding relative to another visual cue(s) or object(s) in space (Figure 2.1; Area C and Area D). Previous functional magnetic resonance imaging (fMRI) studies revealed inconsistent results on the activations of the neural substrates associated with these two types of spatial coding. The inconsistencies could have been due to discrepancies in the theoretical frameworks or the designs of the experimental paradigms. This study was aimed at conducting meta-analysis on the existing fMRI studies for addressing these discrepancies and hence gaining a better understanding of the neural mechanisms underlying allocentric and egocentric spatial coding.

2.1.1. Potential Overlaps between Egocentric and Allocentric Spatial Coding

Dorsal and ventral attention systems are distinct anatomically and functionally (Corbetta & Shulman, 2002; Vossel et al., 2014). Dorsal attention system has been proposed to predominantly mediate encoding of object in an egocentric map whereas ventral attention system predominantly mediates the encoding processes in an allocentric map (Vossel et al., 2014). The ventral attention system for allocentric spatial coding rests with the notion that the

former plays a key role in maintaining spatial relationships of objects in space (Kravitz et al., 2013). The key neural substrates of the dorsal attention system are the intraparietal sulcus (IPS), the superior parietal lobule (SPL), and the frontal eye field (FEF) (Corbetta et al., 2008; Kravitz et al., 2013). The SPL is associated with maintaining head-centred maps of somatosensory and visual spaces, the FEF with encoding spatial relationships, and the IPS with attentional selection (Kravitz et al., 2013; Ptak, 2012; Ptak & Schnider, 2010). The ventral attention system for allocentric spatial coding is grounded on the findings that neurons within it maintained allocentric representations (Kravitz et al., 2011; Kravitz et al., 2013). The key neural substrates of the ventral attention system are the temporoparietal junction (TPJ) (including the superior temporal gyrus, inferior parietal lobule, and lateral occipital regions) and the middle and inferior frontal gyrus (Corbetta et al., 2008; Kravitz et al., 2013; Vossel et al., 2014). These cortical structures were related to processing of salient and behaviourally relevant stimuli, such as identification of cued targets (Corbetta et al., 2008; Vossel et al., 2014) and memory-based identification of objects in space (Ptak, 2012). The TPJ has been revealed to play a higher-level role in the switching between the two neural networks in spatial coding processes: contextual visuospatial updating (Geng & Vossel, 2013; Ptak, 2012) and reorienting of cued targets (Corbetta & Shulman, 2002; Posner, 1980).

The major controversy of the proposed two pathway hypothesis, however, is about the unclear role played by the dorsal attention system in spatial coding (Kravitz et al., 2011; Kravitz et al., 2013). Szczepanski et al. (2013) argued that the dorsal attention system is likely to be involved in both egocentric and allocentric types. These researchers demonstrated that the inter-cortical connections in the dorsal system enable nodes depending on the types of reference frame required. In particular, the IPS2–FEF connectivity supports attentional selection in viewer-centered, i.e., egocentric, spatial coordinates, and the SEF (supplementary eye field)–

SPL1 connectivity supports attentional selection in object-centered, i.e. allocentric, spatial reference frames (Szczepanski et al., 2013). Other studies share similar findings on the dorsal attention system supporting allocentric and egocentric spatial coding in a flexible manner (Galati et al., 2000; Zaehle et al., 2007; Zanto & Gazzaley, 2013). The distinctiveness of the dorsal attention system can shed light on the possible dual role it plays. Kravitz et al. (2011) proposed that the dorsal attention system is composed of three sub-pathways: the parieto-prefrontal (spatial working memory), parieto-premotor (visual-guided behavior), and parieto-medial temporal (navigation) pathways. The occipito-parietal circuit somehow integrates the signal processing of the sub-pathways. According to Kravitz et al., the parieto-premotor pathway is involved in encoding an object in space for the formation of an egocentrically visuospatial map of the objects. The neural substrates previously found to associate with the sub-pathway are the IPS, the middle temporal gyrus, the medial superior temporal gyrus, and the prefrontal cortex (Goodale, 2014; Milner & Goodale, 2008). In contrast, the parieto-medial sub-pathway has been found to mediate allocentric spatial coding (Byrne et al., 2007; Crowe, Averbeck, & Chafee, 2008; Ekstrom et al., 2014). The neural substrates of the parieto-medial sub-pathway are the caudal part of the intraparietal lobule (area PG) (Chafee, Averbeck, & Crowe, 2007; Crowe et al., 2008), the posterior cingulate cortex (Hashimoto, Tanaka, & Nakano, 2010), and the retrosplenial cortex (Vann, Aggleton, & Maguire, 2009). The potential overlaps of neural substrates between the parieto-premotor and parieto-medial sub-pathways support the notion that neural processes associated with egocentric spatial coding could be part of the neural processes in allocentric spatial coding (Galati et al., 2000; Kravitz et al., 2011; Zaehle et al., 2007).

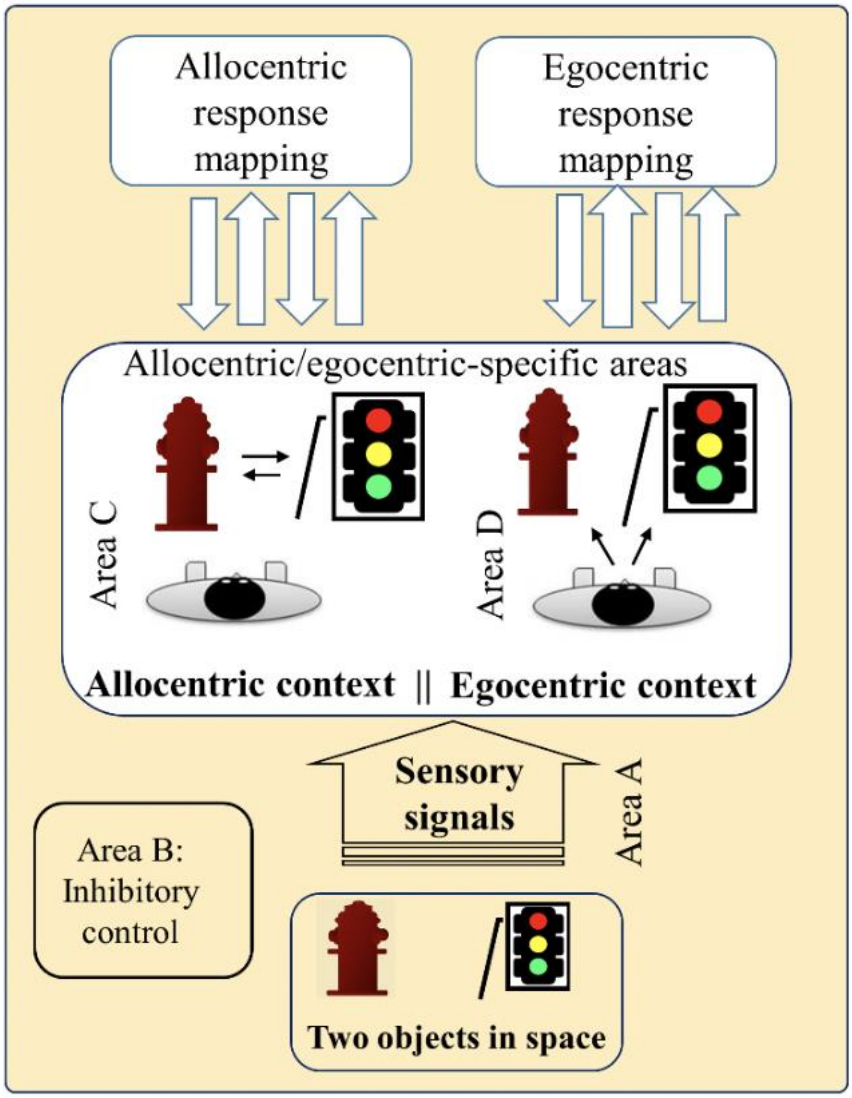

Figure 2. 1. Schematic diagram depicting the cognitive processes of allocentric and egocentric spatial coding. Visuospatial information about the two objects in space (Area A) are attended to. Task-relevant signals inhibitory control (Area B) help to focus volitionally the two objects in space. Depending on the task requirements, relevant signals are selected by means of inhibitory control (Area B). Allocentric spatial coding is characterized with the visuospatial information to be modulated by the coordinates of other object in space (Area C). Egocentric

spatial coding is characterized with the information to be encoded basing on one's bodily coordinates (Area D).

2.1.2. Experimental Paradigms as a Confounding Factor

By reviewing the experimental paradigms used in previous studies on spatial coding, we could largely divide these into spatial judgment (SJ) or spatial navigation (SN) tasks. A common feature of SJ tasks is that the target mapping operates mainly by sensorimotor interactions with little or no mental shifting (e.g.: Liu, Li, Su, & Chen, 2017). Such tasks require participants to indicate a left or right position with reference to the position of an object shown on screen or the midsagittal position of one's body. In contrast, some common features of SN tasks are that the visual targets are embedded in a complex background and that map-like spatial layouts are required to generate visuospatial images for making responses (e.g.: Committeri et al., 2004). Compared with SJ tasks, SN tasks usually require the participants to maintain visuospatial images for relatively long periods of time, which demands additional attention and visuospatial working memory-guided during navigation (e.g.: Committeri et al., 2004; Zhang & Ekstrom, 2013). As expected, these two types of tasks have different task processes supported by different cognitive functions and demands. For instance, the cognitive demands of SJ tasks predominantly consist of allotting visual attention at a location in space, whereas the demands of SN tasks include mainly encoding, retrieval from memory, top-down attention control, and visuospatial working memory (for critical review see: Filimon, 2015).

As the task-specific processes between the two spatial coding methods are different, these differences might have confounded the results of previous studies and hence produced inconsistent findings. To address this potential confounding factor, this study was aimed at separating the tasks into SJ and SN groups. The grouping of the studies based on the task

designs would set controls on the task-specific processes when brain activations were pooled among the SJ or SN studies.

2.1.3. Hypotheses of the Study

It was hypothesized that involvements of the FEF and SPL would be common to both egocentric and allocentric spatial coding, and that neural substrates might not be specific to an allocentric or egocentric strategy. Egocentric spatial coding would be unique to activations in the superior occipital gyrus and the lateral/ventral intraparietal sulcus. Allocentric spatial coding, in contrast, would be unique to activations in the IPL, the superior temporal gyrus, and perhaps the TPJ. To further test the notion that allocentric-related processes involve retrieval of spatial representations from memory, which is not the case in egocentric spatial coding, we hypothesized that there would be differences in the activations in the temporal region, particularly in the medial temporal lobule. It was anticipated that studies involving SJ tasks would be biased with activations of the occipito-parietal circuit compared to studies involving SN tasks, which would be biased with activations of the temporo-parietal circuit.

2.2. Method

The guidelines for neuroimaging meta-analysis (Muller et al., 2018; supplementary file 1) and the Preferred systematic Reviews and Meta-Analysis (PRISMA) (Moher, Liberati, Tetzlaff, Altman, & Group, 2009) were used in this section.

2.2.1. Searching Strategies

Functional neuroimaging studies published between 2000 and 2019 (last updated October) were searched from PubMed. The search strings, which produced 2295 results from PubMed, were as follows: “allocentric” OR “egocentric” OR “viewer-centered” OR “world-centered’

OR “body-centered” OR “frame of reference” OR “spatial navigation” combined (“AND”) with “fMRI” or “PET”.

2.2.2. Selection Criteria

The inclusion criteria for selecting the articles were as follows: 1) articles were published in peer-reviewed journals; 2) Montreal Neurological Institute (MNI) or Talairach and Tournoux (1988) stereotaxic coordinates were provided; 3) task-related brain activations were elicited from tasks involving allocentric and/or egocentric spatial coding; 4) subjects were comprised of healthy and young human adults; and 5) responses on the tasks were obtained by pressing keys on a keyboard or a joystick. Additional papers were included by tracing from the retrieved articles and other review articles. The data extraction procedures were done according to guidelines for ALE meta-analysis (Muller et al., 2018).

The experiments included in this study were classified by SJ (example: Galati et al., 2000) and SN (example: Committeri et al., 2004) task types. SJ tasks predominantly 1) encoded and processed the stimulus by exogenous orienting, 2) had no cue-target association, 3) elicited responses according to the stimulus presented on screen by real-time visual estimates (e.g., judging the location of a vertical line), and 4) involved minimal mental manipulation of the stimulus before responses were made. SN tasks predominantly had the following attributes: 1) encoded with attention being allocated based on exogenous and endogenous orienting, 2) manipulated and perhaps generated images based on the stimulus presented on screen, including off-line retrieval, 3) possibly retrieved visuospatial representation images, and 4) possibly required active maintenance from visual short-term memory.

Twenty-eight articles containing 34 experiments (number of subjects, n = 447) were identified (Figure 2.2 and Table 2.1). Among them, 22 experiments involving allocentric tasks

(n = 352 with 252 foci) were grouped for conducting the meta-analysis 1 (allocentric, number of experiments, N = 22), and the subsequent 10 SJ experiments (1a, n = 136 with 68 foci) and eight SN experiments (1b, n = 157 with 125 foci) were grouped for task-specific meta-analysis. Another 22 experiments involving egocentric tasks (n = 327 with 277 foci) were grouped for conducting the meta-analysis 2 (egocentric, N = 22), and the subsequent 12 SJ experiments (2a, n = 157 with 125 foci) and nine SN experiments (2b, n= 149 with 128 foci) were grouped for task-specific meta-analysis. Five experiments with four allocentric tasks and one egocentric task were excluded from the task-specific meta-analyses, as their tasks did not conform to SJ or SN types (Table 2.1 and Figure 2.2). In summary, four different ALE meta-analyses were performed: meta-analysis 1 (allocentric), meta-analysis 2 (egocentric), meta-analysis 1a (SJ) and 1b (SN) (task-specific allocentric), and meta-analysis 2a (SJ) and 2b (SN) (task-specific egocentric).

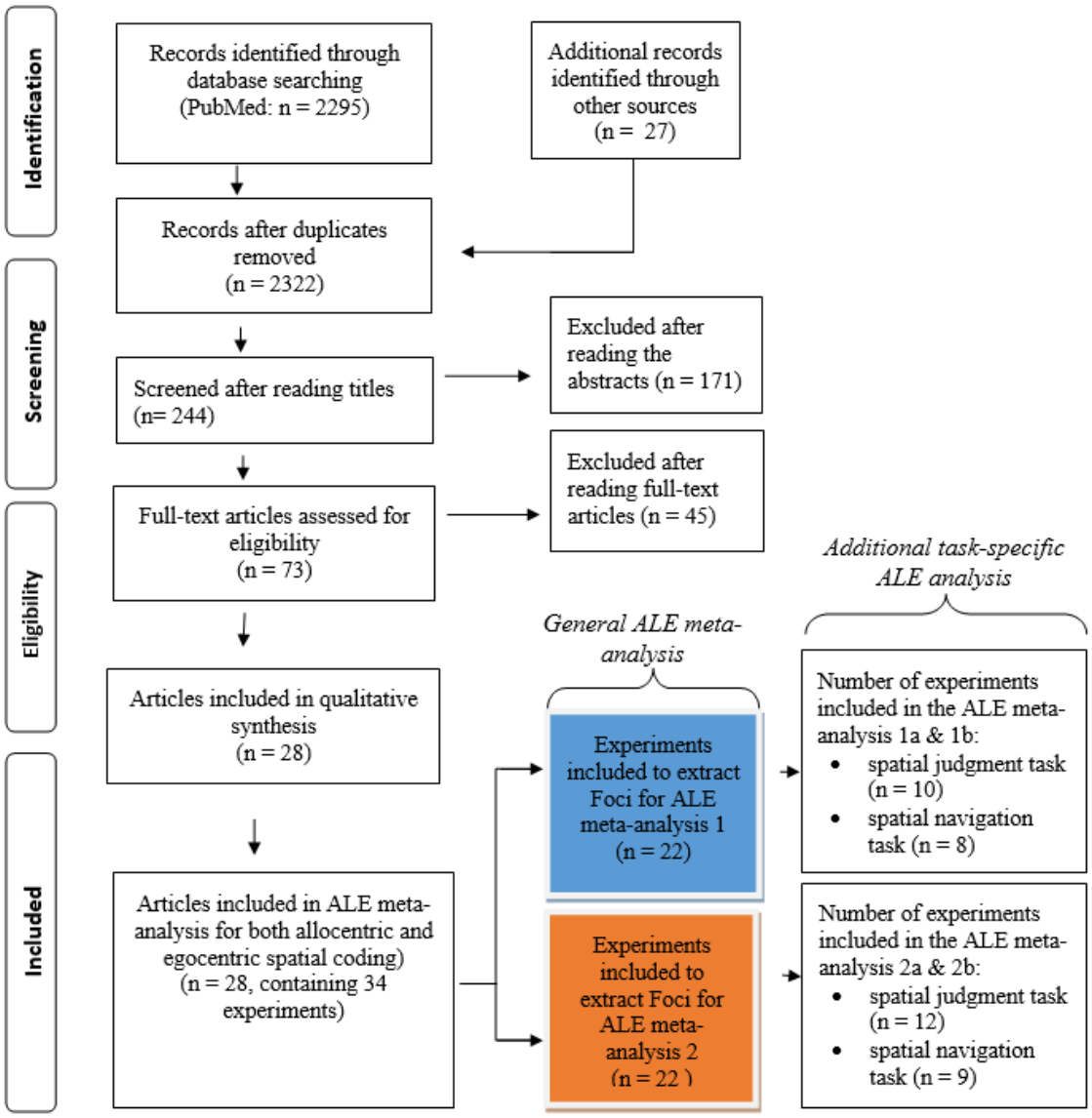

Figure 2. 2. Study selection diagram of the present review and meta-analysis.

2.2.3. Activation Likelihood Estimate (ALE)

ALE is a coordinate-based meta-analysis method and software developed to pool and map common neural trends across different neuroimaging studies. The extracted coordinates were analyzed using the revised ALE algorithm (Eickhoff et al., 2009). The reported foci in each experiment were considered as centers of 3D Gaussian probability distributions, which captured the spatial uncertainty related to each focus (Eickhoff et al., 2009). The probabilities of all the distributions of those foci were then combined at voxel levels and used to create cluster maps (Turkeltaub et al., 2012). Last, using the ALE score, dissociation was made between random and true clusters of convergence (Eickhoff, Bzdok, Laird, Kurth, & Fox, 2012). The analyses were carried out using GingerALE version 3.0.2 (Research Imaging Institute, UT Health Science Center, San Antonio). GingerALE offers conversion of coordinates based on Talairach space to the MNI space. The cluster-wise inference threshold method was used to map the clusters of convergence, producing results with higher specificity and sensitivity than the voxel-wise thresholding method (Eickhoff et al., 2012; Eickhoff et al., 2016). The locations of the clusters were anatomically labelled with the SPM Anatomy Toolbox (Eickhoff et al., 2005).

Two general ALE analyses were performed on the foci derived from the selected articles for each of the allocentric (aSC) and egocentric (eSC) spatial coding types. Conjunction analyses, based on the thresholded z-maps and to be followed by a subsequent ALE analysis, were carried out to test whether the two spatial coding types elicited comparable clusters of convergence. Two contrasting meta-analyses were then conducted on the convergence results: [aSC > eSC] and [eSC > aSC]. Additional meta-analyses were performed to test the possible foci differentiation between the SJ and SN task types. All the derived ALE maps were thresholded at the cluster level $p < .05$, using family-wise error correction for multiple

comparisons, and were based on a Monte Carlo simulation cluster-forming threshold of $p < \cdot 001$ on the voxel level (Eickhoff et al., 2012; Eickhoff et al., 2009). The ALE results were visualized using MANGO (Research Imaging Institute, UT Health Science Center, San Antonio). The "Colin27_T1_seg_MNI.nii" high resolution anatomical template (available at www.brainmap.org/ale) was overlaid onto the visual images in the MNI space

Table 2. 1. List of the selected neuroimaging studies on allocentric and egocentric spatial coding types

Study	N	Age	Imaging technique and design*	Contrast	Modality	*Nature of the task	*Key task specific activated brain region (s) in both all/ego spatial coding		N (Foci mined)	Meta-Analysis No.
							Allo	Ego		
Barra et al. (2012)	26	18-29	fMRI-b	Ego > control Allo > control	Visual	SN	OT (R/L), PHG (R/L) RSC (R/L), OTG (R/L)	Cu (R/L), CS (R)	aSC, 3 eSC, 15	1,2, 1b, 2b
Chen et al. (2014)	13	23-40	fMRI-e	Ego > control Allo > control	Visual Auditory	SJ	SPL-LG (R/L), CF (R/L), Cu (R/L)	PMd (R), SPOC (R/L)	eSC, 3 aSC, 6	1,2, 1a, 2a
Chen et al. (2012)	19	24±3	fMRI-b	Ego > control Allo > control	Visual	SJ	MOG (R/L), SPC (L), ITG (R)	SPC (R), I/MFG (R), SFG (L), IPC (L)	aSC, 6 eSC, 10	1,2, 1a, 2a
Committeri et al. (2004)	14	23-33	fMRI-b	Ego > control Allo > control	Visual	SN	PO (R/L), IFG (R), LOT (R/L), MOT (R)	PO (R/L), SFG (R), IFG (R/L)	eSC, 17 aSC, 27	1,2, 1b, 2b

Creem, Downs, Snyder, Downs III, and Proffitt (2001)	10	NA	fMRI-b	Ego > control Allo > control	Visual	SJ	PrCu (R/L), SPC (L), PoG (L), Cu (R), SFG (R/L), MFG, CRBL (R)	SPC (L), PrCu (R/L), Cu (R/L), SFG (R/L), MFG (R/L), CRBL (R)	aSC, 10 eSC, 14	1,2, 1a, 2a
Creem-Regehr, Neil, and Yeh (2007)	17	20-26	fMRI-b	Ego > fixation	Visual	A/E-GR	NA	LO, IPC (L), SPC (R), Hi (R), CRBL (R)	eSC, 24	2
Fink et al. (2003)	12	19-36	fMRI-b	Allo > control	Visual	SJ	VLPFC (R), LIPC (R), PO (R), EC (R), PMVr (R)	NA	aSC, 9	1, 1a
Frings et al. (2006)	13	21-39	fMRI-b	Allo > control	Visual	SN	PrCu(R/L), IT (L), IPC(R), SFG (R), SPC(L), IFG (R),	NA	aSC, 27	1, 1b
Galati et al. (2000)	8	22-29	fMRI-b	Ego > control Allo > control	Visual	SJ	PPC (R), PMC (R), IPS (R), Hi (R), MO (R)	PPC (R/L), PT (L), PMC (R/L), MFG (L)	aSC, 6 eSC, 24	1,2, 1a, 2a

Galati, Committeri, Sanes, and Pizzamiglio (2001)	10	24-29	fMRI-b	Ego > control	Visual	SJ	NA	PPC (R/L), IPS (R/L), SFG (R/L), IFG (R/L), Pre-SMA (R), aSMG (R/L)	eSC, 24	2,2a
Ganesh, van Schie, Cross, de Lange, and Wigboldus (2015)	23	23 (m)	fMRI-b	Ego > control	Visual	E - GR	NA	TPJ (R/L)	eSC, 2	2
Gomez et al. (2013)	20	17-30	fMRI-b	Ego > control	Visual	SN	NA	PrCu (L), ITG (L), MTG (L), PCC (L)	eSC, 3	2, 2b
Gomez et al. (2014)	18	17-30	fMRI-b	Ego > control Allo > control	Visual	SN	Cu ((R/L), STG (R), SPC (R), IPC (R), PrG (R/L)	SPC (R/L), MFG (R/L), STG (R), MTG (R),	aSC, 12 eSC, 8	1,2, 1b, 2b

Gramann et al. (2006)	10	22-34	EEG source reconstruction	Ego > control Allo > control	Visual	SN	IOG (R/L), OTG (R/L), MTG (R/L)	Cu (R/L), SOG (R), MOG (R), MFG (L), STG (R)	aSC, 9 eSC, 11	1,2, 1b, 2b
Liu et al. (2017)	19	18-25	fMRI-b	Ego > control Allo > control	Visual	SJ	MOG (R/L), SPC (R), MFG (R), SFG (L)	PPC (R), MOG (L), ITG (R/L), MFG (R)	aSC, 5 eSC, 6	1,2, 1a, 2a
Neggers, Van der Lubbe, Ramsey, and Postma (2006)	12	22-29	fMRI-e, rapid)	Ego > control Allo > control	Visual	SJ	MFG, CN (R)	PC (R/L), MTG (R/L), MFG (L)	aSC, 2 eSC, 5	1,2, 1a, 2a
Parslow et al. (2004)	11	19-45	fMRI	Ego > rest Allo > rest	Visual	SN	MFG (R/L), PrCu (R/L), PrG (R), IPC (R), MO, OTG (R), STG (R/L), PHG, Hi	MFG (R/L), PrCu (R/L), PrG (R), IPC (R), MO, OTG (R), STG (R/L)	aSC, 24 eSC, 26	1,2, 1b, 2b

Saj et al. (2014)	16	25.7	fMRI		Visual	SJ	ITG (R), MTG (R), MOG (L), IPL (L) PoG (L), CRBL (R)	ITG (R), MTG (R), MOG (L), IPL (L) PoG (L), CRBL (R)	aSC, 6 eSC, 6	1,2, 1a, 2a
Schindler and Bartels (2013)	12	22-30	fMRI-b	Ego > control	Visual	SN	NA	PrCu (R/L), IPS (R/L), IFG (R/L), PrG (L), IPL (R), SFG (R)	eSC, 21	2, 2b
Shibata and Inui (2011)	18	26(m)	fMRI-b	Allo	Visual	A - GR	Pre-SMA (R), TPO (R), DLPFC (R/L), mSFG (L), IFG (R/L), IPS (L), PoG (L), PrCu (L)	NA	aSC,14	1
Thaler and Goodale (2011)	14	NA	fMRI-b	Allo > target-directed	Visual	A - GR	PMd (R/L), IPS (R/L)	NA	aSC, 5	1
Vallar et al. (1999)	7	21-24	fMRI-b	Ego > control	Visual	SJ	NA	SOG (L), IPS (R), AG (R), PrG (R/L), IFG (R)	eSC, 7	2, 2a

Walter and Dassonville (2008)	16	18-32	fMRI-b	Ego > control	Visual	SJ	NA	SPC (R/L), SOG (R/L), MTG (R), PrG (R), MFG (R), aSMG (R)	eSC, 11	2, 2a
Wegman et al. (2014)	47	23 (m)	fMRI-e	Allo > baseline	Visual	SN	PrCu (R), MOG (R), Hi (R), PHG (R), MFG (R/L), CN (R/L), SFG (R/L)	NA	aSC, 22	1, 1b
Weniger et al. (2010)	19		fMRI-b	Ego > Baseline	Visual	SN	NA	PHG (R/L), OTG (R/L), RSC (R/L), POS (R/l), LG (R/L), MTG (R/L), MOG (R/L), PoG (L), AI (L)	eSC, 17	2, 2b
Werner (2005)	12	24 (m)	fMRI-b	Ego > control Allo > control	Visual	SJ	PPC (R/L), IPS (R), AG (R), MOG (R), SOG (R), S/MFG (R)	PPC (R/L), IPS (R), MOG (R), SOG (R), PrCu (L)	aSC, 8 eSC, 6	1,2, 1a, 2a

Zaehle et al. (2007)	16	20-40	fMRI-b	Ego > control Allo > control	Auditory	SJ	SOG (R/L), IPL (R/L), CS (R/L), SFG (R/L), ITG (R/L)	PrCu (R/L), SOG (R/L), CS (R/L), SFG (R/L), ITG (L), IPL (R)	aSC, 10 eSC, 9	1,2, 1a, 2a
Zhang and Ekstrom (2013)	15	NA	fMRI-b	Allo > control	Visual	SN	IFG (L), SPL (R/L), IPL (L), MOG (R/L), IOG (L), PHG (L), FG (L), AG (R/L), MFG (R/L), PrG (L), PrCu (R/L)	NA	aSC, 32	1, 1b

**Note*: One selected study may have one or more experiment(s) in eSC and/or aSC. SN – Spatial Navigation, SJ –Spatial Judgment, A/E-GR - allocentric/egocentric guided reaching, LER - location encoding recognition, fMRI-b - functional magnetic resonance imaging with block design, fMRI-e - functional magnetic resonance imaging with an event-related deign. R/L - bilateral. OT-occipito-temporal, PHG- parahippocampal gyrus, RSC- retrosplenial cortex, OTG- occipito-temporal gyrus (fusiform gyrus), MOG- middle occipital gyrus, SPC- superior parietal cortex, ITG – inferior temporal gyrus, IFG – inferior frontal gyrus, MFG – middle frontal gyrus, SFG – superior frontal gyrus, IPC – inferior parietal cortex, PO – parietal-occipital, LOT – lateral occipito-temporal, MOT – middle occipito-temporal, PoG – postcentral gyrus, CRBL-cerebellum, LO – lateral occipital, Hi – hippocampus, PMVr - ventral premotor cortex, VLPFC - ventrolateral prefrontal cortex, LIPC – lateral inferior parietal cortex, EC - extrastriate cortex, PrCu – precuneus, Cu – cuneus, MO- middle occipital, PMC – premotor cortex, aSMG – anterior supramrginal gyrus, TPJ – temporo- parietal junction, PCC – posterior cingulate cortex, PC – posterior commissure, CN – caudate nucleus, PMd – dorsal premotor area, AI – Anterior insula, POS – parieto-occipital sulcus, SPOC – superior parieto-occipital cortex, CF - calcarine fissure. NA- not applicable.

2.3. ALE Results

2.3.1. Meta-analysis 1 (allocentric)

Three clusters of convergence were identified for the 22 experiments that employed allocentric spatial coding. The significant clusters were in the right SOG ($z = 5.75$, $p < .001$), the precuneus, including a portion of the left IPL ($z = 4.64$, $p < .001$), and the right superior frontal gyrus (SFG) ($z = 5.08$, $p < .001$) (Figure 2.3: Panel A and Table 2.2).

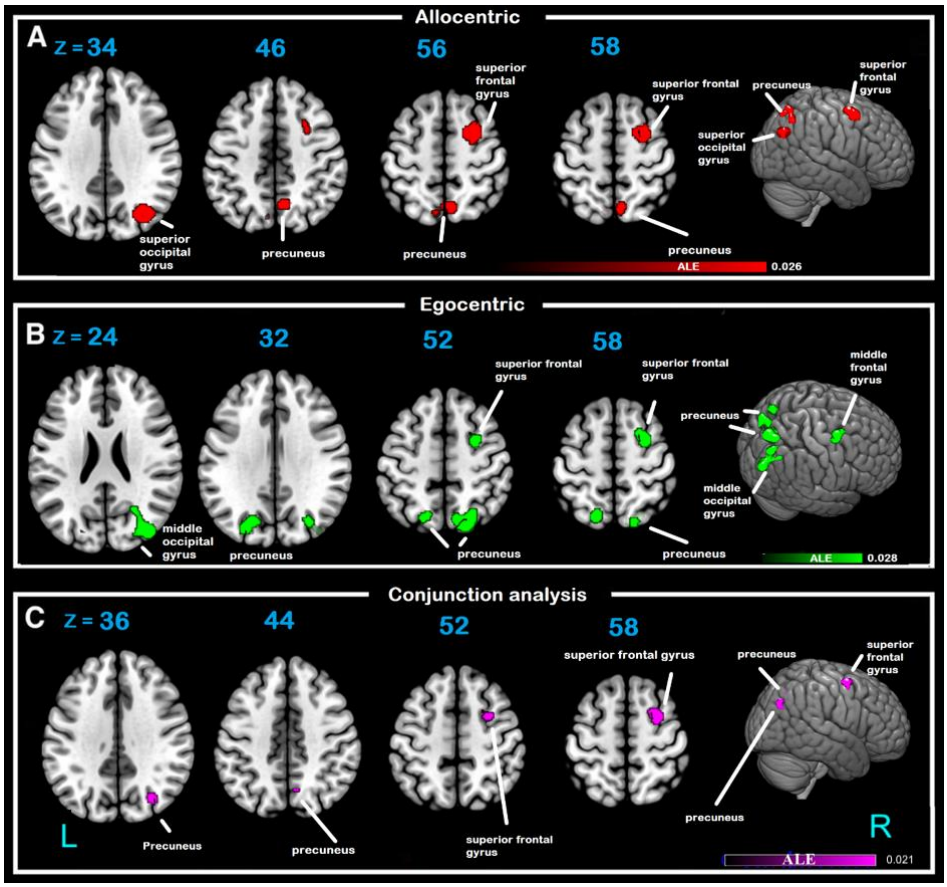

Figure 2. 3. Brain regions showing task-related brain activations in allocentric spatial coding studies (Panel A) and egocentric spatial coding studies (Panel B). Panel C shows common

task-related brain activations appeared in both spatial coding studies. Color bar presents activation likelihood estimation (ALE) z-values.

2.3.2. Meta-analysis 2 (egocentric)

Five clusters of convergence were identified for the 22 experiments that employed egocentric spatial coding. The significant clusters were in the right MOG, including a portion of the posterior cingulate cortex ($z = 6.0$, $p < .001$), the right and left precuneus (RH: $z = 6.04$, $p < .001$; LH: $z = 4.73$, $p < .001$), and the right medial frontal gyrus (MFG) ($z = 5.01$, $p < .001$) (Figure 2.3: Panel B and Table 2.2). The right middle occipital gyrus and a portion of the right posterior cingulate were two other areas of convergence for the egocentric spatial representations.

2.3.3. Conjunction Analysis (allocentric and egocentric)

In general, greater convergence was observed in the right than in the left hemisphere in both meta-analysis 1 (allocentric) and meta-analysis 2 (egocentric) (Table 2.2). This right–left disparity was observed more obviously in the right SOG for the allocentric tasks and in the right MOG and right precuneus for the egocentric tasks. Conjunction analyses of the convergences derived from the two main meta-analyses revealed two clusters of convergence with their main peaks located at the right precuneus and the right SFG (Figure 2.3: Panel C and Table 2.2).

Table 2. 2. ALE results of cluster of convergence on allocentric and egocentric spatial coding types

Cluster	mm^3	Coordinates			ALE	*p*	z-	Hemi	BA	Anatomical Labeling
		X	*y*	*z*	value	value	score			
Meta-analysis 1: allocentric										
1	2264	22	4	56	0.022	<.001	5.08	R	6	Superior frontal gyrus
		28	8	54	0.020	<.001	4.88	R	6	Middle frontal gyrus
2	1952	36	-72	34	0.026	<.001	5.75	R	19	Superior occipital gyrus
		8	-60	46	0.019	<.001	4.64	R	7	Precuneus
3	1872	8	-60	46	0.019	<.001	4.64	R	7	Precuneus
		-6	-70	52	0.014	<.001	3.80	L	7	Precuneus
Meta-analysis 2: egocentric										
1	3656	38	-80	24	0.028	<.001	6.00	R	19	Middle occipital gyrus
		32	-72	40	0.022	<.001	5.03	R	19	Precuneus
		26	-62	22	0.014	<.001	3.73	R	31	Posterior cingulate cortex
2	2896	18	-74	52	0.028	<.001	6.04	R	7	Precuneus
3	1728	28	2	58	0.021	<.001	5.01	R	6	Superior frontal gyrus
		28	-2	50	0.017	<.001	4.31	R	6	Precentral gyrus
4	1448	-26	-78	32	0.020	<.001	4.73	L	31	Precuneus
5	1096	-16	-66	56	0.019	<.001	4.67	L	7	Precuneus
Conjunction Analysis										
1	1048	28	2	58	0.021	NA	NA	R	6	Superior frontal gyrus
2	616	32	-72	36	0.018	NA	NA	R	19	Precuneus
3	88	8	-64	44	0.013	NA	NA	R	7	Precuneus

Note: NA = not available. Conjunction analysis was based on intersection z-maps, which were thresholded and corrected for multiple comparison using FWE at $p < .05$. Thus p-value and z-score cannot be computed.

2.3.4. Meta-analysis 1a (SJ) and 1b (SN) (task-specific allocentric)

The results of ALE for the SJ tasks (allocentric) revealed five clusters of convergence (Figure 2.4 and Table 2.3). The regions with significant convergence were the right MFG ($z = 4.06$, $p < .001$), right precuneus ($z = 4.09$, $p < .001$), right fusiform gyrus ($z = 4.60$, $p < .001$), and right IPL ($z = 4.27$, $p < .001$). Two clusters of convergence were revealed for the SN counterpart, and the regions were the right superior lateral occipital cortex ($z = 4.57$, $p < .001$) and the right precuneus ($z = 4.11$, $p < .001$), which included a portion of the left precuneus ($z = 4.11$, $p < .001$).

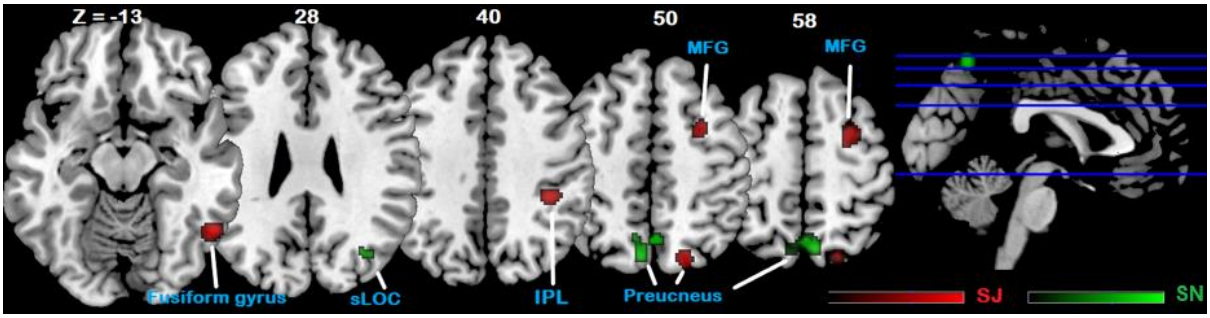

Figure 2. 4. Results of ALE for the SJ (red) and SN (green) in allocentric spatial coding studies. Color bar indicates the ALE values. Note: SJ = spatial judgment tasks. SN = Spatial Navigation tasks. sLOC = superior lateral occipital cortex. IPL = inferior parietal lobule. MFG = middle frontal gyrus.

2.3.5. Meta-analysis 2a (SJ) and 2b (SN) (task-specific egocentric)

The results of ALE revealed two clusters of convergence for the SJ tasks. These clusters were in the right MOG ($z = 6.10$, $p < .001$), precuneus ($z = 5.82$, $p < 001$), right MFG ($z = 5.57$, p

< .001), and partially right SFG (z = 5.04, p < .001). On the other hand, three clusters of convergence were revealed for the SN tasks, which were in the right MOG (z = 4.38, p < .001) and bilateral precuneus (RH: z = 4.78, p < .001; LH: z = 4.84, p < .001) (Figure 2.5 and Table 2.3).

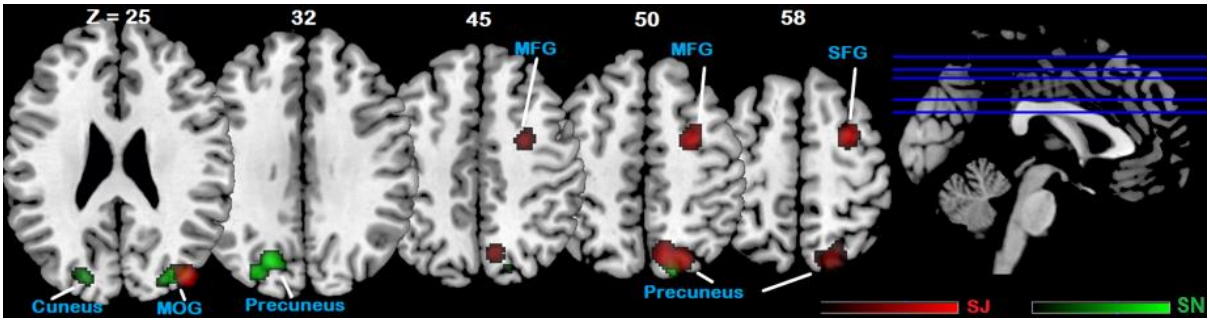

Figure 2. 5. Results of ALE for the SJ (red) and SN (green) in egocentric spatial coding studies. Color bar indicates the ALE values. Note: SJ = spatial judgment tasks. SN = Spatial Navigation tasks. MOG = middle occipital gyrus. MFG = middle frontal gyrus. SFG = superior frontal gyrus.

The allocentric spatial coding type seemed to associate with convergence in the right SFG and SOG (Figure 2.6). In contrast, the egocentric spatial coding type appeared to associate with convergence in the right MFG and MOG. Convergence in the right precuneus seemed to associate with both spatial coding types. Substantial differences in convergence were revealed between the SJ and SN tasks in each of the allocentric and egocentric types. Task-specific allocentric spatial coding appeared to demand the most diverse clusters of convergence, including the right inferior parietal lobule (IPL), superior lateral occipital cortex (sLOC), and right fusiform gyrus (FG).

Table 2. 3. Task-specific related cluster of convergence in SJ versus SN of allocentric and egocentric spatial coding types

Cluster	mm^3	Coordinates			ALE	*p*	z	hemi	BA	Anatomical Labeling
		x	y	Z	value	*value*	score			
Meta-analysis 1a (SJ) (for aSC)										
1	1096	30	4	48	0.011	<.001	4.06	R	6	Middle frontal gyrus
2	872	34	-72	34	0.011	<.001	4.09	R	19	Precuneus
3	840	54	-58	-12	0.013	<.001	4.60	R	37	Fusiform gyrus
4	712	40	-36	42	0.011	<.001	4.27	R	40	Inferior parietal lobule
5	680	20	-74	52	0.014	<.001	4.95	R	7	Precuneus
Meta-analysis 1b (SN) (for aSC)										
1	1472	6	-66	58	0.014	<.001	4.11	R	7	Precuneus
		2	-62	52	0.014	<.001	4.11	L	7	Precuneus
2	816	34	-70	32	0.016	<.001	4.57	R		Superior lateral occipital cortex
Meta-analysis 2a (SJ) (for eSC)										
1	2952	18	-72	54	0.021	<.001	5.82	R	7	Precuneus
2	2192	28	0	58	0.020	<.001	5.57	R	6	Middle frontal gyrus
		28	-2	50	0.017	<.001	5.04	R	6	Superior frontal gyrus
3	1376	40	-82	24	0.023	<.001	6.10	R	19	Middle occipital gyrus
Meta-analysis 2b (SN) (for eSC)										
1	1720	-18	-72	32	0.017	<.001	4.78	L	31	Precuneus
		-28	-80	32	0.013	<.001	4.16	L	19	Superior occipital gyrus
		-22	-80	28	0.012	<.001	3.90	L	18	Cuneus
2	976	36	-80	26	0.015	<.001	4.38	R	19	Middle occipital gyrus
		26	-84	24	0.010	<.001	3.54	R	18	Cuneus
3	728	18	-76	52	0.017	<.001	4.84	R	7	Precuneus

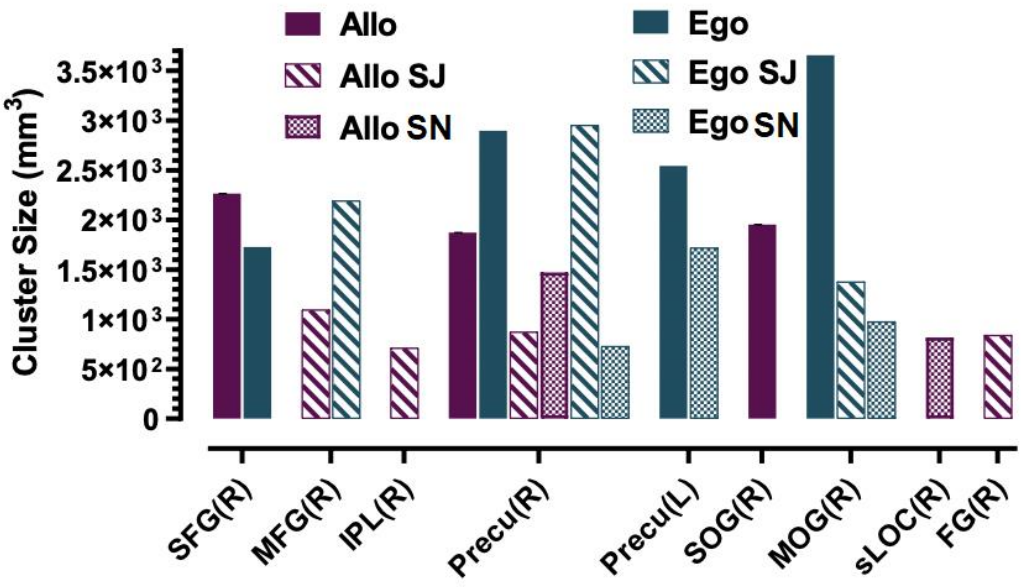

Figure 2. 6. Results of ALE in terms of cluster sizes (in mm3) showing cluster of convergence in allocentric and egocentric spatial coding studies before and after grouped according to the spatial judgment (SJ) or spatial navigation (SN) task-specific features. SFG = superior frontal gyrus. MFG = middle frontal gyrus. IPL = inferior parietal lobule. Precu = precuneus. SOG = superior occipital gyrus. MOG = middle occipital gyrus. FG = fusiform gyrus. sLOC = superior lateral occipital cortex.

2.4. Discussion

In general, the allocentric and egocentric spatial coding types share comparable clusters of convergence in the precuneus and the SFG. The main convergence differences were in the occipital region—that is, in the SOG and MOG for the allocentric and egocentric representations, respectively. Additional controls set on the task types revealed more differences in the

convergences associated with the two types of spatial coding. For the SJ tasks, the MFG clusters of convergence were unique and common to both types, whereas the FG and IPL clusters were unique to the allocentric type, and the middle occipital gyrus cluster was unique to the egocentric type. For the SN tasks, the precuneus cluster of convergence was common but not unique to both spatial coding types, while the sLOC cluster was unique to the allocentric type while the middle occipital gyrus was unique to the egocentric type. It is noteworthy that among all the clusters, the right precuneus cluster of convergence was found to associate with all the spatial coding and task types. In contrast, the left precuneus cluster of convergence was associated only with egocentric spatial coding, particularly with SN tasks.

The convergent results of the precuneus cluster supported the hypothesis that egocentric and allocentric spatial coding are mediated by common neural substrates—that is, by the precuneus, which falls within the SPL/FEF junction. However, the hypothesis that egocentric spatial coding would involve the SOG and lateral/ventral IPS and that allocentric spatial coding would involve the IPL and STG cannot be supported. The task-specific hypothesis that SJ tasks would be biased with convergence in the parieto-occipital clusters and that SN would be biased with convergence in the parieto-temporal clusters is partially upheld.

2.4.1. Neural Processes Underlying Spatial Coding – Similarities and Differences

The finding of the convergence of the bilateral precuneus cluster as common to both spatial coding types is consistent with what has been reported in previous studies employing egocentric (Creem et al., 2001; Gomez et al., 2013; Parslow et al., 2004; Schindler & Bartels, 2013; Zaehle et al., 2007) or allocentric (Creem et al., 2001; Frings et al., 2006; Parslow et al., 2004; Shibata &

Inui, 2011; Wegman et al., 2014; Zaehle et al., 2007; Zhang & Ekstrom, 2013) tasks. Similarly, the right SFG as the second cluster of convergence common to both spatial coding types is consistent with previous studies on egocentric (Committeri et al., 2004; Creem-Regehr et al., 2007; Creem et al., 2001; Fink et al., 2003; Galati et al., 2000; Gramann et al., 2006; Vallar et al., 1999) or allocentric (Frings et al., 2006; Shibata & Inui, 2011; Wegman et al., 2014; Zaehle et al., 2007) task-taking. These two clusters of convergence further indicated that both spatial coding types are mediated by the dorsal attention network. Neural processes, such as attention selection and response mapping (Corbetta & Shulman, 2002) and maintenance of covert spatial attention (Corbetta & Shulman, 2002; Moore & Fallah, 2004; Thompson, Biscoe, & Sato, 2005), are essential for completing the tasks. Besides the dorsal attention network, the convergence revealed in the SFG cluster together with that in the precuneus cluster (as a larger part of the posterior cingulate cortex) is suggestive of the involvement of the fronto-parietal attention network in both types of spatial coding. Additional neural processes for the tasks would be visuospatial attention (Galati et al., 2001; Galati et al., 2000; Liu et al., 2017; Neggers et al., 2006; Werner, 2005; Zhang & Ekstrom, 2013), encoding of objects in space (Foley, Whitwell, & Goodale, 2015; Goodale & Milner, 1992; Milner & Goodale, 2008), and maintenance of spatial representations in working memory (Corbetta et al., 2008; Ptak, 2012).

The main differences in the convergence of clusters between the two types of spatial coding were revealed in the occipital cortex—that is, in the SOG versus the MOG for the allocentric and egocentric types, respectively. Our results on the SOG are consistent with a few previous studies that showed activations in the SOG were higher in an allocentric than in an egocentric condition

(Committeri et al., 2004; Galati et al., 2000; Neggers et al., 2006; Zaehle et al., 2007). The SOG (BA 19) is located in the anterior parieto-occipital region (Galletti et al., 2001), which mediates object-centered image processing (Crowe et al., 2008). Its close connection with the precuneus (van Asselen, Kessels, Kappelle, & Postma, 2008) suggests that the SOG may play a role in visualizing and maintaining the spatial relationships of the objects in space during the allocentric coding process (Boccia, Nemmi, & Guariglia, 2014). The MOG, in contrast, is located rostrally to the parieto-occipital sulcus, which mediates encoding of object locations (Goodale & Milner, 1992). The role of the MOG in egocentric coding is likely to encode the body-centered coordinates during the coding process (van der Stoep, Postma, & Nijboer, 2017). It is noteworthy that the convergent results of the SOG and MOG clusters revealed are not consistent with those reported in a few papers included in this meta-analysis. Three papers reported activations in the lateral occipital complex (comprising both the MOG and the SOG) in both spatial coding types (Liu et al., 2017; Saj et al., 2014; Werner, 2005), and two other papers reported activations in the SOG in the egocentric condition (Werner, 2005; Zaehle et al., 2007). A close look at the tasks used in these experiments indicated that the task processes involved some sort of SJ (see below). The similarity in the coding rules set for these supposedly allocentric and egocentric processes could have confounded the results. For instance, discriminating left/right with reference to the body in the egocentric condition (Saj et al., 2014) is largely comparable to differentiating the movement of an on-screen bar with reference to the midpoint of a line close to the bar in the allocentric condition (Neggers et al., 2006).

2.4.2. Task-Specific Confounding Factor - Spatial Judgment versus Spatial Navigation

The complementary task-specific meta-analyses resulted in two main observations. First, the precuneus was confirmed once again to play a generic role, its convergence having been found in both SJ and SN tasks. Second, the influence of the task-specific processes on the convergence of clusters appeared to be stronger for the allocentric than for the egocentric type. The generic role of the precuneus in both types of spatial coding has been covered in the last section and will not be repeated here. In fact, no task-specific influence was revealed for the egocentric spatial coding, which yielded the MOG cluster of convergence across both SJ and SN conditions. In contrast, for the allocentric spatial coding, SJ task influences were found in the FG and IPL clusters, whereas SN task influences were found in the sLOC cluster.

The results indicated that, during the SJ tasks, allocentric spatial coding might have been biased with increasing demands of object recognition (FG; Weiner & Zilles, 2016), spatial perception (IPL, see Husain & Nachev, 2007), sustained attention (IPL, see Husain & Nachev, 2007) and attention shifting and maintenance (IPL, see Ptak, 2012). The SJ tasks might also have changed the demands of the displacement-related process of the target image in allocentric spatial coding (FG, see Ferber, Humphrey, & Vilis, 2003). To support our proposition, subjects in a few SJ allocentric tasks were required to judge a left or right position against a self-perceived midpoint on the same line (Galati et al., 2000; Saj et al., 2014; Vallar et al., 1999). The task-taking processes would have been dominated by the orienting attention for continuous saccadic eye movements and online SJ, instead of by visualizing and maintaining spatial relationships through such means as memory-guided retrieval, as unique to allocentric spatial coding (see Saj et al., 2014). For the

confounding factor in the SN tasks, the sLOC cluster also included the posterior parietal cortex. The posterior parietal cortex has been reported to be involved in maintaining visuospatial control of primed action (Goodale & Milner, 1992), and the sLOC in an animal study was found to modulate long-term representation of objects in the visual-field (James, Humphrey, Gati, Menon, & Goodale, 2002). SN tasks could inevitably bias allocentric spatial coding with excessive action controls and maintenance of object representations, such as environmental scenes, in the visual field (see Committeri et al., 2004).

2.4.3. Limitations

There are a few limitations associated with the meta-analytic method adopted in this study. First, we did not attempt to elucidate the theoretical basis for attentional spatial coding, as ALE is not capable of examining temporal courses of the underlying neural processes. The results are meant to merely differentiate the main neural processes associated with the allocentric and egocentric types. Second, the conjunction analyses conducted yielded convergent neural clusters, and the results cannot reflect the within-group heterogeneity among the allocentric/egocentric and SJ/SN tasks. Third, the task-specific classifications adopted in this study (meta-analysis 1a, b & 2a, b) excluded a number of experiments and articles from the analyses. This somewhat would have compromised the generalization of the task-specific ALE results. In addition, some of the tasks included in SN (e.g. Committeri et al., 2004) may require SJ processing. Readers should be cautious when interpreting findings of this part of the study.

2.4.4. Conclusion

Allocentric and egocentric spatial coding involve both similar and distinctive cognitive processes. The strong common clusters of convergence in the right precuneus and the right superior frontal gyrus are suggestive of the recruitment of the parieto-frontal circuit in spatial coding. Distinctiveness of the two types of spatial coding was found in the parieto-occipital circuit, where the allocentric coding was dominated by the SOG cluster and the egocentric coding was dominated by the MOG cluster. These findings indicate that spatial coding regardless of type requires attention selection and maintenance as well as response mapping. Allocentric and egocentric types, however, are unique in recruiting the SOG and MOG clusters for mediating the distinct processes required in the tasks. These tasks in the allocentric coding process are the visualization and maintenance of spatial relationships of objects in space, whereas in the egocentric coding process they are the encoding of body-centered coordinates. The testing of task-specific influences indicated that egocentric spatial coding tasks used in previous studies are rather bias-free. In contrast, allocentric spatial coding tasks appear to have been significantly influenced, whether an SJ or a SN design was adopted as the task-taking process. SJ designs were revealed to have been easily biased by decreases in demands of manipulating spatial relationships among the visual objects. SN designs were dominated by demands of action controls and maintaining visual scenes. Our findings offer insights to enhance the design of spatial tasks for assessing spatial coding, particularly of those tasks targeting the allocentric type.

CHAPETR 3

3. Cortical Hemodynamic Response Associated with Spatial Coding: A Near-Infrared Spectroscopy Study

The results of this chapter were published in *Brain Topography* (Derbie et al., 2021)

3.1. Introduction

Decoding visual information for processing involves orienting attention onto the object in space (Chun et al., 2011; Desimone & Duncan, 1995). To respond to a simple question — "Where are you?" for example—an individual must reference an object in space and indicate his or her position, such as saying, "I am to your right" or "I am between two bookshelves." The former is egocentric spatial coding (eSC), in which one's brain encodes an object in space relative to the body's coordinates. The latter is allocentric spatial coding (aSC), in which the brain encodes an object in space and references the coordinates of another object in space (Ekstrom et al., 2014; Filimon, 2015). A review of brain imaging literature suggests three views on the neural processes involved in the two types of spatial coding.

The first view stipulates that the cognitive processes underlying these two spatial coding types are differentially subserved by the dorsal (DAN) and ventral (VAN) attention networks (Corbetta & Shulman, 2002; Vossel et al., 2014). The ventral stream is predominantly involved in aSC, and the dorsal stream is involved in eSC (Burgess, 2006). The second view stipulates that both spatial coding types are mediated by the same group of neural substrates, such as the posterior parietal cortex (PPC)(Castiello, 2005; Culham & Valyear, 2006), the posterior cingulate cortex, and the precuneus

(Burgess, 2008; Epstein, 2008; Iaria et al., 2007). The third view stipulates that the neural substrates mediating aSC subsume those mediating eSC (Zaehle et al., 2007). Compared with eSC, aSC involves more visual working memory (Cooper & Humphreys, 2000) and cognitive resources (for critical review: Ekstrom et al., 2014; Filimon, 2015). As part of the dorsal attention network, the parietal cortex—particularly the precuneus—mediates these additional neural processes (Ekstrom et al., 2014; Zaehle et al., 2007; Zhang & Ekstrom, 2013).

A review of the studies underpinning the three views indicated that, instead of intrinsic diversities in the neural processes, the contradictory results might have resulted from the task-taking processes involved in these studies' various behavioral paradigms. Considering the potential task-specific influences among the three views, a recent study conducted by Szczepanski et al. (2013) offers further evidence to support the third view that aSC processes subsume the eSC processes. They found that the supplementary eye field (SEF) of the superior parietal lobule (SPL) pathway was common to both conditions. However, the frontal eye fields (FEF) of the intraparietal sulcus area two and the SEF were unique to the egocentric and allocentric conditions, respectively (Szczepanski et al., 2013). They employed a cue-to-target paradigm that differed from the overt orienting tasks used in the majority of previous studies in this area. The cue-to-target paradigm's advantage is its covert instead of overt orienting attention, which would largely reduce biases due to the in-task saccade movements (Posner, 1980). Saccade movements elicit activities in the FEF and PPC (Dean & Platt, 2006; Zaehle et al., 2007).

The motivation behind this study is that the task-taking processes for the task in Szczepanski et al.'s (2013) study could have influenced the results. The participants were

instructed to stare at a fixation cross that appeared in the middle of the screen before the cues and targets appeared. The emphasis on the fixation cross as a reference location could have over-emphasized the gaze-centered process (also called a viewer-centered process) in both spatial coding conditions. Thus, it could have artificially inflated the egocentric processes during the allocentric condition. In this study, we aimed to design tasks that minimize the drawback mentioned above. In brief, the participant was to attend to the fixation cross before the cue or target appeared. Second, the participants were to engage in fine-grain visual scan and discrimination instead of simple spatial judging in the eSC and aSC conditions. In contrast to previous neuroimaging studies that employed fMRI, this study used functional near-infrared spectroscopy (fNIRS) to capture brain activity during participants' task performance for various reasons. First, the tasks used to elicit the spatial coding processes were relatively complex, and operating fNIRS would offer more flexibility than fMRI in the task-taking environment arrangements. Second, fNIRS is less stringent than fMRI on controlling head movements and body posture while performing the task (Heinzel et al., 2013). We hypothesized that the neural substrates corresponding to the dorsal attention network (which contains the juncture of the precentral and superior frontal sulcus) would be common to aSC and eSC conditions. The eCS condition would involve the SPL, and the aCS condition would involve the inferior parietal lobule (IPL).

3.2. Method

3.2.1. Participants

Through convenience sampling, we recruited 22 university students with a mean age of 26.9 years (*SD* = 4.5). All participants gave informed consent according to the Human Subjects Ethics Subcommittee's guidelines. The exclusion criteria included a history of epilepsy and/or other psychiatric disorders and being left-handed. All participants were right-handed. We explained the experiment's purpose and procedure to the participants and obtained ethical approval for the experiment from the Human Subjects Ethics Subcommittee at the institution where we conducted the experiment.

3.2.2. The Experimental Paradigm

The task design referenced those of Barrett et al. (2001) and Brian (2014). One trial has five screens arranged in sequence (see Figure 3.1). First, a blank screen appeared for a variable time of 500 to 1000 ms, and we set the mean duration to 600 ms. A 500-ms fixation cross (+) followed the blank screen. The third screen presented a 200-ms group of three circles (called the triad). In the triad, one circle was illuminated to indicate the upcoming target's probable location (for eSC) or position (for aSC). After the cue, another 500-ms fixation cross reappeared. The 1500-ms target stimulus was the same triad, in which each circle contained a "T" oriented in different directions. The circle containing a sideways "T" was the only target circle. The participants responded by pressing the "Z" or "M" key on a keyboard. There were valid and invalid trials in each condition. For aSC, a valid trial referred to the target circle occupying the same relative

position as the cue. For eSC, a valid trial referred to the target circle occupying the cue's absolute location. A block design was used to organize the trials. All trials were counterbalanced regarding the hemi-field distributions and the valid and invalid responses.

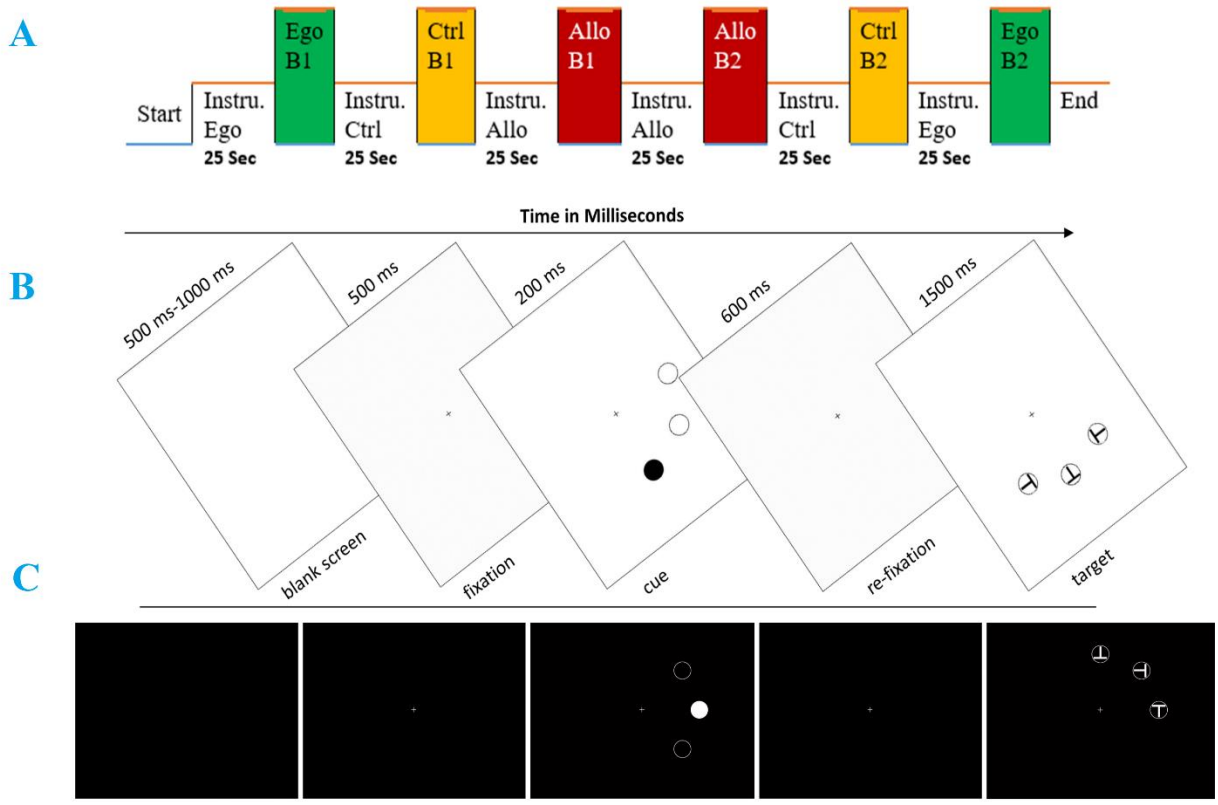

Figure 3. 1. Design of the experimental task. A: Sequence of the six task blocks for the three conditions. B: Presentation schedule of fixing, cue, and target screens of a trial in the egocentric condition. C: Cue and target in a valid trial for the egocentric condition. Note: Ego = Egocentric; Allo = Allocentric; Ctrl = Control; B1 = Block 1; B2 = Block 2; Instru = Instruction.

Stimuli

The cue triad stimulus contains three circles on a black background. One illuminated circle indicates the upcoming target's probable location or position, and the other two circles are the distractors. A total of 22 cue circles appeared at various degrees with reference to the middle of the screen (0°, 45°, 90˚, 135°, 180°, 225°, 270°, and 315°), equally distributed in the right and left hemi-fields. The target triad stimulus contains one target and two distractor circles (Figure 3.1B). The target circle is denoted by a 90° or -90° slanted "T," and the distractor circle is denoted by upright or inverted "Ts". Target and distractor circles are presented in a systematically varied order. The stimuli for the control condition are the same as the cue and target stimuli in the eSC and aSC conditions. The only difference was that participants were instructed to view the cue stimulus but disregard the location/position information in it.

Task-taking Procedure

The participants completed six task blocks with two blocks for each of the aSC, eSC, and control conditions. Each block had 24 trials. The blocks' order was counterbalanced (Figure 3.1A), and each participant received training on performing the task before engaging in the experiment. The training continued until the participant responded according to the response rules within 1500 ms in all three conditions. Before starting the task, participants sat in front of the computer screen with the subjective midline of their body aligned with the screen's center. Participants viewed the instructions on the specific response rules at the beginning of the task block. By the end of each trial, participants responded within 1500 ms by pressing the "M" (90° tilted "T") or "Z" key (-90°

tilted “T”) to indicate the target circle’s specific orientation. Participants were reminded throughout the task to respond as quickly as possible. We used the E-prime 2.0 software (Psychology Software Tools, Pennsylvania, USA) for Windows 7 with a refresh rate of 56.9 ms for stimulus presentation and for behavioral data management.

3.2.3. NIRS Data Acquisition and Preprocessing

Capturing O_2-Hb concentration data employed a 52-channel configured Hitachi optical topography (ETG-4000, Hitachi™ Medical. Co., Kashiwa, Japan) equipped with laser diodes of two wavelengths (695 nm and 830 nm). There were 44 channels (22 channels in each hemisphere composed of two 3 x 5 optode probe sets), each comprising eight emitters and seven detectors. The data sampling rate was 10 Hz. The right fNIRS probe was mounted over the right superior frontal region, covering the hot sites reported in previous studies on aSC and eCS. The hot sites included the occipitoparietal circuit (e.g. Ekstrom et al., 2014; Filimon, 2015; Galati et al., 2001; Galati et al., 2000; Liu et al., 2017; Neggers et al., 2006) and the right SFG (e.g. Committeri et al., 2004; Fink et al., 2003) (Figure 3.2). The left probe was mounted at 3 cm posterior to the left occipital lobe, covering the left temporoparietal junctions and left occipitoparietal circuits. Previous studies revealed that these sites modulate allocentric spatial coding more than those in the right superior frontal region (e.g. Chen et al., 2012; Gomez et al., 2014; Saj et al., 2014). The distance between the corresponding source and the detector was 3 cm for detecting the O_2-Hb concentration at 2 to 3 cm below the scalp (Toronov et al., 2001).

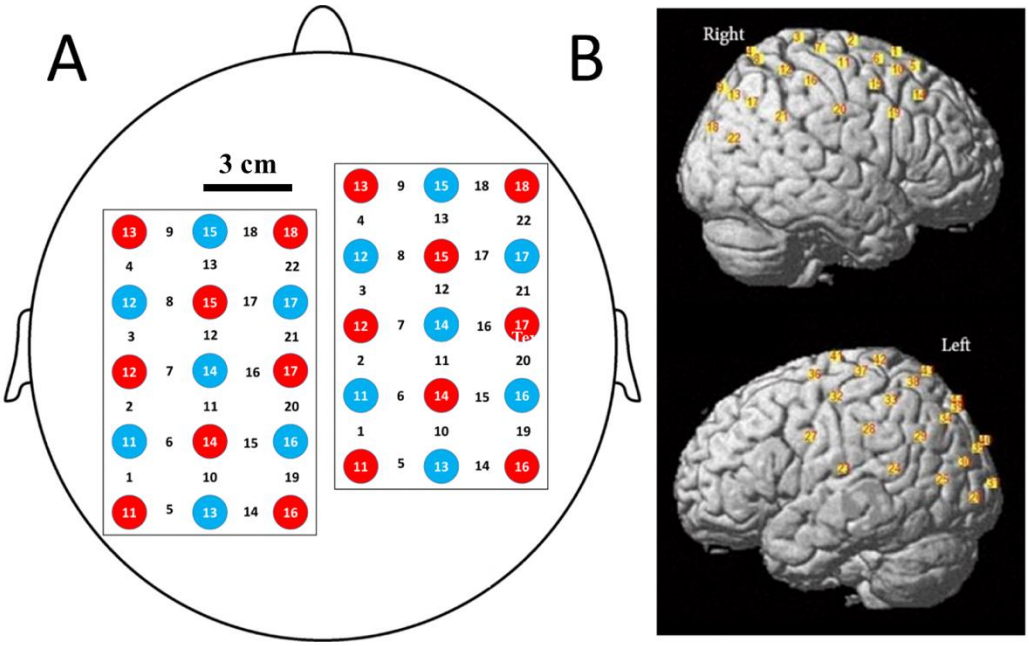

Figure 3. 2. A: Probe set configuration. Red circles represent emitters and blue circles represent detectors. B: Channel configurations superimpose onto T1 image (Montreal Neurological Institute space).

Participant-specific NIRS channel positions were obtained with a 3-D digitizer before transforming them into the Montreal Neurological Institute (MNI) space equipped in the SPM-NIRS toolbox. An estimation of changes in the O_2-Hb level was computed with the modified Beer-Lambert law approach (Cope & Delpy, 1988):

$$A = In\frac{I_{inc}}{I_{det}} = L\mu_a + G$$

whereby Lg (l_0/l): light extinction; I_{inc}: incident light intensity; I_{det}: light intensity as detected; L: path length; $L\mu_a$: tissue absorption coefficient; and G: signal loss due to light scattering (Kocsis, Herman, & Eke, 2006).

3.2.4. Individual and Group Spatial Analysis

An individual-level spatial analysis was conducted using the *nfri_mni_estimation* function (Singh, Okamoto, Dan, Jurcak, & Dan, 2005). The NIRS probe positions were "probabilistically" converted into the MNI-152-compatible canonical brain map to derive each participant's mean cortical surface MNI coordinates. The individual functional data were entered into the aSC > control and eSC > control comparisons. Each contrast's *t* values for each channel were extracted and then pooled to form the group values. The group mean *t* values for each channel were converted into the functional data and plotted onto the MNI template (Figure 3.5). The SPM Anatomy Toolbox (Eickhoff et al., 2005) in the SPM5 software package (www.fil.ion.ucl.ac.uk/spm/software/spm5/) was used to produce the anatomical labeling. All operations were conducted in the Matlab environment R2009b (Mathworks, Boston, MA, USA).

3.2.5. Statistical Analysis

Participants' between-condition reaction times (RTs) from the experimental task were compared with repeated variance analysis measures. The Validity × Condition effects were tested. Validity was valid versus invalid trials, and Condition was aSC versus eSC. Post hoc comparisons for significant effects used paired *t* tests. The analyses were conducted with IBM SPSS v.23 for Windows®.

Changes in the O_2-Hb concentration were defined as the O_2-Hb concentration of the aSC or eSC condition subtracted by that of the control condition. We preprocessed the fNIRS data using the wavelet-minimum description length detrending algorithm method and a hemodynamic

response function-based low-pass filter to remove artifacts related to cardiac, breathing, and vasomotor changes (Jang et al., 2009). For all participants, the onset vectors were specified manually, and each block's onset and duration were defined from those registered in each scan. The changes in the O_2-Hb concentration at the participant and group levels were derived using NIRS-SPM (Tak et al., 2011). The group-level changes in O_2-Hb concentration were derived using an SPM *t* statistic map with the statistical significance set at $p \leq 0.05$. The *t* statistics were used to plot the channel-specific fNIRS, as shown in Figure 3.5 (see Results). Pearson's correlation coefficients of the changes in O_2-Hb concentration among the channels were computed for the aSC and eSC conditions using the R packages for statistical computing (R Core Team, 2017). A hierarchical clustering method was employed to further group and visualize the patterns of correlograms available in the R package (Murtagh, 1985).

The least absolute shrinkage and selection operator-regularized principal component (LASSO-RPC) (e.g. Ryali, Chen, Supekar, & Menon, 2012), a machine learning-based regression analysis, was conducted to explore relationships between the behavioral responses and brain activities. That is, LASSO-RPC was meant to predict the participants' RTs from the 44 channel-specific changes in the O_2-Hb concentration.

The advantage of LASSO-RPC is minimizing the overfitting shortcomings due to the large number of multiple comparisons used in other statistical methods. The LASSO-RPC model was:

$$\hat{\beta}^{lasso} = min\beta(y - Z\beta)'(y - Z\beta) + \lambda \sum_{J=1}^{p} |\beta j|$$

whereby $\sum_{J=1}^{p} |\beta j|$ is the absolute size of the least square estimate, and Z is the channel-specific change in the O_2-Hb concentration. When Z_j weakly relates with Y, the value of βj approaches zero. To further control within group variability, the RT of the control condition was entered as a regressor variable in the regression model. All the LASSO-related analyses were conducted with the R packages of statistical computing (Friedman, Hastie, & Tibshirani, 2009).

3.3. Results

3.3.1. Behavioural Results

One participant's data were excluded from the analyses because the corresponding data was discarded from the NIRS-SPM analysis. The main effect on mean RTs of valid trials among the three experimental and control conditions was significant ($F(2,60) = 55.33$, $p = <.001$, $\eta p^2 = .65$) (Figure 3). The mean RTs of both eSC ($t(20) = -10.79$, $p < .001$) and aSC ($t(20) = -7.68$, $p < .001$) conditions were significantly faster than that of the control condition. The aSC condition (91.4 ± 2.6%) had significantly lower accuracy rate than the eSC condition (91.5 ± 2.6%) ($t(40) = -3.35$, $p < .001$). The two-way RM-ANOVA revealed significant Condition ($F(1,20) = 200.20$, $p < .001$, $\eta p^2 = .91$) and Validity ($F(1,20) = 14.45$, $p = .001$, $\eta p^2 = .42$) effects on the participants' mean RTs. The Condition × Validity effect was significant ($F(1,20) = 10.44$, $p = .004$, $\eta p^2 = .34$).

The mean RTs of valid trials were significantly faster than those of the invalid trials in both the aSC (t (20) = -7.85, p < .001) and eSC conditions (t (20) = -14.01, p <.001). The mean RTs of valid trials of the eSC conditions were significantly faster than those of the aSC condition (t (20) = -5.63, p <.001). However, the differences in mean RTs of invalid trials were not statistically significant between eSC and aSC conditions (t (20) = -1.05, p = .305).

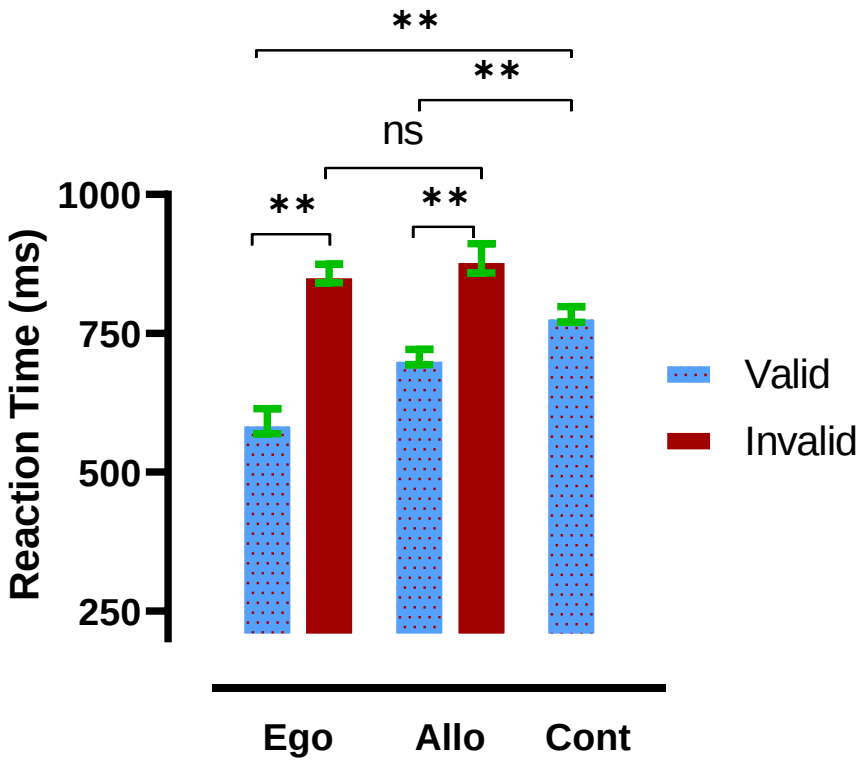

Figure 3. 3. Comparisons of reaction times across the egocentric, allocentric, and control conditions. Note: Error bars are standard errors. ** = p < .001.

3.3.2. fNIRS Results

The NIRS-SPM-based contrast analysis included 21 participants because one participant's data had errors during signal recording. No significant activation clusters were revealed in the eSC > aSC contrast or vice versa. Significant changes in O_2-Hb concentration were found for the aSC > Control contrast in a large right cluster of activation, including in the right post-central gyrus (Ch. 16) (t (20) = 3 (maxima), $p < .05$), IPS (Ch. 12) (t (20) = 3 (maxima), $p < .05$), IPL (Ch. 20) (t (20) = 3 (maxima), $p < .05$), TPJ (Ch. 21) (t (20) = 3 (maxima), $p < .05$), and a small left cluster in the IPL (Ch.20) (t(20) = 3 (maxima), p <.05) (Figure 3.4). Significant activation clusters found in the eSC > Control contrast were in the right post-central gyrus (Ch. 16) (t (20) = 2.6 (maxima), $p < .05$) and IPL (t (20) = 2.6 (maxima), $p < .05$).

Channel-specific fNIRS t values plotted on an MNI-compatible canonical brain show that the left hemisphere had lower t values (i.e. cortical activities) than the right hemisphere did in both spatial coding conditions (t (20) = 1.83 - 2.20, $p = .05$) (Figure 3.5).

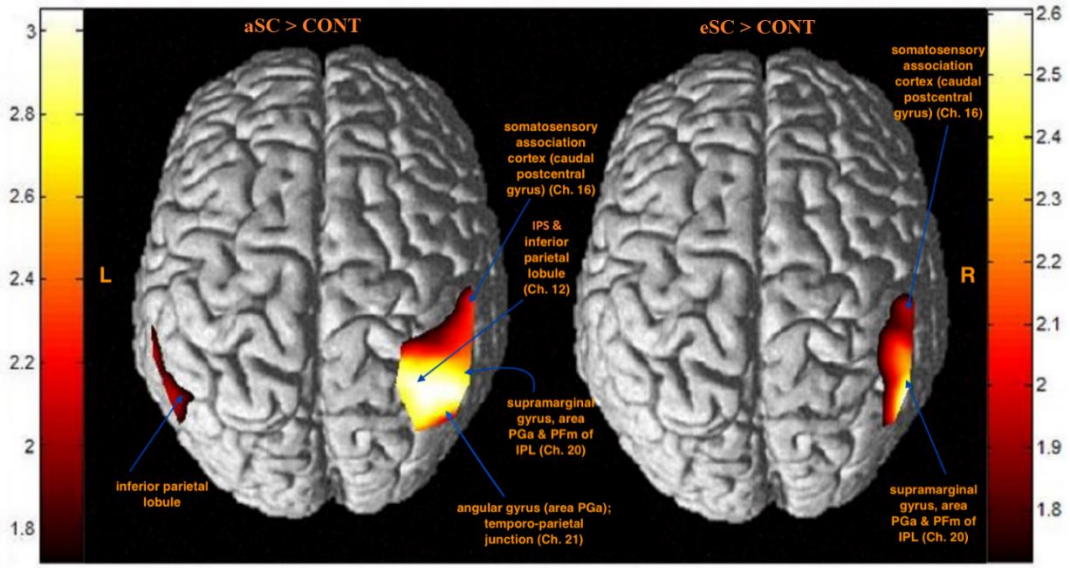

Figure 3. 4. Significant cortical activities in the right and left hemispheres for the aSC > Control and eSC > Control contrasts. The group mean t-values on O_2-Hb were superimposed onto the T1 template mapped on the MNI coordinate values. Note: The channel numbers shown correspond to those in Figure 2.

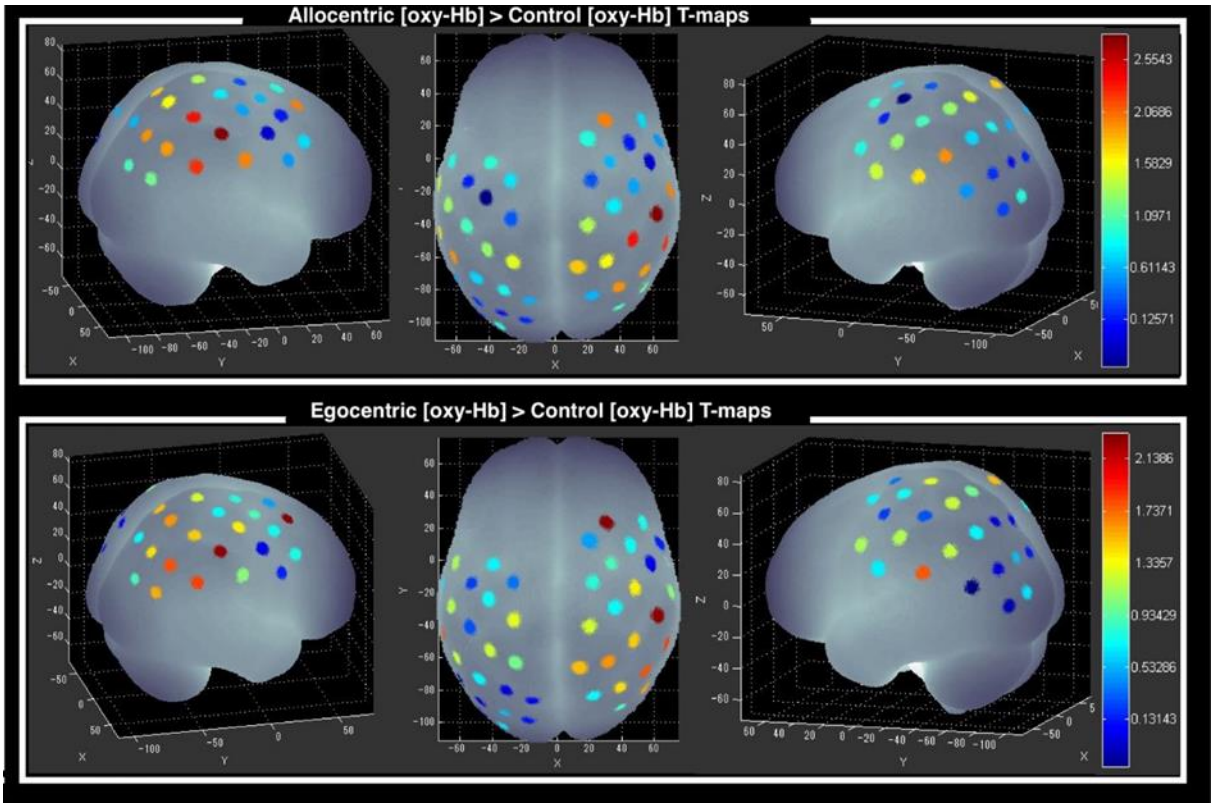

Figure 3. 5. Channel-specific fNIRS plot on the right and left hemispheres for both the allocentric and egocentric conditions. Note: t-values are group-based O2-Hb mapped on the channels 1 to 44 for allocentric > control and egocentric > control comparisons.

We explored correlations of the aSC minus Control or eSC minus Control O_2-Hb concentration changes among the channels. The aSC condition's right hemisphere showed significant positive correlations between the channels in the right frontal region (channels 2, 10, and 14) and those in the right parietal region at the right SPL (channels 12 and 16) ($p < .01$; Figure 3.6). Significant negative correlations were observed between a cluster of channels in the right frontal regions at MFG (channels 10 and 14) and SFG (channels 1 and 2) and those channels in the right parietal region (channels 9, 13, and 21) ($p < .01$). In the left hemisphere, similar positive correlations were revealed between a cluster of channels in the left precentral gyrus (channels 27, 36, 37, and 41) and in the left parietal regions at the SPL (channels 38, 43, and 44) and the IPL (channels 24, 29, and 39) ($p < .001$ to .01). Another clusters of channel correlations were between the left SFG (channel 41) and the left parietal region (channels 24 and 29) ($p < 0.001$). For the eSC condition, significant frontal to parietal channel correlations were found between the frontal region (channels 2, 10, and 14) and the SPL (channels 12 and 16) ($p < .01$; Figure 3.7). In the left hemisphere, the frontal to parietal correlations were between the precentral gyrus (channels 27, 36, 37, and 41) and the SPL (channels 38, 43, and 44; $p < .01$) and IPL (channels 24, 29, 39; $p < .001$); and between the SFG (channel 41) and the parietal region (channels 24 and 29; LH: $p < 0.001$).

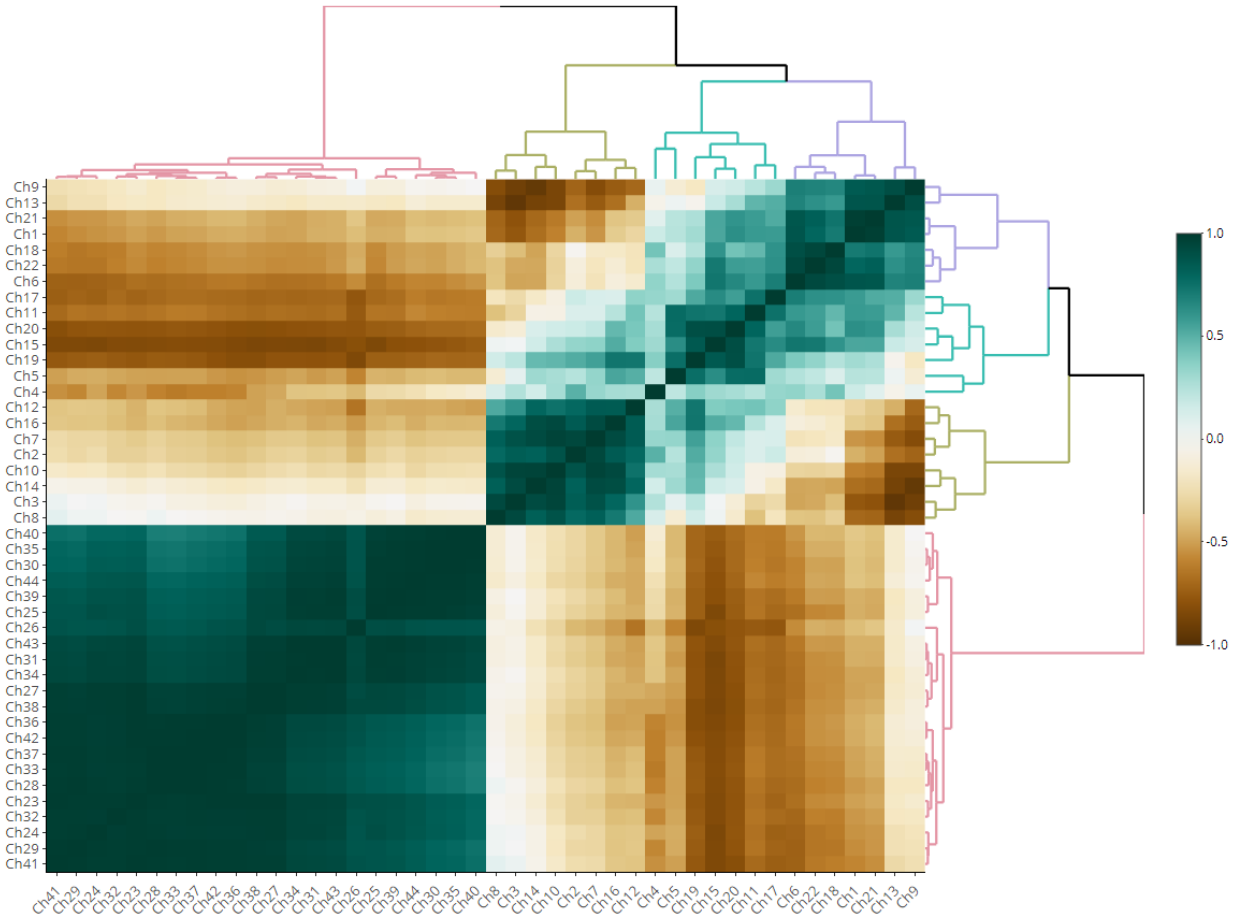

Figure 3. 6. Correlational matrix of channel-specific change in O2-Hb concentration of Allocentric > Control condition. Hierarchical clustering is used to group the correlation coefficients.

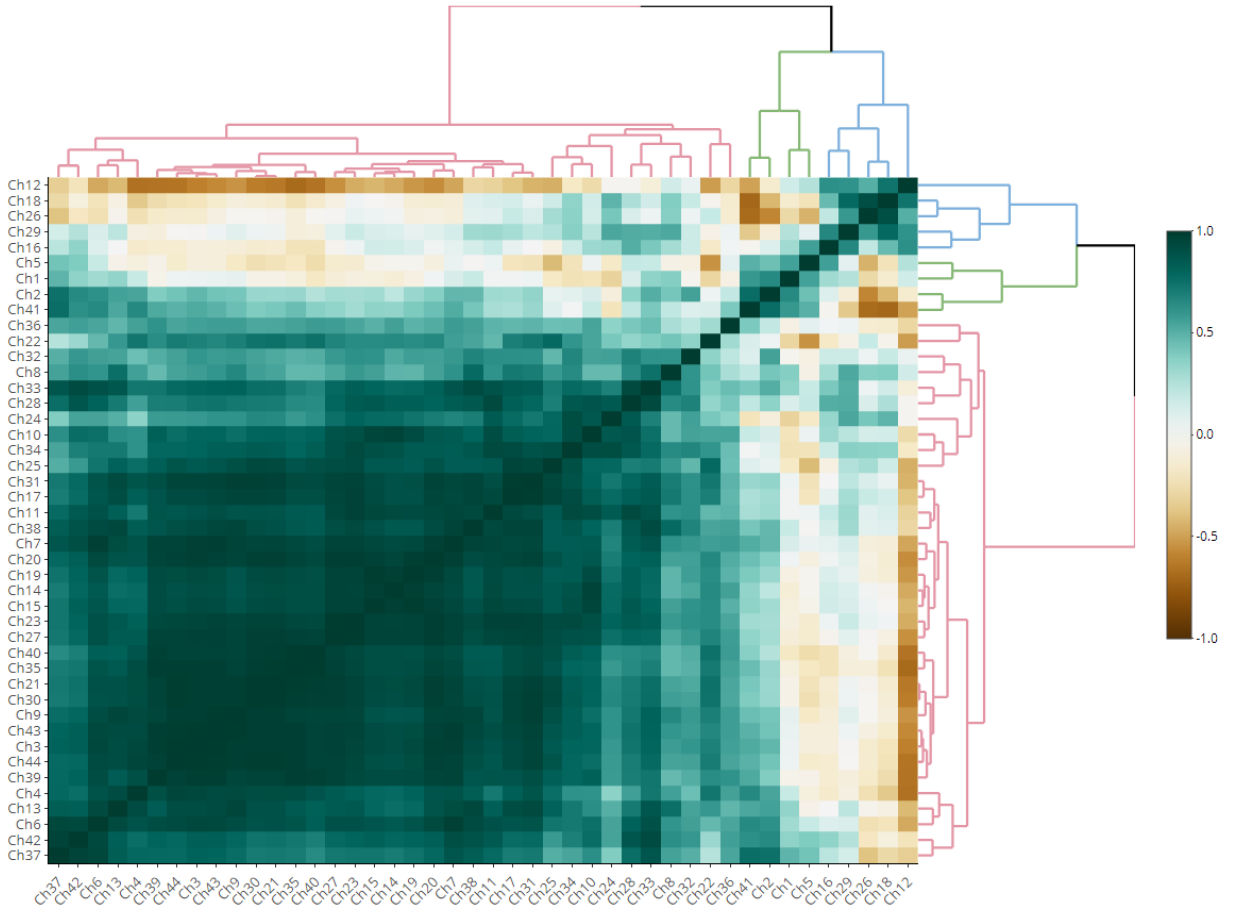

Figure 3. 7. Correlational matrix of channel-specific change in O2-Hb concentration of Egocentric > Control condition. Hierarchical clustering is used to group the correlation coefficients.

3.3.3. LASSO-RPC Regression

The regression model built for the aSC condition included six channels, which explained 59.5% of the total variance (Table 3.1a). Among them, the changes in the O_2-Hb concentration in two channels significantly predicted the RTs. Channel 2 corresponded to the right SFG F (6, 17) = 6.63, p = 0.04, and channel 27 corresponded to the left precentral gyrus (PG) F (6, 17) = 6.63, p = 0.038. In contrast, the model built for the eSC condition included eight channels, which explained 54.1% of the total variance (Table 3. 1b). Among them, all three significant channels predicting the RTs were in the right hemisphere: channel 1 F (8, 15) = 4.38, p = .029 and channel 5 F (8, 15) = 4.38, p = .002 corresponded to the right SFG. Channel 22 F (8, 15) = 4.38, p < .001 corresponded to the right IPL's caudal part and the right middle temporal gyrus (MTG).

Table 3. 1. Summary of LASSO-RPC regression of changes in O_2-Hb concentration in fNIRS channels predicting RTs in allocentric and egocentric conditions.

	Estimate	Std. Error	t-value	*p*-value	MNI Coordinates	Anatomical Labelling
a. Allocentric SC						
Ch.26	-38.00	43.51	-0.87	.394	-44, -91, 5	MOG (L)
Ch.27	-242.90	108.45	-2.24	.038*	-60, -2, 41	PG (L)
Ch.02	281.97	126.77	2.22	.040*	21, -13, 76	SFG (R)
Ch.04	179.01	96.27	1.86	.080	14, -64, 71	SPL (R)
Ch.05	-62.25	41.38	-1.50	.150	30, 22, 62	SFG (R)
Ch.06	-76.29	147.18	-0.52	.610	32, -2, 68	SFG (R)
b. Egocentric SC						
Ch.26	-98.84	108.02	-0.92	.374	-44, -91, 5	MOG (L)
Ch.31	-39.14	172.14	-0.23	.823	-32, -99, 11	MOG (L)
Ch.36	-231.55	127.13	-1.82	.088	-38, -3, 65	PG (L)
Ch.01	-327.73	136.33	-2.40	.029*	20, 12, 71	SFG (R)
Ch.05	770.58	215.26	3.58	.002*	30, 22, 62	SFG (R)
Ch.14	-161.74	229.72	-0.70	.492	51, 23, 44	MFG (R)
Ch.15	-127.62	235.01	-0.54	.595	56, -2, 53	PoG (R)
Ch.22	477.39	111.12	4.29	<.001	52, -76, 26	pIPL (R)

Note. *p<.05. MNI=Montreal Neurological Institute. MOG = middle occipital gyrus. PG = precentral gyrus. SFG = superior frontal gyrus. MFG = middle frontal gyrus. pIPL = posterior inferior parietal lobule. SPL = superior parietal lobule. PoG = postcentral gyrus.

3.4. Discussion

The custom-designed cue-to-target paradigm revealed various cortical activity patterns for allocentric and egocentric spatial coding. First, the predictive model based on the O_2-Hb concentration changes suggested that cortical activities happen in the right SFG. The cortical activities in the bilateral IPL, including the PoG, were also common to both types of spatial coding, but bilateral activities for allocentric spatial coding were only compared to the right hemispheric activities for the egocentric condition. They suggested a possible top-down attention shift, maintenance (i.e. IPL), and response mapping (i.e. SFG) occurred in both spatial coding types. The common cortical activities supported this study's first hypothesis set that aSC and eSC would both involve the dorsal attention network. Cortical activities unique to allocentric spatial coding were in the left IPL, the right TPJ, the right caudal parts of the IPL, the right IPS, and the left PG for allocentric—these were not observed in egocentric spatial coding. These results suggested the plausible involvement of additional visuospatial memory and updating (i.e. precuneus) (Wolbers, Hegarty, Büchel, & Loomis, 2008) and maintaining object-directed actions (i.e. IPS) (to maintain object-directed actions; James et al., 2002).

This study's cue-target paradigm involved orienting attention and attention control. The behavioral results showed that the allocentric spatial coding had longer RTs than the egocentric spatial coding. Egocentric spatial coding is location based, so the longer RTs suggest that the position-based processing in the allocentric spatial coding might have involved additional steps in the cue-to-target process. Our results are comparable to previous studies in which tasks had an orienting component in the cue phase (Barrett et al., 2001; Brian, 2014). However, the results differ

from two other studies that embedded similar cognitive processes but found no significant between-condition differences in RTs (see e.g.: Committeri et al., 2004; Kozhevnikov, Motes, Rasch, & Blajenkova, 2006). The inconsistent results are perhaps due to the difference in the task rules. In Committeri et al. (2004) and Kozhevnikov et al. (2006), the navigation of spatial locations was based on the fixed target-mapping rules set at the beginning of the task condition, compared with the time-locked trial-by-trial rule informed by this study's cue.

The activities in the SFG were the strongest predictor of the subjects' task performances in the allocentric and egocentric conditions. In the montage, the SFG corresponds to the SFG's posterior subregion (SFGp), which mediates motor control in sensorimotor-related tasks (Li et al., 2013). Besides, the SFG involves control attention pertinent to location when the cue was time locked to the anticipation of the upcoming target stimuli (Corbetta & Shulman, 2002; Hopfinger, Buonocore, & Mangun, 2000). The activities in the SFG suggested that attention control and stimulus-response mapping processes are neural processes common to both types of spatial coding. The other regions involved in both types were the IPL and PoG, which were reported as parts of the "task positive network" (Fox et al., 2005). Together with SFG, IPL related to attention control of cue stimuli (Noudoost, Chang, Steinmetz, & Moore, 2010). The PoG—which includes SMA, SEF and pre-SMA—mediates vigilance for visually guided task-switching (Nachev, Kennard, & Husain, 2008) and responses to target stimuli (Ptak, 2012). Our findings reinforce findings reported in previous studies that had both spatial coding types with task-taking processes involving stimulus-response mapping and responses to target stimuli in addition to attention control (e.g. Fink et al., 2003; Liu et al., 2017; Neggers et al., 2006; Saj et al., 2014).

The main differences between the two spatial coding types were in the results of the right TPJ and the left PG. The fNIRS results showed significant cortical activities in the TPJ, the IPS, and the PG in the allocentric condition—but not in the egocentric condition. The TPJ reportedly plays a major role in mediating reorienting attention (Corbetta, Kincade, Lewis, Snyder, & Sapir, 2005; Krall et al., 2015). Compared to egocentric spatial coding, our results suggest that allocentric spatial coding would have demanded more reorienting attention when encoding the spatial relationships among objects. In this study, subjects engaging in the allocentric trial were required to identify the distractor-target triad, of which the locations were at least a 45° angled distance from the cued location. Participants had to reorientate their attention to capture the new positions of the distractor-target triad before making a response. The significant results for the cortical activities in the caudal parts of IPL (aka angular gyrus) (channels 17, 21 and 22) supported our proposition that the reorienting attention process is unique to allocentric spatial coding. Angular gyrus, as part of the task-negative network (Fox et al., 2005), mediate the manipulation of mental representation and reorient attention to relevant information.

The main discrepancies between our study's results and those of Szczepanski et al. (2013) are the latter not revealing the involvements of TPJ and SPL in the allocentric condition and the IPL in the egocentric condition. For TPJ and IPL, our results align with those of a previous study (review: Kravitz et al., 2011), suggesting that updating visuospatial information was a process in both spatial coding conditions. The SPL results indicated that maintaining a working memory during top-down processing (Corbetta & Shulman, 2002) may be unique to allocentric—but not egocentric—spatial coding. Nevertheless, the discrepancies in Szczepanski et

al. (2013) results may have resulted from the difference in the two studies' task designs. A future study could verify this speculation.

This study has several limitations, and readers should interpret the results with caution. First, the experimental task was more complex than the tasks employed in other spatial coding studies, particularly in identifying the target among the distractors. A generalization of the results must consider the task-specific differences. Second, the NIRS method captures cortical activities that occurred superficially to the cortex (2–3 cm below the scalp) (Toronov et al., 2001), so activities emitted from deeper neural structures (such as those from MTL) could have been excluded in this study. Third, due to the limited coverage by the fNIRS probe montage adopted in this study, activities not emitted from the dorsal aspect of the scalp might have been missed, such as those from the middle temporal cortex. Last, but not least, is the block design used to group the same spatial coding trials that could have inflated biases due to the task-taking strategies adopted by the participants. A future study should test the results' robustness by using a similar test design but varying the task's difficulty. Other methods of brain imaging, such as functional magnetic resonance imaging, and an event-related design should be used to explore the possible involvement of other brain structures in spatial coding.

To conclude, this study's results revealed similarities and differences between the allocentric and egocentric spatial coding processes. The similarities rest with the cortical activities in the SFG and IPL, including PG, suggesting that both spatial coding types involve attention control and stimulus-response mapping. The dissociation between the two types of spatial coding exists in the cortical activities in the left IPL, the IPS, and the right TPJ, suggesting that a

reorienting of attention and visual working memory are involved in allocentric but not egocentric spatial coding. The findings offer a plausible explanation for individuals' difficulties in performing allocentric spatial coding but not egocentric spatial coding. Older individuals with neurodegeneration (Colombo et al., 2017; Lithfous, Dufour, Blanc, & Després, 2014) reportedly to present with decline performances in allocentric but not egocentric spatial coding tasks. Future studies should test the robustness of the uniqueness of allocentric and egocentric spatial coding by employing visuospatial tasks with different designs. Studies involving post-stroke patients with specific brain lesions could inform the application of spatial coding tests in clinical practices.

CHAPTER 4

4. Model of Spatial Coding: A Revisit

The meta-analyses conducted on previous fMRI studies reported in Chapter 2 indicate common and unique neural substrates associated with the two types of spatial coding. The between-type convergence was in the superior occipital gyrus for allocentric spatial coding and the middle occipital gyrus for egocentric spatial coding. The between-type common convergence was in the right precuneus and the right superior frontal gyrus. The results also revealed that the design of the task paradigms used for eliciting the spatial coding processes showed effect on the allocentric but not egocentric spatial coding. The results reported in Chapter 3 are found to corroborate with those in Chapter 2. Using a fine-grained cue-to-target paradigm and functional near-infrared spectroscopy (fNIRS) revealed that the between-type differences were in the left precentral gyrus (PG), intraparietal sulcus (IPS), and angular gyrus for the allocentric spatial coding and the right IPL for the egocentric spatial coding. Common neural activities were found located in the right superior frontal gyrus (SFG) and in the post-central gyrus (PoG) for both spatial coding types. Consistent results presented in the two chapters suggested that spatial coding involves top-down attention, encoding visual representation, and response-mapping processes, which is sub-served by neural substrates in the parieto-frontal regions, whereas functional dissociation of the two spatial coding types were observed in parieto-occipital circuits (Figure 4.1).

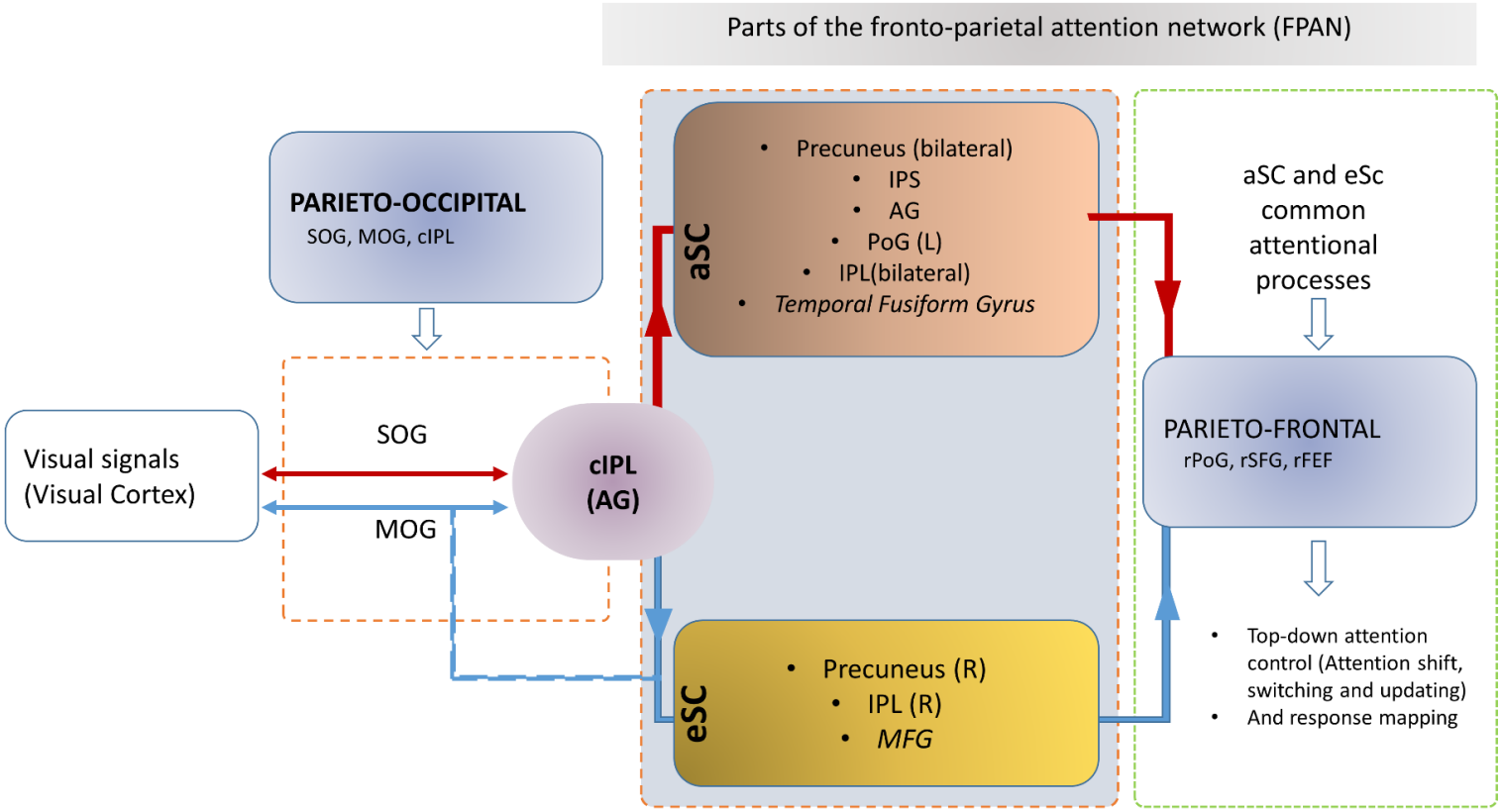

Figure 4. 1. Collated model of spatial coding. The signals projected from visual cortex feedforward to the caudal parts of the IPL (AG) via SOG for aSC and via MOG for eSC. SOG and MOG may have carried the feedforward and feed-backward loops representing aSC and eSC respectively. cIPL mediates the feedforward and feed-backward loops in aSC and eSC signals equally, and serve as a

circuit-breaker for aSC only. MOGs eSC signal may have bypassed the cIPL and directly projected to precuneus for example (indicated in broken blue line). It updates based on its top-down attention allocation and further processed and projected encoded signals involving IPS, IPL, AG, PoG, and task-specific signals to temporal fusiform gyrus for allocentric and precuneus, IPL and task-specific signals to middle frontal gyrus for egocentric. Both aSC and eSC integrates for its respective top-down attention control and response mapping involving common parieto-frontal regions (PoG, SFG, and FEF). Note: aSC=allocentric spatial coding; eSC=egocentric spatial coding.

4.1. Functional Networks of Spatial Coding

The common involvement of the fronto-parietal region, identified as the dorsal attention network, in both aSC and eSC suggest that spatial coding is dominated by top-down attention shift and maintenance (by the IPL), and response mapping and attention control (by the SFG) processes. The proposition that aSC is likely to involve additional visuospatial memory, updating processes, and maintaining object-directed actions than eSC is supported by the unique activations in the right TPJ (comprising SOG and caudal parts of IPL) and the right IPS. The importance of the caudal parts of the IPL (AG) to the task relevant nodes of functional and structural connections to the key neural regions subserving aSC as deliberated in Chapter 1 and 3 and in line with the three theoretical framework is re-visited below.

4.1.1. The Caudal Parts of IPL (AG) As A Nexus to the Feed-Forward and Feed-Backward Loops

The caudal part of IPL (cIPL), also known as angular gyrus (AG) has been found to mediate visuospatial attention particularly conveying and integrating visual signals (Seghier, 2013). The cIPL is also structurally connected to the parieto-frontal and the occipito-tempo-frontal projections (Seghier, 2013; Uddin et al., 2010). According to Kravitz et al. (2011), the three sub-pathways of the dorsal attention network are connected to the cIPL: parieto-prefrontal, parieto-premotor, and parieto-medial temporal sub-pathways. They are associated with the spatial working memory, visual-guided behaviour, and navigation processes respectively. To be specific, the parieto-premotor sub-pathway (involving MIP, dPMC, VIP, and SMA) mediates object in space for forming an egocentrically visuospatial map. The parieto-medial sub-pathway (involving PCC, RSC, MTL, and parahippocampal cortex) is to mediate allocentric spatial coding (Byrne et al., 2007; Crowe et al., 2008; Ekstrom et al., 2014). The parieto-prefrontal sub-pathway (LIP, VIP, MT and MST) is to mediate spatial working memory. The evidence gathered in Chapter 2 and 3 indicates that cIPL is common to both spatial coding types as it connects to key neural substrates such as IPS and FEF in the dorsal attention network. The cILP also serve as the marker for dissociating aSC and eSC as described under Kravitz et al.'s sub-pathway architecture parieto-occipital and the shared parieto-frontal circuits were mainly mediated by the cIPL (Figure 4.1.). Functionally, the two division of cortical visuospatial processing into distinct dorsal and ventral attention networks shown to initiate from cIPL (Kravitz et al., 2011).

A good way to understand the role of cIPL is to investigate its structural connectivity within the neural system. Structurally, the cIPL is connected with IPS and FEF within the dorsal attention network via the splenium corpus callosum (SPN) (Park et al., 2008), with the frontal and opercular cortex via the SLF (Makris et al., 2005), with the posterior division of STG via the middle longitudinal fasciculus (MLF) (Frey, Campbell, Pike, & Petrides, 2008), and with the SFG via the occipitofrontal fasciculus (Makris et al., 2007). The left and right IPL is connected via splenium of the corpus callosum (SPN) (Park et al., 2008). As Figure 4.2. shows, the fibre tract passing through inferior and middle longitudinal fasciculus (ILF and MLF) and ILF connects IPL with SOG, MTG, and ITG; inferior occipitofrontal fascicle (IOF) connects IPL with precuneus and SFG via caudate; SLF connects IPL with MFG and IFG (Seghier, 2013). The potential overlaps of neural substrates between the parieto-premotor and parieto-medial sub-pathways support the notion that the neural processes associated with egocentric spatial coding could be part of those in allocentric spatial coding (Galati et al., 2000; Kravitz et al., 2011; Zaehle et al., 2007). The evidence highlighted above suggested that cIPL, as a circuit-breaker for aSC and feedforward and feed-backward (Figure 4.1) functional mechanisms for both aSC and eSC, are heavily relied on the scaffolding of structural connectivity projected to the near and far brain regions (Ptak, 2012; Seghier, 2013). The intricacy of the connectivity involving cIPL also accounts for the functional dissociation of aSC and eSC.

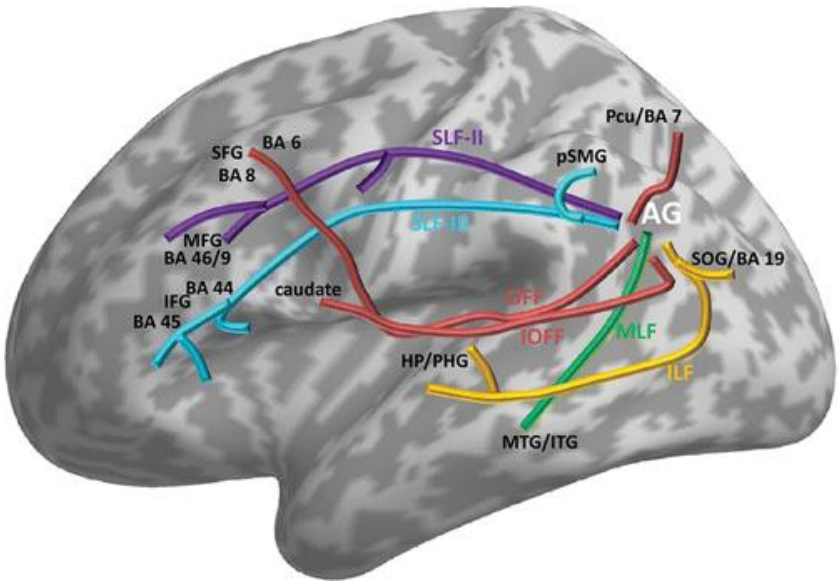

Figure 4. 2. Schematic illustration of structural connectivity of the AG (cIPL) to the near (e.g. precuneus, SOG, and pSMG) and far regions (e.g. SFG and MFG) of the white-matter and gray-matter content of the brain. SFG = superior frontal gyrus. MFG = middle frontal gyrus. IFG = inferior frontal gyrus. Pcu = precuneus. pSMG = posterior division of the supramarginal gyrus. AG = angular gyrus. MTG = middle temporal gyrus. ITG = inferior temporal gyrus. HP = hippocampus. PHG = parahippocampal gyrus. SOG = superior occipital gyrus. BA = Brodmann area. SLF-II = superior longitudinal fasciculus–tract second. SLF-III = superior longitudinal fasciculus–tract third. MLF = middle longitudinal fasciculus. IOFF = inferior occipitofrontal fascicle. OFF = occipitofrontal fascicle. ILF = the inferior longitudinal fascicle. Adopted from Seghier (2013; p. 46, Fig. 2), The Neuroscientist, 19(1), 43-61. Copyright 2013 by Sage Publications.

Both aSC and eSC share the fronto-parietal attention network (FPAN) (Figure 4.1). Functional connectivity during visuospatial attention within the FPAN has been shown to be mediated by the fibre tracts passing through the SLF (Ptak & Schnider, 2010) (Vaessen, Saj, Lovblad, Gschwind, & Vuilleumier, 2016). Top-down attention processes, which is crucial to both the spatial coding types, relies heavily on the structural integrity, particularly the PPC function and the feedforward loops in projecting the signals towards frontal regions (Ptak, 2012). Reaction times (RT) during visuospatial task has been associated with the functional connectivity within the core nodes of the FPAN (Prado, Carp, & Weissman, 2011). Taken together, the differences in the RTs between the eSC and aSC conditions reported in Chapter 3 suggest potential differences in the functional connectivity underpinned by the respective structural connectivity/integrity unique to the different spatial coding types. The differences in the structural connectivity between eSC and aSC and their contributions to the respective functional connectivity and behavioral responses and whether age-related changes in WM integrity could be accounted for age-related changes in aSC and eSC could are the key questions to be asked in Chapter 5 of this thesis.

4.1.2. Structural-Functional Interplay in Spatial Coding – An Integrated Model

To recap, aSC and eSC are functionally dissociative in the parieto-occipital circuits and sharing similar parieto-frontal regions along the FPAN. As mentioned in the previous section, cIPL serves as a feedforward and feed-backward loop connecting the parieto-occipital and parieto-frontal in both aSC and eSC. Besides, the cIPL is a circuit-breaker for the feedforward signals in aSC for specialized brain areas including to the ventral attention network (VAN). Efficient functional modulations of the FPAN has been shown to relate to the structural connectivity within

the network (Burzynska et al., 2013; Chechlacz, Gillebert, Vangkilde, Petersen, & Humphreys, 2015). The structural-functional relationship has been demonstrated in studies showing efficient modulation of visuospatial attention was associated with involvement of fewer number of neural substrates or nodes activated within the structural network (Burzynska et al., 2013; Chechlacz et al., 2015; Neubauer & Fink, 2009). The study of the functional and structural nodes of the cIPL (AG) would further inform the common and distinct neural mechanisms of aSC and eSC. In particular, depicting the interactions between the white matter (WM) integrity and gray matter (GM) functions can help building an enhanced model of spatial coding which deliberate further on the roles of cILP in the feedforward (to parieto-frontal circuits) and feed-backward (to parieto-occipital) loops of the two spatial coding types.

4.1.3. Test on Robustness of an Integrated Model of Spatial Coding – Aging Effect

Ageing is characterized by degeneration of white matter integrity, demyelination and axonal loss, altering the projection of neural signals to near and far brain regions (Maniega et al., 2015; Sullivan, Rohlfing, & Pfefferbaum, 2010). Exploring how the aging effects would impact on the functional-structural interplay built from the younger participants would gain further insights into the robustness of the proposed enhanced model for spatial coding. Age-related changes of the fibre bundles, as indexed by fractional anisotropy (FA) - a marker of brain WM integrity, would inform how the nodes of the distributed task-relevant networks could have modulated the efficiency of the functional connectivity for mediating visuospatial attention in eSC (Tuch et al., 2005; Westlye, Grydeland, Walhovd, & Fjell, 2011), and for mediating visuospatial working memory in aSC (Fjell et al., 2016; McNab et al., 2015).

The myelinated fibre bundles of SLF, as indexed by the fractional anisotropy (FA), have been correlated with neural activities in FPAN during visuospatial attention (Vaessen et al., 2016). Age-related changes in orienting and re-orienting was associated with the disruption of WM integrity in the SLF and ILF (De Schotten et al., 2011). WM integrity in SLF and ILF have been associated with slower RT among older adults (Bennett, Motes, Rao, & Rypma, 2012). SLF and ILF fibre tracts affected more prominently the PFC which was associated to reduced capacity in reorienting (attention control) and in PPC related to orienting to a task relevant stimuli (Grady, 2012). Putting together, these studies suggested processing of visuospatial attention in ageing relies on the complex structure-function interactions along the FPAN. Therefore, illuminating the comprehensive structure-function association during spatial coding tasks and whether age-related differences in WM integrity accounts for the difference in GM allocentric and egocentric-function will inform the enhanced model.

To test the enhanced spatial coding model and the robustness of the model in ageing, Chapter 5 is to use a combined diffusion tensor imaging (DTI) and functional magnetic resonance imaging (fMRI) data from 27 younger adults and 24 older adults.

CHAPTER 5

5. Functional and Structural Architectures of Allocentric and Egocentric Spatial Coding: The Effect of Aging

5.1. Introduction

Visuospatial functions such as those mediated by the fronto-parietal attention network (FPAN) rely on how the near and far neural nodes are connected by the white-matter (WM) tracts (Burzynska et al., 2013). Degeneration of WM integrity, demyelination and axonal loss due to normal aging have been found to impact on the functional connectivity of the FPAN (Bennett et al., 2012; Madden et al., 2007; Sullivan et al., 2010). In other words, normal aging is supposed have negative impacts on the neural structure as well as the neural functions. In spatial coding, it was found that aging tended to modulate the key neural signals sub-serving the allocentric but not the egocentric type (Colombo et al., 2017). Putting this together with the enhanced functional model presented in Chapters 2 and 3, the study described in this chapter is to add WM integrity to the functional model for exploring the structure-function architecture based on younger subjects for mediating spatial coding. The younger model will then be compared with that constructed based on older subjects. The results will shed light on the variability of the structure-function architecture due to the aging-effect and hence inform the robustness of the integrated model proposed for theorizing allocentric and egocentric spatial coding.

The occipito-parietal circuit, the caudal part of the inferior parietal lobule (cIPL), has been revealed to mediate both egocentric and allocentric processing along with the frontoparietal attention network (FPAN) (Kravitz et al., 2011; Zaehle et al., 2007). The signals reaching cIPL

(also known as angular gyrus, AG) are to project to the parieto-premotor and parieto-medial temporal pathways (Kravitz et al., 2011). The parieto-premotor pathway is to encode object in space in an egocentric map. The core neural substrates underlying the parieto-premotor pathway are the cIPL, superior parietal lobule (SPL; including IPS), somatosensory motor area (SMA), and FEF (Fattori et al., 2010; Galletti et al., 2001; Kravitz et al., 2011). The parieto-medial temporal pathway, on the other hand, is to encode visual inputs in allocentric map (Kravitz et al., 2011). The key neural substrates of the parieto-medial temporal pathway are cIPL (area PG) (Chafee et al., 2007; Crowe et al., 2008), posterior cingulate cortex (PCC) (Hashimoto et al., 2010), and the retrosplenial cortex (RSC), temporoparietal junction (TPJ), and medial temporal lobule (MTL) (Erel & Levy, 2016; Vann et al., 2009).

The core neural substrate of interest is cIPL which forms strong connection with the posterior cingulate cortex (PCC) and TPJ. The TPJ plays a major role in mediating reorienting attention (Corbetta et al., 2005; Derbie et al., 2021; Krall et al., 2015). Compared to egocentric spatial coding, our results suggest that allocentric spatial coding would have demanded more reorienting attention when encoding the spatial relationships among objects. The PCC has been proposed to mediate the cIPL for transforming inputting information into allocentric representations (Byrne et al., 2007). Besides, PCC is also suggested to mediate shifting the spatial attention during allocentric spatial coding (Byrne et al., 2007; Hopfinger et al., 2000; Kravitz et al., 2011). Disruption of structural integrity of cIPL would have an impact on allocentric spatial coding particularly on the formation of the spatial representation process. The fibre tracts connecting cIPL with other spatial coding related neural substrates are the inferior and middle longitudinal fasciculus (ILF and MLF), and the inferior occipitofrontal fascicle (IOF). The inferior

frontooccipital fasciculus (IFOF) has been found to disrupt the function of cILP and hence allocentric spatial coding (Chechlacz et al., 2010; Ptak & Schnider, 2010; Vaessen et al., 2016). These fibre tracts will be tested for their involvements in forming the structure-function architecture of spatial coding.

Superior longitudinal fasciculus (SLF) is the main fibre tract which has been reported to facilitate functional connectivity among the near and far neural nodes of FPAN (Ptak & Schnider, 2010) during visuospatial attention (Vaessen et al., 2016). Previous studies showed consistent evidence on aging effects on FPAN were disruptions on the optimal balance among these neural nodes (Erel & Levy, 2016) (Bennett et al., 2012) (De Schotten et al., 2011; Prado et al., 2011). These disruptions resulted in compromised alerting (Gola, Kamiński, Brzezicka, & Wróbel, 2012), orienting (Gamboz, Zamarian, & Cavallero, 2010), and attention control functions (Turner & Spreng, 2012). Other fibre tracts which have been showed to be sensitive to aging effect and visual and visuospatial attention include splenium of the corpus callosum (SPN) (Madden et al., 2007), the right posterior thalamic radiation (PTR) (Tuch et al., 2005), the bilateral inferior longitudinal fasciculus (ILF) (Bennett et al., 2012), the anterior corona radiata (ACR) (Yin et al., 2013), and the posterior corona radiata (PCR) (Yin et al., 2009). The anterior corona radiata (ACR) was related to aging effect on modulating attention control (Niogi et al., 2008). Together with MT, the ACR was found to strongly linked to the disruption of the feedforward and feedback loop of signals projected to the frontal eye-fields (FEF) and LPFC (Amso & Scerif, 2015). These fibre tracts henceforth will be added to the exploration of the structure-function relationships in this study.

Studies revealed aging effects modulated allocentric but not egocentric spatial coding (Colombo et al., 2017; Harris & Wolbers, 2014; Rodgers, Sindone III, & Moffat, 2012). The impact on allocentric spatial coding may be due to the age-related deterioration of the functional connectivity between LPFC and parietal regions (Grady, 2012) particularly when allocentric processes involve visual short-term memory (Montefinese, Sulpizio, Galati, & Committeri, 2015). Another possibility is the age-related decline in the PCC which mediates the strategies in the retrieval (recent review: Colombo et al., 2017) and transformation of the visual representations for forming an allocentric map (Boccia, Sulpizio, Nemmi, Guariglia, & Galati, 2017; Byrne et al., 2007; Kravitz et al., 2011). With these in mind, this study will test the aging effects on SPL, PCC, MTL, and LPFC for influencing the structure-function relationships for spatial coding.

This study is to enrich the current neural model of spatial coding by comparing the structure-function relationships between those built from younger subjects with those built from healthy older subjects. Based on the previous findings that aging effect would have stronger impacts on allocentric than egocentric spatial coding, the comparisons between the two subject groups are expected to provide additional evidence on the on the enhanced and integrated neural model spatial representations. The theoretical underpinning is that the cIPL receives visuospatial information from the posterior regions of the brain, which couples with attentional feedforward and feed-backward processes. These processes are proposed to be mediated by the LPFC, PCC, MT/ST for allocentric, but be mediated by the FEF, IPS, and LPFC for egocentric. Given that ageing is likely to modulate activations of the MTL and LPFC, the between-group comparisons will show differences in the feedforward and feed-backward loops in the FPAN network, and the relationships between the functional connectivity among these neural substrates and its interaction

with structural integrity among the longitudinal WM tracts, i.e. ILF, IFOF, SLF and to those non-longitudinal WM tracts in ACR, SPN, PCR, and anterior thalamic radiation (ATR). The hypotheses set for this study are:

1. There would be differences in the structural integrity and connectivity associated with the neural activations mediating the feedforward and feed-backward loop between aSC and eSC spatial coding. It is anticipated that eSC would recruit the WM tracts in the parieto-frontal regions (i.e. IPS-FEF), while aSC would extend the WM tracts to those located in the LPFC and superior temporal regions. The integrity and connectivity of the involved WM tracts would differentially relate to the functional connectivity associated with aSC or eSC.
2. Functional connectivity among PCC, MT and LPFC in the older group would be different from that in the younger group. The decline in the aSC-related functional connectivity in the older group would be relate to the decrease in the structural integrity of the ILF, SLF, ACR and SPN. The structure-function relationships observed in aSC however would not occur in eSC in the older group.

5.2. Methods

5.2.1. Participants

The total sample size in this part of the study was 51. Twenty-seven of them were younger adults (mean age 22.37, SD = 0.88, 18 female) and 24 were older adults (mean age 68.29, SD = 3.59, 13 female). All subjects were right-handed and had normal or corrected-to-normal vision. All of them were screened with the Chinese version of Montreal Cognitive Assessment (MoCA;

Lu et al., 2011). The optimal cut-off score set for individuals with one to six years of education was 19/20 and that for individual with seven and above years or above education was 24/25, suggesting without obvious cognitive dysfunction. Ethical approval was obtained from the ethics committees of the Rehabilitation Hospital, Fujian University of Traditional Chinese Medicine and written informed consent was obtained from all subjects prior to the experiment.

5.2.2. The Experimental Paradigm

The cue-to-target paradigm was adapted from the task used in Wilson, Woldorff, and Mangun (2005) for initiating the aSC and eSC processes. The design of a trial follows presentation of a cue screen, a stimulus-onset asynchrony (SOA) for a fixed duration, and then a target screen (Figure 5.1A). The cue screen shows a Chinese character located at the center for 350 ms that indicates the potential position of the target to be presented later in the trial (e.g. Figure 5.1B). The character is "L" (left, 左) or "R" (right, 右) indicating the likelihood that the target would appear on the left or right side of the screen/stimulus window respectively (see below). The cue character also informs the subject the type of spatial coding processes required in the trial, with the italic font (*L*, *左*) or (*R*, *右*) indicates an eSC condition and the regular font indicates an aSC condition. Besides the cue, the screen also shows three stimulus-windows: two squares (subtended 3.75° vertically and horizontally to the center) and one rectangle (displayed at 3.75° vertically and 12.2° horizontally to the center). All the stimulus-windows are empty during the cue phase. The second screen is SOA shows a dot which replaces the cue character. The target screen lasts for 1500 ms during which one target and three distractors will appear inside the three stimulus-windows. The rectangular shape stimulus-window is at the upper part of the screen, contains the target in an aSC

condition, will appear on the left or right side of the screen. The window is further divided into three equal parts, with the two ends presents either a target (a [+] sign) or a distractor (an [*] sign). The two squared stimulus-windows are at the lower part of the screen, contains the target in an eSC, in fixed left and right locations. Similar to aSC, each window will contain the same target or distractor depending on the types of trials. In an aSC condition, after the presentation of the cue and the SOA screen, the target will appear in the left or right end of the rectangular stimulus-window. The subject regardless of the left or right position of the window on the screen was to indicate the location of the target with reference to the position within the stimulus-window. The response was made by pressing 'Z' (for left) or 'M' (for right) button on a MRI-compatible keyboard with the right index or middle finger respectively. Inter-trial intervals were set at 500, 2500, or 4500 ms randomized among all the trials within one block. To avoid attention biases, both the rectangle and squares were counterbalanced for both conditions.

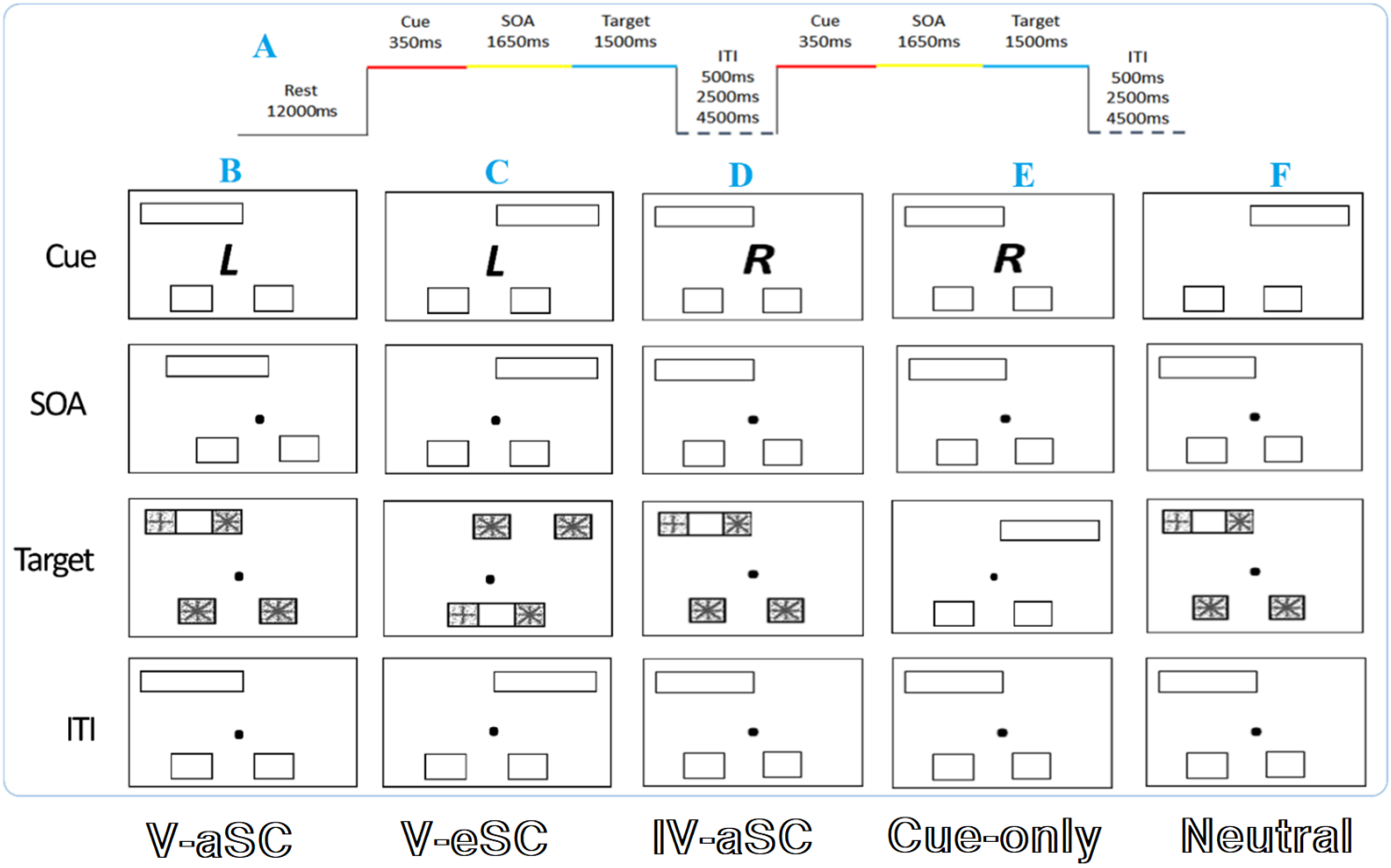

Figure 5. 1. The experimental paradigm and timing parameters. (A) Overall design and time sequence; (B) Valid allocentric trial is the position indicated by the cue is consistent with the position of the target appeared in the rectangular stimulus-window; (C)

Valid egocentric trial is the position indicated by the cue is consistent with the position of the target appeared in one of the squared stimulus-window; (D) Invalid allocentric trial is the position indicated by the cue is not consistent with the position of the target appeared in the rectangular stimulus-window; (E) Cue-only trial is the cue presented does not follow by presentation of target and distractors; (F) Neutral trial is no cue is presented but followed by presentation of target and distractors. Note: The cues ("L" and "R": left and right) is enlarged for better illustration. In actual experiment, "L" and "R" were replaced with "左" and "右" respectively. The stimuli displayed in here are in reversed contrast and the actual appearances in the experiment were white figures on a black background. SOA = stimulus onset asynchrony. ITI = inter-stimulus interval. ms = milliseconds.

There are four types of trials in the cue-to-target paradigm. They are valid, invalid, neutral, and cue-only. For a valid trial, the position of the target is consistent with the information provided by the cue (Figure 5.1B and C). Consistent allocentric position means the location of the target is in the corresponding relative position as indicated by the cue within the rectangular stimulus-window regardless its position on the screen. Consistent egocentric position means the location of the target is in the corresponding position as indicated by the cue with reference to the bodily coordinates of the subject. For an invalid trial, the location of the target is not consistent with the information provided by the cue (Figure 5.1D). For a cue-only trial, after presentation of a cure, no target or distractor is presented inside the stimulus-windows after the SOA screen (Figure 5.1E). For a neutral trial, no cue is presented on the first screen, the SOA and target screen are presented as in other types of trials. There are 288 trials (144 valid, 48 invalids, 72 cue-only,

and 24 neutral) organized in three runs, with 96 trials in each run. The distribution of the trial types and cue types were counterbalanced across the runs. Each run lasted for 7 minutes and 50 seconds. The total duration for a subject to complete the paradigm inside the MRI scanner was 24 minutes including two one-minute rest periods in between the runs.

5.2.3. Procedure of Data Collection

To prepare for the functional MRI scan, the subject completed a training session to familiarize with the cue-to-target paradigm before entering in the scanner. The trials used for the training and the actual experiment were similar, except in the training session the response made by end of each trial was followed by a feedback indicating the correctness of the response. Subject had to achieve an accuracy rate of at least 80% before commencing the actual experiment. The MRI scan was conducted in the brain imaging laboratory of a rehabilitation hospital affiliated with the Fujian University of Traditional Chinese Medicine. Siemens Prisma 3.0 T MRI system with a 64-channel head and neck coil was used.

5.2.4. Functional Imaging - Data Acquisition and Pre-processing

Functional MRI was used to generate the data for contributing to the structure-function relationship for both the younger and older subjects. High-resolution structural T1-weighted images were acquired: echo time (TE) = 2.27 ms, repetition time (TR) = 2300 ms, field of view (FOV) = 250 × 250 × 240 mm^3, voxel size = 0.98 ×0.98× 1 mm^3, image matrix= 256 × 256). Functional images were acquired using a T2*-weighted echo planar imaging (EPI) sequence: TE = 30 ms; TR = 2000 ms; field of view (FOV) = 230 × 230 × 146 mm^3; voxel size = 3.6 × 3.6 × 3.6 mm^3; image matrix= 64 × 64.

Diffusion-weighted spin-echo planar images for diffusion tensor imaging (DTI) were obtained: TR = 5000 ms, TE = 69 ms; flip angle, 90°; matrix, 96 × 96; FOV = 224 mm x 224 mm; bandwidth = 1954 Hz/Voxel; voxel size = 1.8 × 1.8 × 3.5 mm^3. Diffusion-weighting gradients were applied at a b value of 1000 s/mm^2. Twelve images with no diffusion gradients (b0) was also acquired for each subject.

Pre-processing of the fMRI data was carried out by using FSL version 6.0.0 (FMRIB Software Library; University of Oxford; www.fmrib.ox.ac.uk/fsl) (Smith et al., 2004). The pre-processing included removal of non-brain voxels using brain extraction tool (BET; Smith, 2002), motion correction using MCFLIRT (Jenkinson, Bannister, Brady, & Smith, 2002), temporal high-pass filtering with 100s cut-off, slice timing correction, spatial smoothing by a Gaussian kernel with full-width half-maximum of 8 mm. Functional images were, then, registered to its native anatomical image using FMRIB's Linear Image Registration Tool (FLIRT) and then linearly registered to the MNI152 template with 12 degree of freedom affine transformation (Greve & Fischl, 2009; Jenkinson et al., 2002). To allow for signal stabilization, the first two dummy scans of each run were discarded.

5.2.5. Functional Imaging - Whole-brain Data Analysis

Each subject had three runs containing 96 trials in each run. First-level analysis was performed on the data of each run with general linear model (GLM) separately for the younger and older subjects. There were four cue conditions, namely aSC, eSC, neutral, and invalid, and their first-order derivatives were modelled. The regressors were convolved with a gamma function with a standard deviation of 3 s and a mean lag of 6 s. Temporal autocorrelation correction was performed using the improved linear model (FILM) of the FSL (Woolrich, Ripley, Brady, &

Smith, 2001). Each within-subject run was collapsed using FSL's fixed effect analysis. fMRI time-series was modelled using the onset period of the cue. Between subject higher-level analysis was performed by using FMRIB's Local Analysis of Mixed Effects (FLAME) option 1. The resulting statistical map was tested using Gaussian random-field based cluster thresholding with non-parametric cluster forming threshold of Z>2.3 and a multiple-comparison corrected cluster significance threshold of $p = 0.05$ (Worsley, 2001). The three explanatory variables (EV) covered in this analysis were aSC cue, eSC cue, and neutral cue. Between and within group contrasts for aSC cue > neutral cue, eSC cue > neutral cue, eSC cue > aSC cue and aSC cue > eSC cue were performed. Each subject's average parameter estimates in percentage for both the aSC and eSC cue-related signals were extracted from each predefined regions of interest (ROIs) using the 'Featquery' distributed as part of FSL. See bellow how the ROI's were defined. The results generated from this part of the analyses indicated neural substrates which showed significant activations associated with each of the aSC and eSC conditions and comparisons were made to test the differences in these activations between the younger and older groups. The results also formed the basis for the constructions of ROIs for building the functional connectivity models.

5.2.6. Structural Imaging - Diffusion Weighted Image Processing

The DTI data was analyzed using the FMRIB Software Library. The image with no diffusion gradients (b0) from each subject was skull-stripped using FSL's Brain Extraction Tool (Smith, 2002). All diffusion weighted data from all subjects were pre-processed for eddy-current induced distortions and motion correction using the FSL's top-up and Eddy tool. After distortions and motion correction, using the FDT toolbox (Smith et al., 2004), raw DTI data was fit into the

diffusion tensor model from which the FA (fractional anisotropy) maps for each subject was generated.

5.2.7. Structural Imaging - Tract-based spatial statistics (TBSS)

Whole-brain voxel-wise statistical analysis was carried by using tract-based spatial statistics (TBSS; Smith et al., 2006) of the FSL (Smith et al., 2004). First, subject's FA images were aligned into FMRIB58_FA 1×1×1mm standard-space using FNIRT (FMRIB's Nonlinear Registration Tool) (Andersson, Jenkinson, & Smith, 2007). Second, to achieve skeletisation, the aligned FA images were then affine transformed into 1x1x1mm MNI152 space. Third, using the mean FA image, FA skeleton common to cross-subject and cross-group white-matter tracts were created. This was achieved by thresholding the centre of white-matter bundles with a value of 0.2. Each subject's aligned FA maps was then projected onto the mean FA skeletonised map and the resulting data was subjected for cross-group voxel wise statistics. Correction for multiple testing was conducted using threshold-free cluster enhancement (TFCE) method (Smith & Nichols, 2009) and determined at $p \leq 0.05$. As additional quality assurance, we tested the differences in the FA values between the younger and older groups. The results of the comparisons were found to be consistent with those reported in other studies (Madden et al., 2010; Madden et al., 2007; Voineskos et al., 2012). The between-group differences revealed were SLF, PCR, ILF, ATR, and posterior limb of internal capsule (Figure 5.2). The comparability of the age-related results with other studies supported the validity of using the FA values in the subsequent ROI and structure-function relationship analyses. The mean FA values were extracted from each subject according to the predefined ROIs.

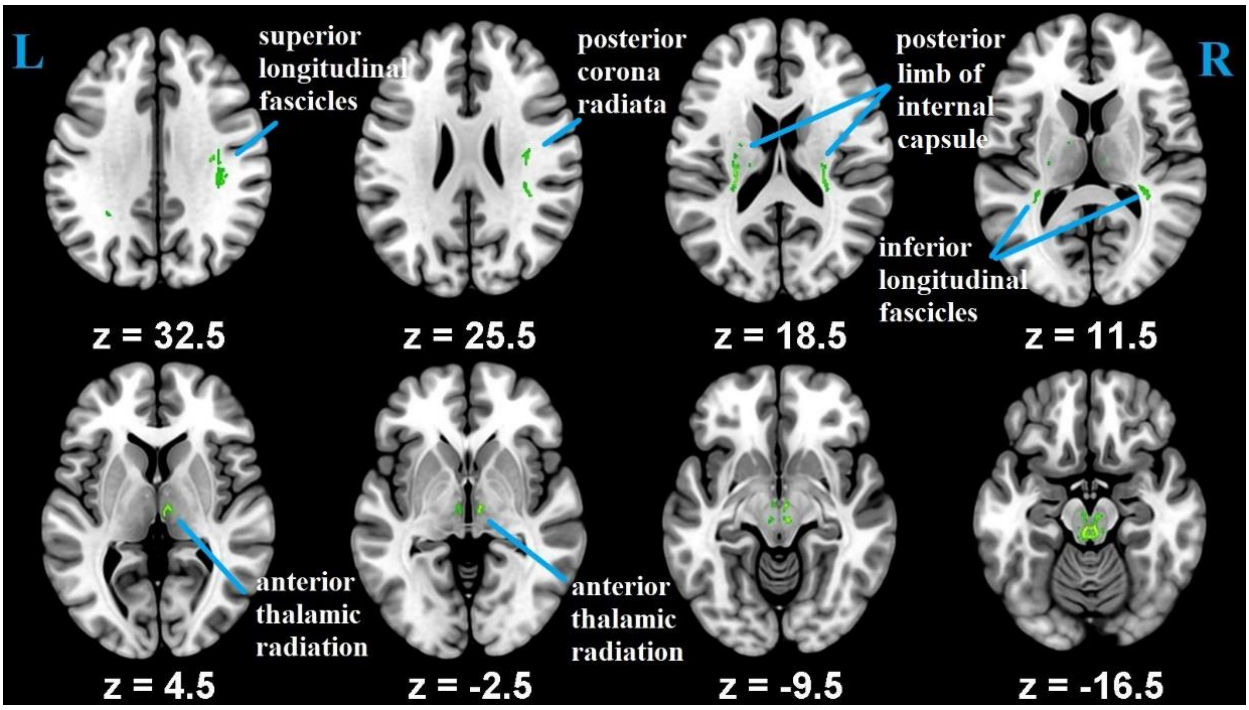

Figure 5. 2. Age group differences in FA measures. Corrected for multiple comparisons using threshold-free cluster enhancement (TFCE) ($p < 05$).

5.2.8. Structure-Function Relationship - Construction of Functional and WM ROIs

There are two types of ROIs in the analyses: functional and structural. For the functional ROIs, they were determined by using activation likelihood activation (ALE) method for the identification and extraction based on the existing datasets from other studies (Eickhoff et al., 2005). The datasets came from previous neuroimaging studies on spatial coding listed in PubMed. Peaks of the activation coordinates were obtained from 22 papers on allocentric and 20 papers on egocentric spatial coding. They were then aggregated after conducting ALE meta-analysis. Five clusters of convergence were identified for each of the aSC and eSC conditions (see Chapter 2). ROI masks were produced by drawing a 5 mm kernel sphere in each cluster at the location whereby showing maximum ALE values ($Peak_x$, $Peak_y$, $Peak_z$). The ROIs derived were the right FEF (x = 22, y = 4, z = 56), right precuneus (x = 8, y = -60, z = 46), left SPL (x = -24, y = -62, z = 58), right IPL (x = 56, y = -54, z = 29) and right SOG (x = 36, y = -72, z = 34) for aSC condition, and the right FEF (x = 28, y = 2, z = 58), bilateral precuneus (RH: x = 18, x = -74, z = 54; LH: x = -16, y =-66, z = 56), right IPL (x = 56, y = -54, z = 29), and left SOG (x = -26, y = -78, z = 32) for the eSC condition (Figure 4.3). These ROIs were largely consistent with those reported in previous ALE studies on spatial coding (e.g. Committeri et al., 2004; Liu et al., 2017; Wegman et al., 2014; Weniger et al., 2010; Zaehle et al., 2007; Zhang & Ekstrom, 2013).

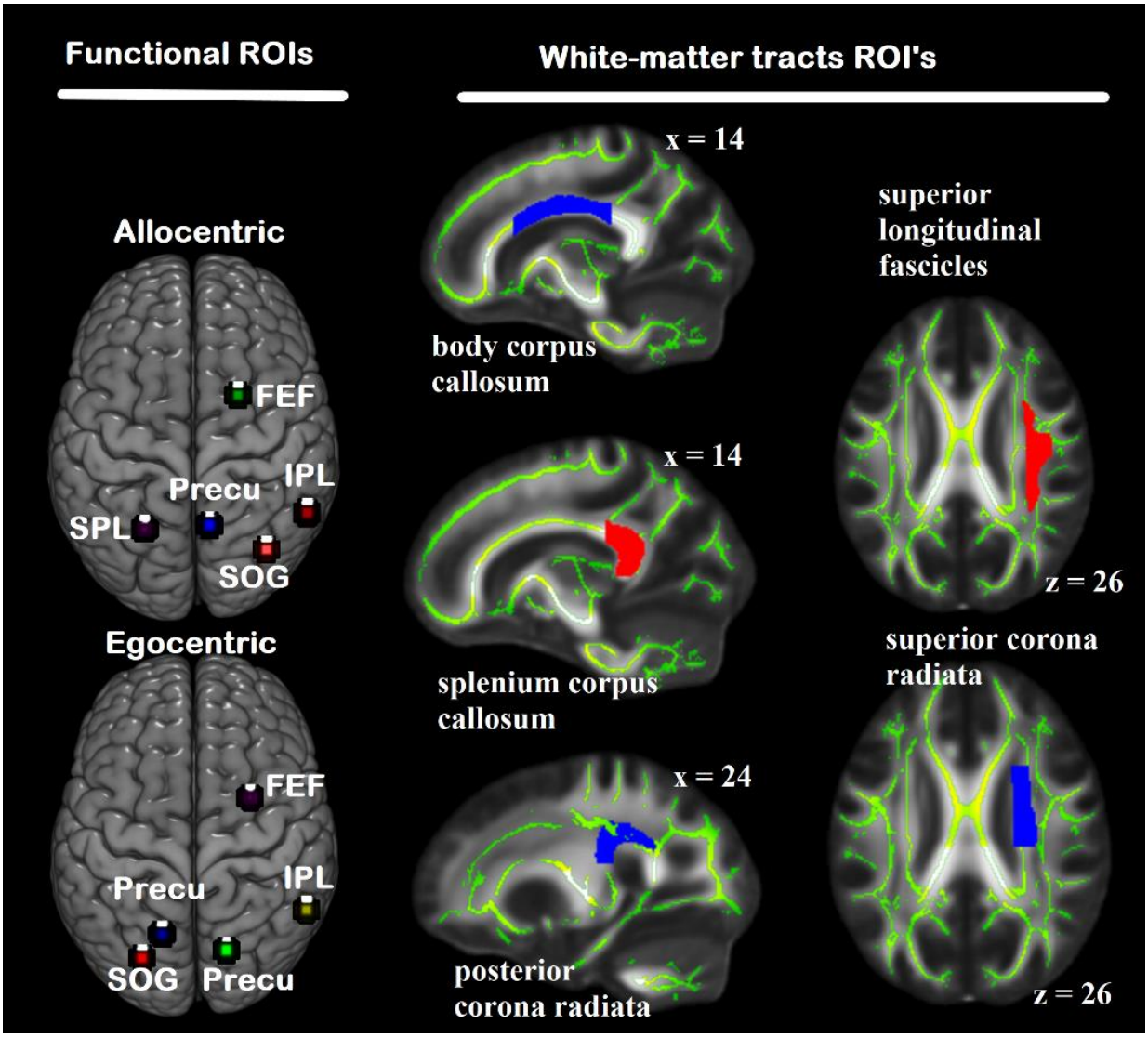

Figure 5. 3. Functional and white-matter ROIs identified for modelling the structure-function relationship for spatial coding. The white-matter ROIs are overlaid on FMRIB58_FA 1 mm standard-space and the mean FA skeleton of both the younger and older groups (the tracts

shown in green). FEF: frontal eye field. Precu: precuneus. IPL: inferior parietal lobule. SOG: superior occipital gyrus. SPL: superior parietal lobule.

Constructing of the WM ROIs involved two steps. First, we identified published studies on white matter (particularly FA) in relation with ageing and visuospatial attention. Ten key white-matter tracts associated with ageing and visuospatial attention from five studies were collated (Bennett et al., 2012; Chechlacz, Humphreys, Sotiropoulos, Kennard, & Cazzoli, 2015; Madden et al., 2007; Tuch et al., 2005; Voineskos et al., 2012). The WM tracts related to aging and visuospatial attention were identified for constructing their ROIs. They were the bilateral anterior and superior corona radiata (SCR), bilateral posterior corona radiata (PCR), body corpus callosum (BCC), splenium corpus callosum (SPN), bilateral superior longitudinal fasciculus (SLF), and bilateral posterior thalamic radiation (PTR) (see Introduction). White-matter labelling and parcellation were done by using FSL atlas tools ("JHU ICBM-DTI-81"; Mori et al., 2008). To select the tracts for further analyses, the FA values obtained from each of these tracts were correlated with subjects' performances (RTs) on the cue-to-target paradigm. The results showed significant correlations in the FA values of five tracts with the RTs of subjects in the older group and/or younger group in allocentric and/or egocentric condition. They were the right SCR, right PCR, BCC, SPN, and right SLF (Figure 5.3). These tracts were adopted as the binary WM ROIs for interrogating the brain structural organization of each subject using 'fslmeants' on all_FA_skeletonised image in FSL.

5.2.9. Structure-Function Relationship - Seed-to-Voxel Connectivity Analysis

Relationships were tested between the functional and WM ROIs by correlating their BOLD signals and FA values separately for the aSC and eSC conditions using R statistical computing (R Core Team, 2017) followed by hierarchical multiple regression for ROIs with significant correlations. Each WM RO's were entered as a dependent variable and BOLD changes in each functional ROI's were entered as the independent variable. There were four models set for the regression analyses for predicting BOLD signals (aSC-neutral or eSC-neutral) of each of the significant functional ROIs by the FA values of the WM ROIs. They were young-aSC, young-eSC, old-aSC and old-eSC. In each model, semi-partial correlation (sr^2) and changes in the coefficient of determination (ΔR^2) of were examined for the contribution made from the FA of WM ROIs to activations of the functional ROIs associated with spatial coding processes. The results of the regression analyses in terms of BOLD-FA relationships were used to corroborate with the differences in the fMRI findings on aCS and eSC for the younger subjects reported in Chapter 4. The significant WM tracts also formed the basis for conducting the subsequent functional connectivity analyses on the differences between the younger and older subjects.

The aging effect on the proposed neural models of aSC and eSC was tested in terms of the differences in the seed-to-voxel connectivity between the younger and older subjects. The method used for constructing the functional connectivity models was the generalized psychophysiological interaction analyses (gPPI) (McLaren, Ries, Xu, & Johnson, 2012) in the CONN toolbox (Whitfield-Gabrieli & Nieto-Castanon, 2012). The gPPI required extracting the time-series average BOLD signals from the functional ROIs. The criteria set for selecting these ROIs were: 1)

consistent with the those of the proposed enhanced spatial model presented in Chapter 4; 2) related to visuospatial attention; and 3) in order to delimit the analysis and reduce type I error, given the number of voxels to ROI comparisons, two key networks associated to visual attention supported by top-down attention control (dorsal attention network [DAN] and fronto-parietal network [FPN]). Four ROIs which exclusively located in the right hemisphere were identified and they were mapped onto the anatomical areas from the Harvard-Oxford atlas included in CONN (Desikan et al., 2006; Fox et al., 2006). The ROIs entered for the gPPI analyses were the right FEF, IPS, lateral PFC, and PPC. Studies have shown that visuospatial attention mainly involved neural substrates the right hemisphere (Corbetta & Shulman, 2002; Kravitz et al., 2011), and thus only the seed regions in the right hemisphere in these two functional networks were drawn. The FA values of the three WM ROIs (PCR, SLF and SCR) revealed in the significant hierarchical multiple regression models became the covariates of interest to see its effect to the task-modulated connectivity of the DAN and FPN. The PPI regressors were modelled as follow:

1. Three task regressors for each of aSC, eSC and neutral conditions convolved with the hemodynamic response function (HRF);
2. The seeds of the time-series BOLD signals were IPS, FEF, LPFC and PPC for each of the three task regressors; and,
3. The interaction terms of seed regions time-series with task regressors.

The seed-to-voxel connectivity analyses were conducted on the younger and older subjects. The task regressors mentioned above were submitted to a gPPI model. Each subject had three seed-to-voxel gPPI maps with each representing one task regressors. The seed-to-voxel gPPI maps were

used to test for possible between-subject and between-condition effects to the task-related modulation of functional connectivity patterns. The next level of analyses was conducted to investigate whether age-related changes in FA could be accounted for age-related differences in the aSC-eSC functional connectivity. Similar to the first gPPI procedure, the four seeds of the time-series BOLD signals were PPC, LPFC, IPS and FEF. In addition, the FA values of PCR, SLF and SCR were entered in the gPPI model, separately and every location in the brain were measured. Two models were set for the gPPI analyses: 1) testing the task effects on the WM tract modulated functional connectivity for the younger and older groups respectively, with aSC > NEU (neutral condition) and eSC > NEU contrasts; and 2) testing the age effects on the WM tract modulated functional connectivity for the aSC and eSC conditions respectively, with YOUNG-FA> OLD-FA as in between subject's contrasts aSC > NEU and eSC > NEU as in between condition contrasts and one seed region at a time. Using the CONN toolbox, the gPPI contrast maps for each design were generated and results were displayed using Statistical Parametric Mapping (SPM12) and its corresponding group-level beta-weights for each contrast, corrected for multiple comparison using FDR at .05, were extracted and plotted along the connectivity strength brain maps.

5.3. Results

5.3.1. Subjects' Task Performances

The RTs of the subjects for the valid trials were significantly faster than those for the invalid trials in both the younger (aSC: t = 2.35, $p \leq .05$; eSC: t = 2.82, $p < .01$) and older groups (aSC: t = 2.16, $p \leq .05$; eSC: t = 3.20, $p < .01$) (Figure 5.4). Compared to older subjects, younger subjects responded faster in both aSC (t = -8.27, $p < .01$) and eSC trials (t = -7.79, $p < .01$). Subjects' RTs for valid trials in aSC and eSC condition were significantly faster than those for the neutral trials in both the younger (aSC: t = -7.77, $p < .01$; eSC: t =-8.43, $p < .01$) and older groups (aSC: t = -7.32, $p < .01$; eSC: t =-6.30, $p < .01$). The condition effects (aSC versus eSC) on the RTs were statistically not significant for both groups. The behavioral results suggest that the cue-to-target effects were significant on facilitating the subjects' responses on both spatial coding conditions. Significant aging effects were observed, which impacted on the longer time taken by the older subjects to respond to the target.

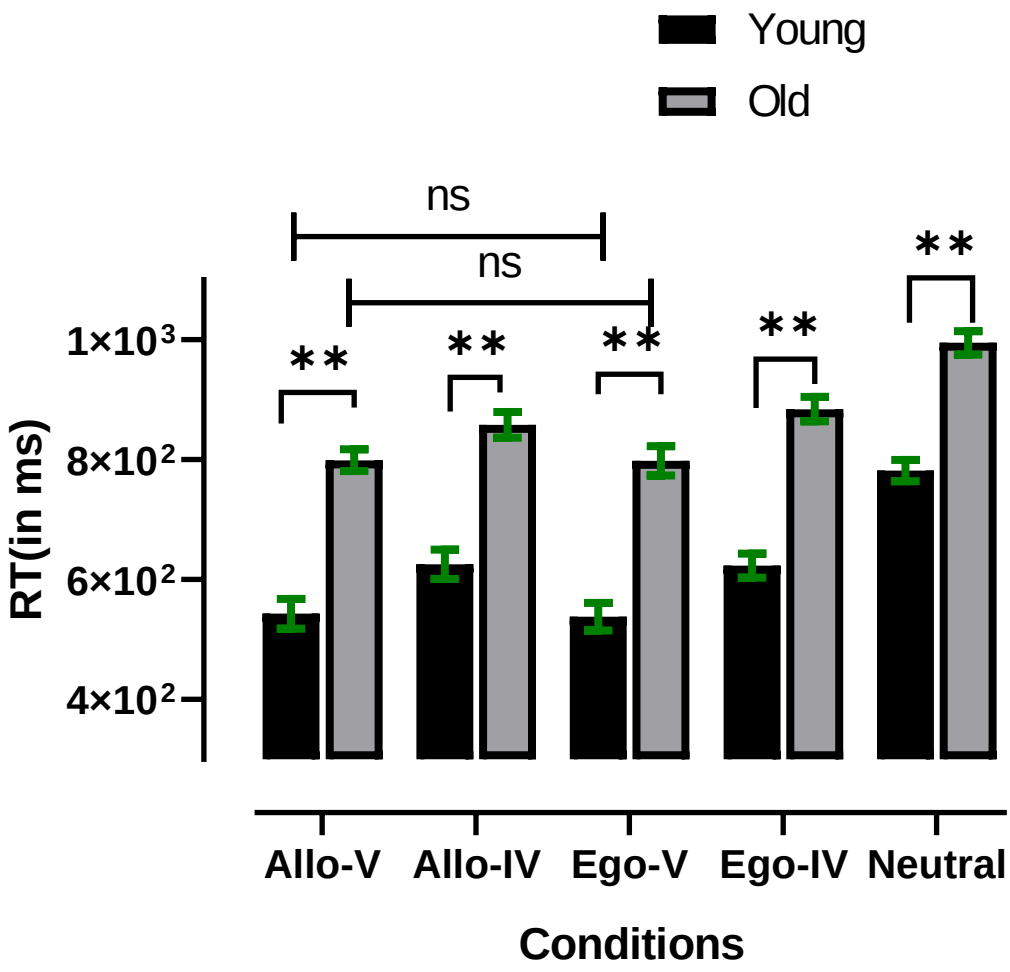

Figure 5. 4. Group comparisons of reaction times (RTs) across the egocentric, allocentric and neural conditions. Error bar shows the standard error of the mean RT per conditions. ** p<.01. ns = non-significant. ms = milliseconds. aSC-V = allocentric valid trials. eSC-V = egocentric valid trials. aSC-IV = allocentric invalid trials. eSC-IV = egocentric invalid trials.

Functional brain activities associated with allocentric and egocentric processing

There were two contrasts set for the whole-brain functional MRI analyses: aSC > NEU (neutral condition) and eSC > NEU. Among younger subjects, significantly stronger activations were found in the bilateral PreCG, IFG, MOG, and FusiFG for the aSC > NEU contrast (Figure 5.5). Other sites with significantly stronger activations were the right ACC, PMd, and left PoCG and MFG. For the eSC > NEU contrast, stronger activations were revealed in the bilateral precuneus and PCC, the right LG, left SFG and AG.

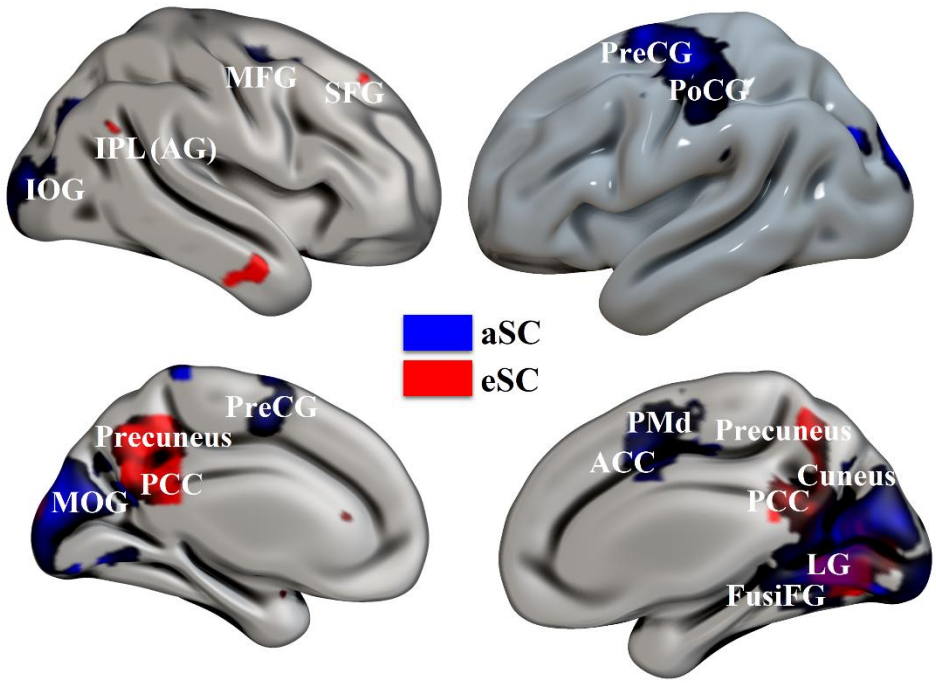

Figure 5. 5. Whole-brain functional MRI analyses on aSC_{valid} > NEU and eSC_{valid} > NEU contrasts among younger subjects. Activations blobs are corrected for multiple comparison using P_{FWE} < .05. Colour labels blue = allocentric spatial coding and red = egocentric spatial coding. Right and left medial, and posterior three-dimensional views of a standard brain are shown. IOG = inferior occipital gyrus. MOG = middle occipital gyrus. PCC = posterior cingulate cortex. LG = lingual

gyrus. FusiFG = fusiform gyrus. IPL = inferior parietal lobule. PreCG = precentral gyrus. PoCG = postcentral gyrus. ACC = anterior cingulate cortex. PMd = premotor cortex. MFG = middle frontal gyrus. SFG = superior frontal gyrus.

Among the older subjects, stronger activations in the bilateral PreCG, PoCG, and IOG for the aSC > Neutral contrast (Figure 5.6). Other neural substrates showed stronger activations for the aSC were the right LG, right precuneus, left FusiFG, left MTG, left STG, and left MFG. For the eSC > Neutral contrast, stronger activations were observed in the right PoCG and IPL.

Among the younger subjects, the main difference between the two types of spatial coding were in the left PreCG and PoCG, and the right ACC for aSC condition, and the bilateral precuneus and PCC including the left SFG for the eSC condition. Among the older subjects, the main between-condition differences were in the bilateral IOG, PreCG and PoCG, and the right precuneus and left ACC for the aSC condition, and the left PoCG and IPL for the eSC condition.

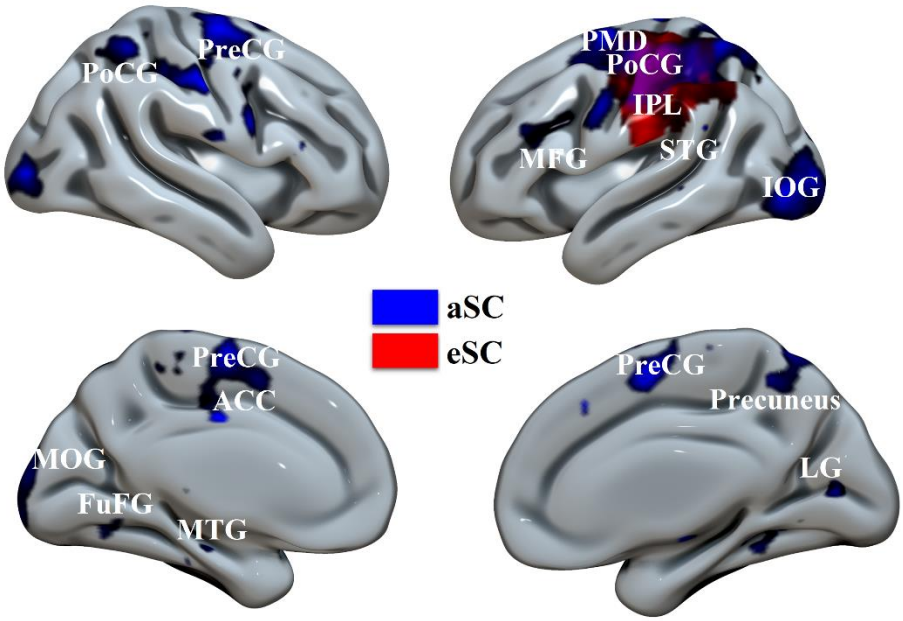

Figure 5. 6. Whole-brain functional MRI analyses on aSC_{valid} > NEU and eSC_{valid} > NEU contrasts among older subjects. Activations blobs are corrected for multiple comparison using $P_{FWE} < .05$. Colour labels blue = allocentric spatial coding and red = egocentric spatial coding. MOG = middle occipital gyrus. LG = lingual gyrus. FuFG = fusiform gyrus. MTG = middle temporal gyrus. STG = superior temporal gyrus. IPL = inferior parietal lobule. PreCG = precentral gyrus. PoCG = postcentral gyrus. ACC = anterior cingulate cortex. PMD = premotor cortex. MFG = middle frontal gyrus.

5.3.2. BOLD-FA Relationships

The results of exploring the relationships between BOLD signal changes and WM integrity have two parts: one was correlation coefficient and the one was hierarchical multiple regression. The BOLD signals were from five functional ROIs while the FA values were from four structural ROIs (or tracts). Separate sets of correlations were computed for each of the aSC and eSC conditions, and for the younger and older groups. Among younger subjects, only the PCR was revealed to relate to the functional ROIs. For the aSC condition, BOLD signal change in the right SOG was significantly and negatively correlated with the FA value of PCR ($r = -.51$, number of subjects (n) = 27, $p<.01$). Similar significant and negative correlation was found between the FA values of PCR and BOLD signal change in the right precuneus ($r = -.44$, $n = 27$, $p< .05$) (Figure 5.7).

Among the older subjects, for aSC condition, significantly positive correlations were found between the BOLD signal change in the right FEF and FA values in the SCR ($r = .48$, $n = 24$, $p<.05$), the right precuneus and the PCR ($r = .46$, $n = 24$, $p< .05$), the right IPL and BCC ($r = .41$, $n = 24$, $p<.05$), and the right IPL and PCR ($r = .44$, $n = 24$, $p<.05$) (Figure 5.7). For the eSC condition, older subjects showed positive correlations between the right IPL and BCC ($r = .42$, $n = 24$, $p<.05$), the right IPL and SPN ($r = .42$, $n = 24$, $p<.05$). All other correlations between the BOLD signal changes of the functional ROIs and the FA values of the structural ROIs were not statistically significant.

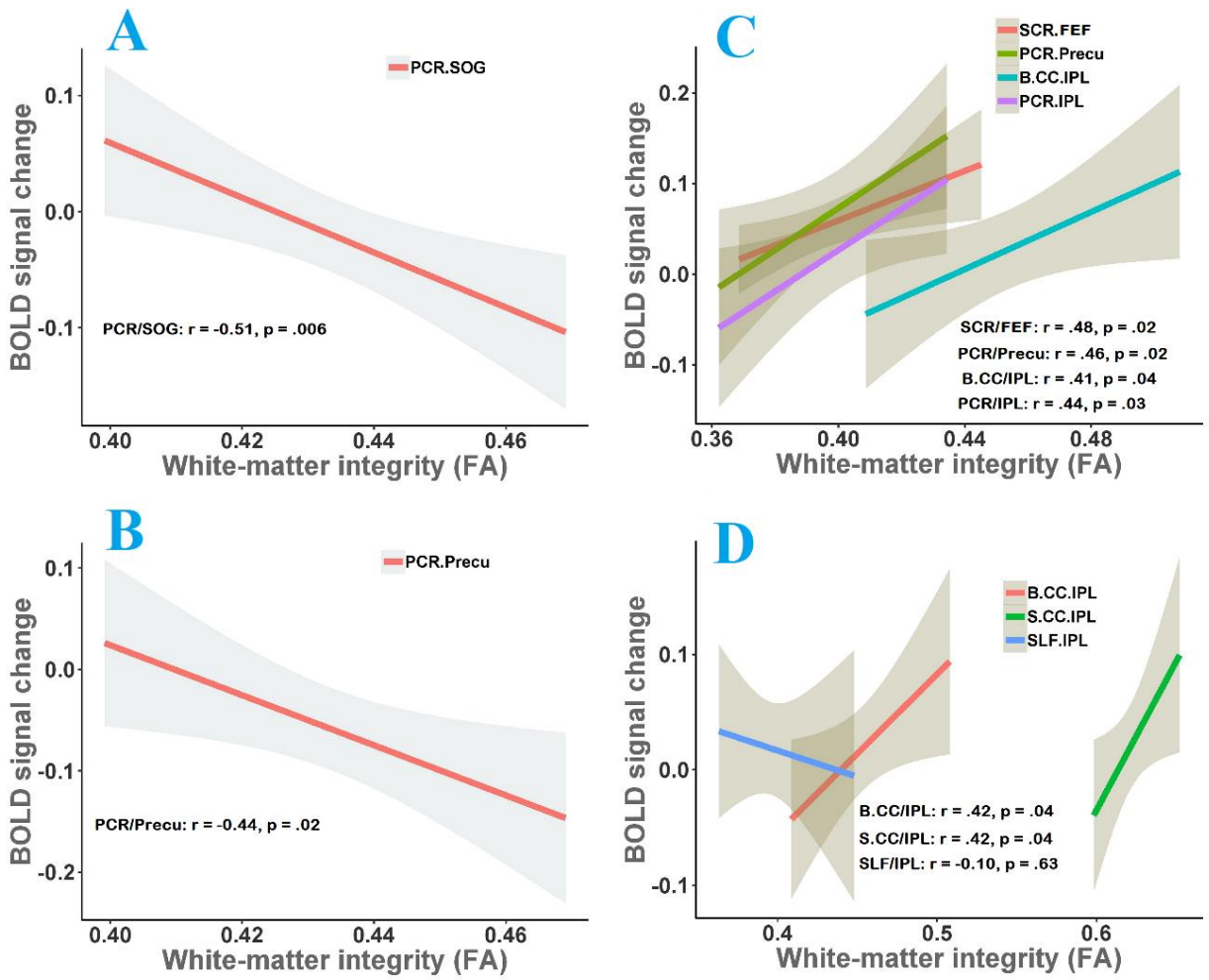

Figure 5. 7. The relationships between FA values of the structural ROIs and BOLD signal changes in the functional ROIs for aSC and eSC conditions and younger and older subjects. A) aSC BOLD signals changes and FA values among younger subjects. B) eSC BOLD signals changes and FA values among younger subjects. C) aSC BOLD signals changes and FA values among older subjects. D) eSC BOLD signals changes and FA values among older subjects. SCR: superior corona radiata. FEF: right frontal eye-fields. PCR: posterior corona radiata. Precu: right

precuneus. BCC: body corpus callosum. SPN: splenium corpus callosum. IPL: right inferior parietal lobule. SLF: superior longitudinal fasciculus.

The results showed differences in the BOLD-FA relationships both between the aSC and eSC conditions and the age groups. The younger subjects showed fewer structure-function relationships. More importantly, their significant and negative relationships appear to exist in the same PCR tract with different functional ROIs involved, i.e. SOG in aSC and precuneus in eSC. In contrast, the older subjects showed relatively more substantial but positive structure-function relationships. Significant relationships were found in four functional ROIs with three WM tracts for aSC condition and two functional ROIs with two WM tracts in egocentric. The right IPL and BCC relationship was the only structure-function pair common to both types of spatial coding.

Hierarchical multiple regression analyses were conducted separately for the aSC and eSC conditions, and the younger and older subjects. The predictors were the FA values of the significant WM tracts from the correlational analyses and the dependent variables were the BOLD signal changes in the significant functional ROIs reported above. Tables 5.1 to 5.4 show the variances of the BOLD signals accounted for by the WM tract FA values yielded from the different regression analyses.

In younger subjects, the results of hierarchical multiple regression analyses further confirm the FA values of PCR significantly predicted BOLD signal changes in the right SOG for aSC (Table 5.1 and Figure 5.7) and the right precuneus for eSC (Table 5.2. and Figure 5.7). Among all the structural ROIs, only PCR brought significant increases in the activation change of the right SOG in the aSC condition (Table 5.1, $\Delta R^2 = .250$, $r = -.51$, $p < .05$). Similar results yielded from PCR were that it was the only significant structural ROI significantly increased the activation in

the right precuneus in the eSC condition (Table 5.2, $\Delta R^2 = .190$, r = -.44, $p < .05$). In older subjects, three significant prediction models were yielded for the IPL, FEF and precuneus for the aSC condition. BOLD signal changes in the right IPL were significantly predicted by the FA values of both PCR and BCC for aSC accounting for 17.3% of the variances (Table 5.3, $\Delta R^2 = .173$, r = .44, $p < .05$). Between the two structural ROIs, PCR appears to have slightly larger contributions to the prediction than BCC (*ß = .46, p<.05).* BOLD signal changes in the right FEF was significantly predicted by the FA values of SCR which accounted for 24.5% of the variances (Table 5.3, $\Delta R^2 = .245$, r = .48, $p < .05$). BOLD signals changes in the right precuneus was significantly predicted by the FA values of PCR which accounted for 18.1% of the variances ((Table 5.3, $\Delta R^2 = .181$, r = .46, $p > .05$). One only prediction model was significant for the eSC condition, which was on the right IPL. BOLD signals changes in the right IPL was significantly predicted by the FA values of BCC and SPN which accounted for 15.7% of the variances (Table 5.4, $\Delta R^2 = .157$, r = .48, $p < .05$).

Among older subjects, FA values of BCC and SPN were positively correlated with eSC-related PE changes in IPL. At any steps of the model specification, the accounted variances of both BCC ($\Delta R^2 = .078$, r = .42, $p > .05$) and SPN ($\Delta R^2 = .025$, r = .43, $p > .05$) were not above and beyond the other tracts. Surprisingly, it was revealed that eSC-related BOLD signal changes in IPL explained by SLF was above and beyond the accounted variance of other all the white-matter ROI's ($\Delta R^2 = .157$ r = -.10, $p < .05$). From the semi-partial correlation, SLF was accounted for 16% of the observed variance of IPL's egocentric activity (*$sr^2 = .16, p<.05$*). SLF was attributed for the BOLD signal change of the IPL by -.51% of the BOLD signal change (*ß = -.51, p <.05*).

The significant prediction models derived from hierarchical multiple regression indicated the unique WM integrity and BOLD signal change relationships in aSC and eSC. These results

further supported and implicated for the next step of analyses for exploring the effective functional connectivity. The between-group results indicated that the integrity of the structural ROIs had more significant involvements in influencing the BOLD signal changes in the functional ROIs in older than younger subjects, and in aSC than eSC.

Table 5. 1. Hierarchical multiple regression results on prediction of BOLD signal changes in right SOG for younger subjects in allocentric spatial coding

Predictor	*B*	*B* 95% CI LL, UL	*β*	*β* 95% CI LL, UL	sr^2	sr^2 95% CI LL, UL	*r*	Fit		Difference	
								R^2	95% CI	ΔR^2	95% CI
Model 1											
SLF	0.34	-1.26, 1.93	0.09	-0.32, 0.50	.01	.00, .17	.09	.007	.00,.17		
Model 2											
SLF	0.14	-2.15, 2.44	0.04	-0.55, 0.63	.00	-.02, .02	.09				
SCR	0.31	-2.30, 2.93	0.07	-0.52, 0.66	.00	-.04, .04	.10	.010	.00,.11	.003	-.04, .04
Model 3											
SLF	0.40	-1.97, 2.77	0.10	-0.51, 0.71	.01	-.05, .06	.09				
SCR	0.75	-2.03, 3.52	0.17	-0.46, 0.79	.01	-.07, .10	.10				
BCC	-0.77	-2.40, 0.85	-0.25	-0.78, 0.28	.04	-.10, .18	-.10	.050	.00,.18	.040	-.10, .18
Model 4											
SLF	0.69	-2.32, 3.71	0.18	-0.60, 0.95	.01	-.06, .08	.09				
SCR	0.90	-2.08, 3.87	0.20	-0.47, 0.87	.02	-.08, .11	.10				
BCC	-0.62	-2.53, 1.30	-0.20	-0.82, 0.42	.02	-.08, .12	-.10				

SPN	-0.79	-5.65, 4.06	-0.15	-1.10, 0.79	.00	-.05, .06	-.00	.055	.00,.14	.005	-.05, .06
Model 5											
SLF	-0.83	-3.72, 2.06	-0.21	-0.96, 0.53	.01	-.06, .08	.09				
SCR	1.41	-1.24, 4.05	0.32	-0.28, 0.92	.04	-.08, .16	.10				
BCC	-0.04	-1.78, 1.70	-0.01	-0.58, 0.55	.00	-.01, .01	-.10				
SPN	-0.24	-4.53, 4.05	-0.05	-0.88, 0.79	.00	-.01, .01	-.00				
PCR	-2.62*	-4.61, -0.64	-0.57	-1.00, -0.14	.25	-.03, .53	-.51**	.305	.00,.45	.250*	-.03, .53

Note. * = $p < .05$. ** = $p < .001$. SLF: superior longitudinal fasciculus. BCC: body of corpus coliseum. SPN: splenium of corpus coliseum. PCR: posterior corona radiata. SCR: superior corona radiata. SOG: superior occipital gyrus

Table 5. 2. Hierarchical multiple regression results on prediction of BOLD signal changes in right precuneus for younger subjects in egocentric spatial coding

Predictor	*B*	*B* 95% CI LL, UL	*β*	*β* 95% CI LL, UL	sr^2	sr^2 95% CI LL, UL	*r*	Fit		Difference	
								R^2	95% CI	ΔR^2	95% CI
Model 1											
SLF	-0.41	-2.36, 1.53	-0.09	-0.50, 0.32	.01	.00, .17	-.09	.008	.00,.17		
Model 2											
SLF	0.31	-1.98, 2.59	0.06	-0.42, 0.55	.00	-.04, .04	-.09				
BCC	-1.06	-2.87, 0.75	-0.28	-0.77, 0.20	.06	-.11, .23	-.25	.065	.00,.25	.057	-.11, .23
Model 3											
SLF	-0.38	-3.80, 3.03	-0.08	-0.80, 0.64	.00	-.03, .04	-.09				
BCC	-1.41	-3.63, 0.82	-0.38	-0.97, 0.22	.07	-.11, .25	-.25				
SPN	1.49	-3.92, 6.90	0.24	-0.63, 1.11	.01	-.07, .10	-.09	.078	.00,.23	.013	-.07, .10
Model 4											
SLF	-0.39	-4.01, 3.23	-0.08	-0.85, 0.68	.00	-.03, .04	-.09				
BCC	-1.41	-3.71, 0.89	-0.38	-0.99, 0.24	.07	-.11, .25	-.25				

SPN	1.47	-4.35, 7.30	0.24	-0.70, 1.17	.01	-.07, .09	-.09				
SCR	0.03	-3.54, 3.61	0.01	-0.66, 0.67	.00	-.00, .00	-.09	.078	.00,.19	.000	-.00, .00
Model 5											
SLF	-2.00	-5.61, 1.60	-0.42	-1.19, 0.34	.05	-.09, .18	-.09				
BCC	-0.80	-2.97, 1.37	-0.21	-0.79, 0.37	.02	-.07, .11	-.25				
SPN	2.06	-3.30, 7.41	0.33	-0.53, 1.19	.02	-.07, .12	-.09				
SCR	0.57	-2.73, 3.88	0.11	-0.51, 0.72	.00	-.04, .05	-.09				
PCR	-2.78*	-5.25, -0.30	-0.50	-0.94, -0.05	.19	-.07, .45	-.44*	.268	.00,.41	.190*	-.07, .45

Note. * = p < .05. ** = p < .001. SLF: superior longitudinal fasciculus. BCC: body of corpus coliseum. SPN: splenium of corpus coliseum. PCR: posterior corona radiata. SCR: superior corona radiata.

Table 5. 3. Hierarchical multiple regression results on prediction of BOLD signal changes in right IPL, FEF, and precuneus for older subjects in allocentric spatial coding

	B	*B*	*ß*	*ß*	sr^2	sr^2	*r*	Fit		Difference	
Predictor		95% CI LL, UL		95% CI LL, UL		95% CI LL, UL		R^2	95% CI	ΔR^2	95% CI
4.1a: IPL											
Mode l											
SLF	-0.07	-2.39, 2.25	-0.01	-0.45, 0.43	.00	.00, .05	-.01	.000	.00,.05		
Model 2											
SLF	-0.95	-3.51, 1.62	-0.18	-0.67, 0.31	.03	-.09, .14	-.01				
SCR	1.76	-0.67, 4.18	0.35	-0.13, 0.84	.10	-.13, .32	.27	.098	.00,.31	.098	-.13, .32
Model 3											
SLF	-0.93	-3.42, 1.56	-0.18	-0.65, 0.30	.02	-.09, .14	-.01				
SCR	0.75	-1.95, 3.46	0.15	-0.39, 0.70	.01	-.07, .10	.27				
BCC	1.44	-0.49, 3.36	0.37	-0.13, 0.87	.10	-.12, .31	.41*	.196	.00,.39	.098	-.12, .31
Model 4											

SLF	-1.28	-4.03, 1.47	-0.24	-0.77, 0.28	.04	-.10, .18	-.01				
SCR	0.67	-2.10, 3.43	0.14	-0.42, 0.69	.01	-.06, .08	.27				
BCC	0.94	-1.54, 3.42	0.24	-0.40, 0.89	.03	-.09, .14	.41*				
SPN	1.57	-3.27, 6.41	0.22	-0.46, 0.89	.02	-.08, .12	.34	.215	.00,.38	.019	-.08, .12
Model 5											
SLF	-2.15	-4.79, 0.48	-0.41	-0.91, 0.09	.10	-.09, .29	-.01				
SCR	1.15	-1.41, 3.71	0.23	-0.28, 0.75	.03	-.08, .14	.27				
BCC	0.40	-1.91, 2.72	0.10	-0.49, 0.70	.00	-.04, .05	.41*				
SPN	1.48	-2.93, 5.89	0.21	-0.41, 0.82	.02	-.06, .10	.34				
PCR	2.36*	0.16, 4.56	0.46*	0.03, 0.89	.17	-.07, .42	.44*	.387	.00,.52	.173*	-.07, .42
4.1b: FEF											
Model 1											
SLF	0.71	-0.58, 2.01	0.24	-0.19, 0.67	.06	.00, .29	.24	.056	.00,.29		
Model 2											
SLF	0.69	-0.68, 2.07	0.23	-0.22, 0.69	.05	-.12, .22	.24				
BCC	0.06	-0.95, 1.07	0.03	-0.43, 0.48	.00	-.02, .02	.08	.057	.00,.25	.001	.02, .02

Model 3											
SLF	0.83	-0.74, 2.40	0.28	-0.25, 0.80	.06	-.12, .24	.24				
BCC	0.25	-1.18, 1.67	0.11	-0.53, 0.75	.01	-.05, .07	.08				
SPN	-0.56	-3.50, 2.37	-0.14	-0.85, 0.58	.01	-.06, .07	.08	.065	00,.21	.007	-.06, .07
Model 4								.			
SLF	0.78	-0.90, 2.46	0.26	-0.30, 0.82	.05	-.12, .21	.24				
BCC	0.22	-1.27, 1.70	0.10	-0.57, 0.77	.00	-.05, .06	.08				
SPN	-0.56	-3.58, 2.45	-0.14	-0.87, 0.59	.01	-.06, .07	.08				
PCR	0.18	-1.31, 1.67	0.06	-0.45, 0.57	.00	-.04, .05	.14	.068	.00,.17	.003	-.04, .05
Model 5											
SLF	0.05	-1.55, 1.66	0.02	-0.51, 0.55	.00	-.01, .01	.24				
BCC	-0.39	-1.79, 1.02	-0.17	-0.81, 0.46	.01	-.06, .09	.08				
SPN	-0.87	-3.56, 1.81	-0.21	-0.86, 0.44	.02	-.07, .11	.08				
PCR	0.46	-0.88, 1.80	0.16	-0.30, 0.61	.02	-.07, .11	.14				
SCR	1.88*	0.32, 3.43	0.66*	0.11, 1.21	.25	-.04, .53	.48*	.313	.00,.45	.245*	-.04, .53

4.1c: Precuneus

Model 1											
SLF	0.84	-1.42, 3.10	0.16	-0.27, 0.60	.03	.00, .24	.16	.026	.00,.24		
Model 2											
SLF	0.28	-2.30, 2.86	0.05	-0.44, 0.55	.00	-.03, .04	.16				
SCR	1.12	-1.31, 3.56	0.23	-0.27, 0.73	.04	-.11, .19	.26	.067	.00,.27	.041	-.11, .19
Model 3											
SLF	0.28	-2.35, 2.92	0.05	-0.45, 0.56	.00	-.03, .04	.16				
SCR	0.80	-2.06, 3.67	0.16	-0.42, 0.75	.02	-.08, .11	.26				
BCC	0.46	-1.58, 2.49	0.12	-0.41, 0.65	.01	-.07, .09	.22	.078	.00,.24	.010	-.07, .09
Model 4											
SLF	0.25	-2.70, 3.20	0.05	-0.52, 0.62	.00	-.03, .03	.16				
SCR	0.80	-2.17, 3.76	0.16	-0.44, 0.77	.02	-.08, .11	.26				
BCC	0.41	-2.25, 3.06	0.11	-0.59, 0.80	.00	-.05, .06	.22				
SPN	0.16	-5.02, 5.34	0.02	-0.71, 0.75	.00	-.01, .01	.21	.078	.00,.19	.000	-.01, .01

Model 5											
SLF	-0.63	-3.49, 2.23	-0.12	-0.67, 0.43	.01	-.06, .07	.16				
SCR	1.28	-1.50, 4.06	0.26	-0.31, 0.83	.04	-.09, .17	.26				
BCC	-0.14	-2.65, 2.38	-0.04	-0.69, 0.62	.00	-.02, .02	.22				
SPN	0.07	-4.73, 4.86	0.01	-0.67, 0.69	.00	-.00, .00	.21				
PCR	2.39	-0.01, 4.78	0.47	-0.00, 0.95	.18	-.09, .45	.46*	.258	.00,.40	.181	-.09, .45

Note. *B* is the coefficient of the unstandardized regression model, whereas *ß* (beta) is the standardized regression coefficient. sr^2 is the squared value of the semi-partial correlation coefficient. *r* is the zero-order correlation coefficient. *LL* and *UL* is the lower and upper limits of a confidence interval, respectively. * = $p < .05$. ** = $p < .001$. SLF: superior longitudinal fasciculus. BCC: body of corpus coliseum. SPN: splenium of corpus coliseum. PCR: posterior corona radiata. SCR: superior corona radiata. IPL: inferior parietal lobule. FEF: frontal eye-fields.

Table 5. 4. Hierarchical multiple regression results on prediction of BOLD signal changes in right IPL for older subjects in egocentric spatial coding

Predictor	*B*	*B* 95% CI LL, UL	*ß*	*ß* 95% CI LL, UL	sr^2	sr^2 95% CI LL, UL	*r*	Fit		Difference	
								R^2	95% CI	ΔR^2	95% CI
Model 1											
PCR	0.58	-1.30, 2.46	0.13	-0.30, 0.57	.02	.00, .22	.13	.018	.00,.22		
Model 2											
PCR	0.40	-1.46, 2.25	0.09	-0.34, 0.52	.01	-.06, .08	.13				
SCR	1.30	-0.49, 3.10	0.31	-0.12, 0.74	.10	-.13, .32	.33	.114	.00,.33	.096	-.13, .32
Model 3											
PCR	0.06	-1.83, 1.95	0.01	-0.43, 0.45	.00	-.01, .01	.13				
SCR	0.57	-1.51, 2.65	0.14	-0.36, 0.64	.01	-.07, .10	.33				
BCC	1.12	-0.57, 2.80	0.34	-0.17, 0.86	.08	-.12, .27	.42*	.192	.00,.39	.078	-.12, .27
Model 4											
PCR	-0.05	-1.98, 1.89	-0.01	-0.46, 0.44	.00	-.01, .01	.13				
SCR	0.35	-1.84, 2.55	0.08	-0.44, 0.61	.00	-.04, .05	.33				
BCC	0.71	-1.34, 2.75	0.22	-0.41, 0.84	.02	-.08, .12	.42*				
SPN	1.40	-2.40, 5.19	0.23	-0.40, 0.86	.02	-.09, .13	.43*	.216	.00,.38	.025	-.09, .13

Model 5											
PCR	0.54	-1.34, 2.42	0.13	-0.31, 0.56	.01	-.06, .08	.13				
SCR	1.18	-1.00, 3.36	0.28	-0.24, 0.81	.05	-.09, .18	.33				
BCC	0.12	-1.85, 2.09	0.04	-0.57, 0.64	.00	-.01, .02	.42*				
SPN	2.79	-0.97, 6.55	0.46	-0.16, 1.08	.08	-.10, .26	.43*				
SLF	-2.27*	-4.52, -0.03	-0.51*	-1.02, -0.01	.16	-.08, .40	-.10	.374	.00,.51	.157*	-.08, .40

Note. * = $p < .05$. ** = $p < .001$. SLF: superior longitudinal fasciculus. BCC: body of corpus coliseum. SPN: splenium of corpus coliseum. PCR: posterior corona radiata. SCR: superior corona radiata. SOG: superior occipital gyrus

5.3.3. The effects of WM tracts on aSC and eSC-modulated connectivity of the DAN and FPN in younger and older adults

To recap, the gPPI procedure was conducted on constructing the functional connectivity network based on the four functional ROIs, namely the right IPS and FEF which are within the DAN and the right LPFC and PPC which are within the FPN. There are two types of results for each of the PCR, SLF and SCR tracts. The first type of results is on how each of aSC and eSC influenced the WM-modulated functional connective within the DAN or FPN for the younger and older groups. The second type of results is on the between-group differences in the WM-modulated functional connectivity within DAN or FPN for each of aSC and eSC conditions.

Ageing effects on modulating PCR on DAN or FPN connectivity

The PCR showed significant effects on the task-modulated connectivity (Figure 5.8). Among the younger subjects, the effects were observed on the FPN but not DAN. For the right PPC, it showed an increase in connectivity with the right SMG but a decrease in connectivity with the left AG during eSC condition (Figure 5.8A). In the same task condition, for the right LPFC, it showed an increase in connectivity between with the right SMG but decreases in connectivity with the left SFG and sLOC (including portion of the precuneus) (Figure 5.8B). The right LPFC also showed decreases in connectivity with the left SFG, sLOC and precuneus during aSC condition (Figure 4.8C). Modulations of connectivity were substantially less among the older subjects, which was only observed in DAN but not FPN. For the right IPS, it showed an increase in connectivity with the right anterior division of the superior temporal gyrus (aSTG) during aSC condition (Figure 5.8D).

Direct comparisons between the younger and older subjects, under the influences of the PCR, showed increases in connectivity within the DAN particularly in the parieo-occipital regions (Figure 5.9). When compared with older subjects, the increases in the younger subjects were among the right FEF, right sLOC and left occipital fusiform gyrus (OFusG) for eSC condition (Figure 5.9A), and between the IPS and intracalcarine cortex (ICC) for aSC condition (Figure 5.9B); and increases in connectivity between the right IPS and the right caudate for eSC condition (Figure 5.9D). The PCR effects on the FPN connectivity were observed in aSC condition only and limited to LPFC. When compared with younger subjects, older subjects showed increases in connectivity between the right LPFC and the left sLOC for aSC condition (Figure 5.9C).

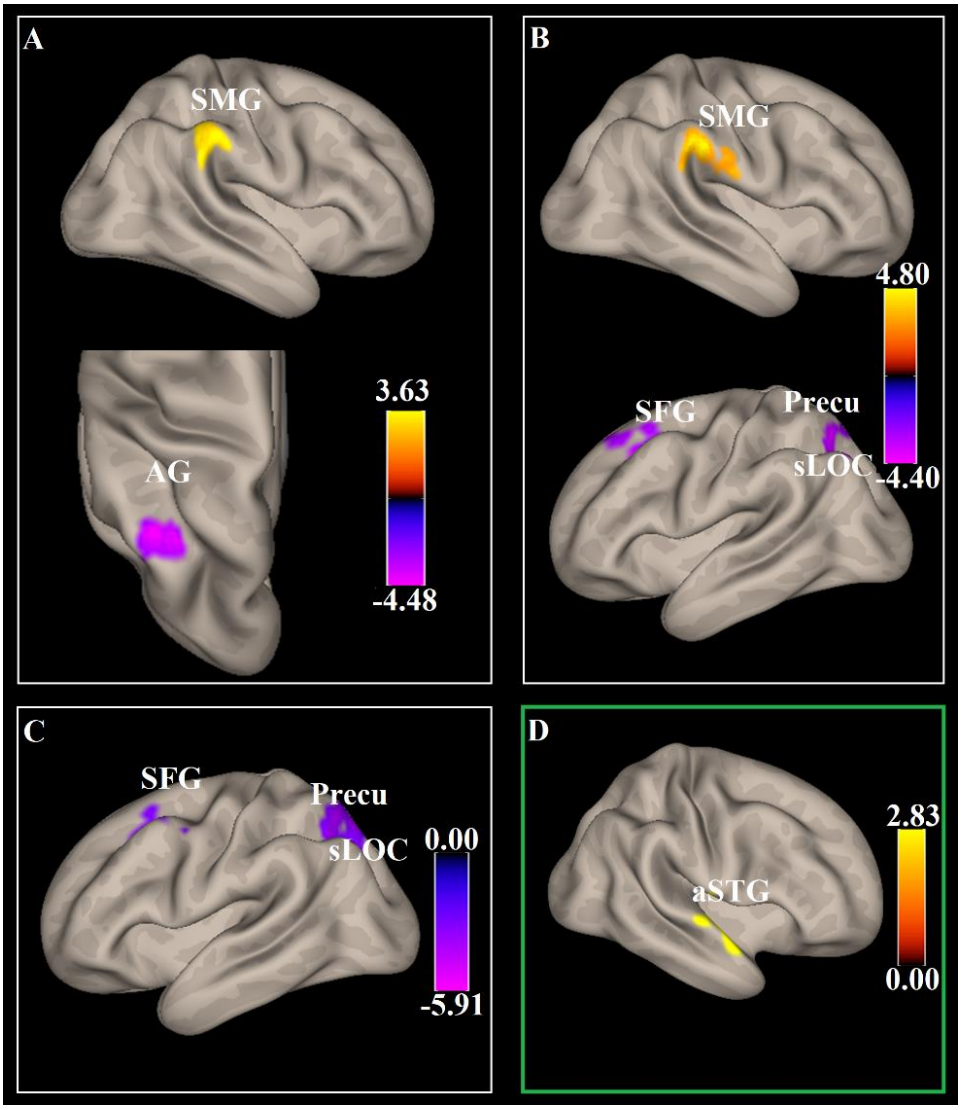

Figure 5. 8 The effects of PCR WM tract on the connectivity of the task-modulated FPN and DAN in younger (white boxes) and older (green box) subjects. A: PCR ~ PPC in eSC > NEU in younger subjects. B: PCR ~ LPFC in eSC > NEU in younger subjects. C: PCR ~ LPFC in aSC > NEU in younger subjects. D: PCR ~ IPS in aSC > NEU older subjects. The connectivity blobs are thresholded and cluster level corrected using FDR for multiple comparison at p = .05. SMG: supramarginal gyrus. AG: angular gyrus. SFG: superior frontal gyrus. Precu: precuneus. sLOC: superior division of lateral occipital cortex. aSTG: anterior division of superior temporal gyrus.

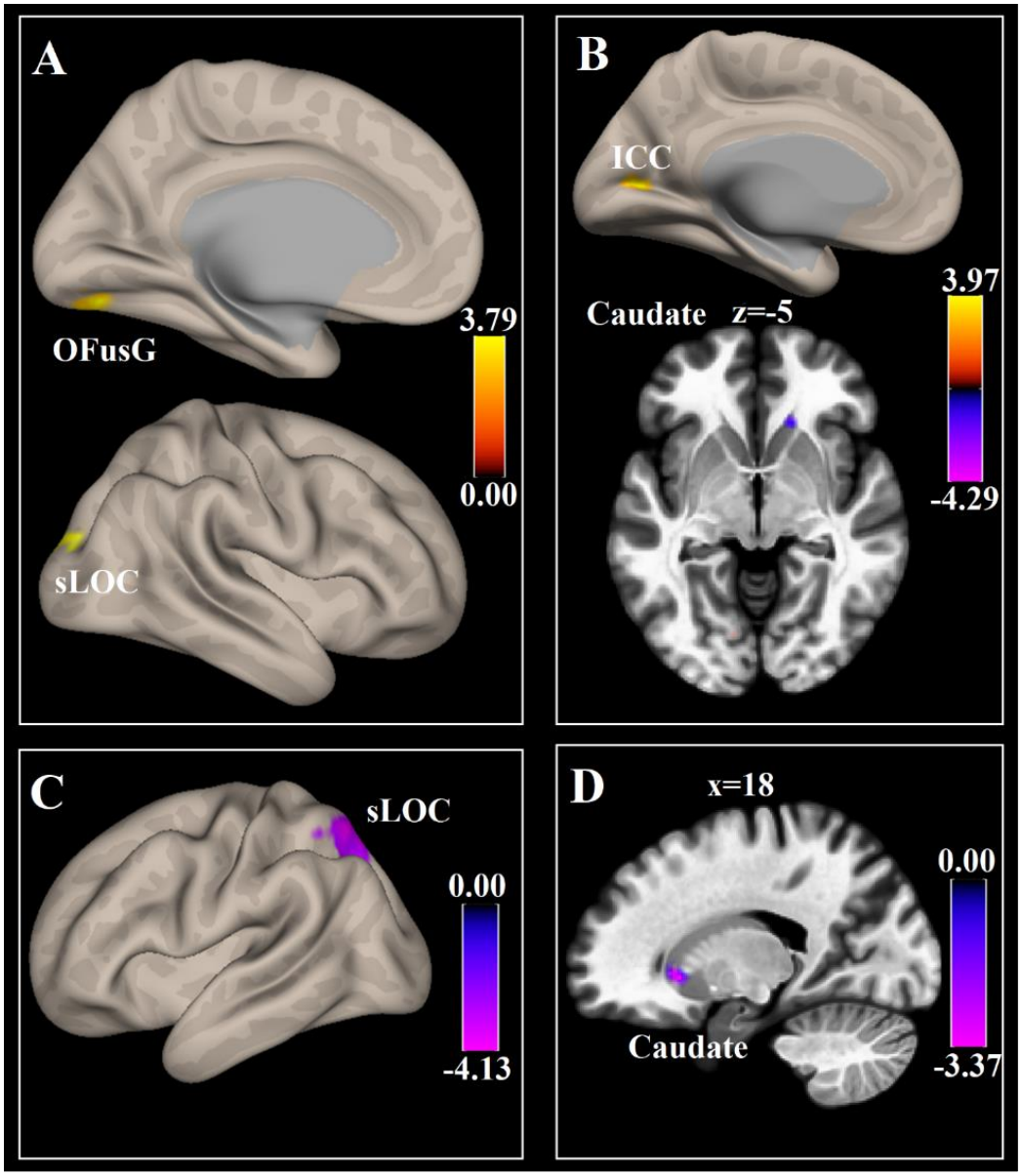

Figure 5. 9. Significant differences between the older and younger subjects in the effects of PCR WM tract on the connectivity of the task-modulated DAN and FPN. A: Right FEF as seed for YOUNG_PCR > OLD_PCR as in-between subject contrast and eSC > NEU as in-between condition contrasts. B: Right IPS as seed for YOUNG_PCR > OLD_PCR as in-between subject contrast and aSC > NEU as in-between condition contrasts. C: Right LPFC as seed for YOUNG_PCR > OLD_PCR as in-between subject contrast and aSC > NEU as in-between

condition contrasts. D: Right IPS as seed for YOUNG_PCR > OLD_PCR as in-between subject contrast and eSC > NEU as in-between condition contrasts. The connectivity blobs are thresholded and cluster level corrected using FDR for multiple comparison at $p = .05$. sLOC: superior division of lateral occipital cortex. ICC: intracalcarine cortex. OFusG: occipital fusiform gyrus.

Aging effect on modulating SLF on DAN or FPN connectivity

The SLF showed significant effects on the task-modulated connectivity (Figure 5.10). Among the younger subjects, the effects were observed on both DAN and FPN. For the right FEF, it showed increases in connectivity with the right MFG and inferior lateral occipital cortex (iLOC) (Figure 5.10A) for aSC condition; and increases in connection with the right MFG, right frontal pole and right central opercular cortex (CO), but a decrease in connectivity with the right MFG and frontooperculum cortex (FO) for eSC condition (Figure 5.10D). For the right IPS, there were decreases in connectivity with the right iLOC and frontoorbital cortex (FOrb) for eSC condition (Figure 5.10B), and decreases in connectivity among the right MFG, STG and ITG for aSC condition (Figure 5.10C). Among the older subjects, the SLF effects were observed only in FPN. For the right LPFC, there were decreases in connectivity with the right MFG and IFG for aSC condition (Figure 5.10E). For the right PPC, its connectivity with the bilateral FP was decreased for eSC (Figure 5.10F) and with the right FP and left PaCiG was decreased for aSC condition (Figure 5.10G).

Direct comparisons between the younger and older subjects, under the influences of the SLF, showed modulations in connectivity only in aSC condition (Figure 5.11). When compared with younger subjects, within the DAN, a decrease in connectivity in the older subjects were between the right FEF and right FP (Figure 5.11A), but an increase in connectivity between the right IPS and MFG and posterior portion of ITG (pITG) for aSC condition (Figure 5.11B). Within

the FPN, the older subjects showed an increase in connectivity between the right LPFC and the right posterior portion of SMG (pSMG) (Figure 5.11C).

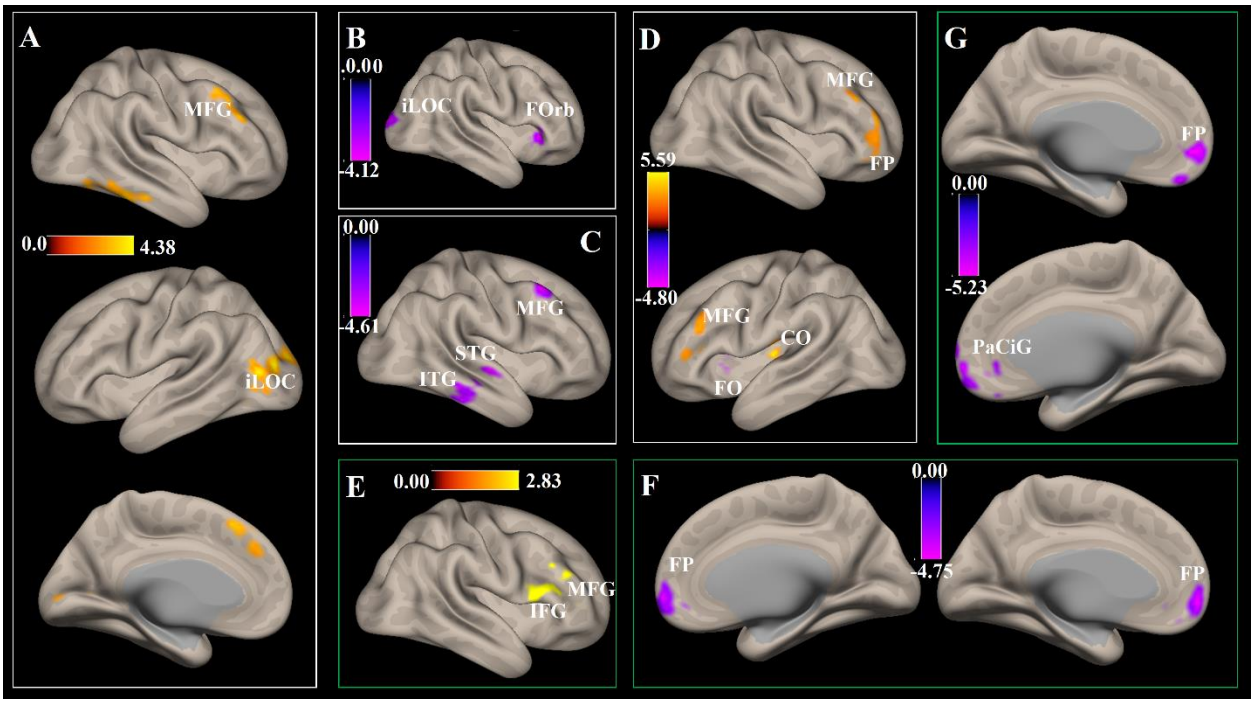

Figure 5. 10. The effects of SLF WM tract on the connectivity of the task-modulated FPN and DAN in younger (white boxes) and older (green box) subjects. A: SLF ~ FEF for aSC > NEU. B: SLF ~ IPS for eSC > NEU. C: SLF ~ IPS for aSC > NEU. D: SLF ~ FEF for eSC > NEU. E: SLF ~ LPFC for aSC > NEU. F: SLF ~ PPC for eSC > NEU. G: SLF ~ PPC for aSC > NEU. The connectivity blobs are thresholded and cluster level corrected using FDR for multiple comparison at p =.05. MFG: middle frontal gyrus. iLOC: inferior division of lateral occipital cortex. Forb: Fronto-orbital cortex. STG: superior temporal gyrus. ITG: inferior temporal gyrus. IFG: inferior

frontal gyrus. FP: frontal pole. PaCiG: para-cingulate gyrus. FO: fronto- Operculum cortex. CO: central opercular cortex.

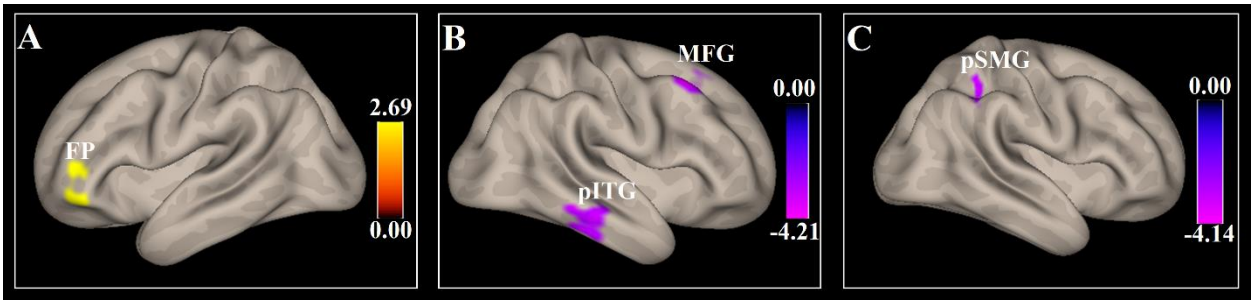

Figure 5. 11. Significant differences between the older and younger subjects in the effects of SLF WM tract on the connectivity of the task-modulated DAN and FPN. A: Right FEF as seed for YOUNG_SLF > OLD_SLF as in-between subject contrast and aSC > NEU as in-between condition contrasts. B: Right IPS as seed for YOUNG_SLF > OLD_SLF as in-between subject contrast and aSC > NEU as in-between condition contrasts. C: Right LPFC as seed for YOUNG_SLF > OLD_SLF as in-between subject contrast and aSC > NEU as in-between condition contrasts. The connectivity blobs are thresholded and cluster level corrected using FDR for multiple comparison at p = .05. FP: frontal pole. MFG: middle frontal gyrus. pITG: posterior division of the inferior temporal gyrus. pSMG: posterior division of the supramarginal gyrus.

Aging effect on modulating SCR on DAN or FPN connectivity

The SCR showed significant effects on the task-modulated connectivity (Figure 5.12). Among the younger subjects, the effects were observed on the DAN and FPN. For the right FEF of DAN, it showed an increase in connectivity with the right MFG for aSC condition (Figure 5.12A), and with the right MFG and lingual gyrus (LG) for eSC condition (Figure 5.12D). For the right IPS of DAN, it had decreases in connectivity with the bilateral precuneus (Figure 5.12) for aSC condition (Figure 5.12B), and with the bilateral PaCiG for eSC condition (Figure 5.12E). For

the right PPC of FPN, it showed an increase in connectivity with the right occipital pole (OP) but decreases in connectivity with the right ACC, PaCiG and temporooccipital parts of middle temporal gyrus (toMTG) for aSC condition (Figure 5.12C), and an increase in connectivity with the left OFusG for eSC condition (Figure 5.12F). In older subjects, the SCR effect also acted on the DAN and FPN. For the right FEF in DAN, it showed a decrease in connectivity with the caudate (Figure 5.12G) for aSC condition but an increase in connectivity with the left angular gyrus (AG) for eSC condition (Figure 5.12I). For the right LPFC, it had an increase in connectivity with the right IFG for eSC condition (Figure 5.12H).

Direct comparisons between the younger and older subjects, under the influences of the SCR, showed modulations in connectivity in both aSC and eSC conditions (Figure 5.13). When compared with younger subjects, within the DAN, an increase in connectivity in the older subjects was between the right FEF and left precuneus and left SMA, and left PreCG but decreases in connectivity between the right FEF and the right MFG (Figure 5.13A). Within the same DAN, the older subjects showed increases in connectivity between the right IPS and the bilateral medial frontal cortex (MedFC) for eSC condition (Figure 5.13B). Within the FPN, the older subjects had decreases in connectivity between the right PPC and the right sLOC for eSC condition (Figure 5.13C).

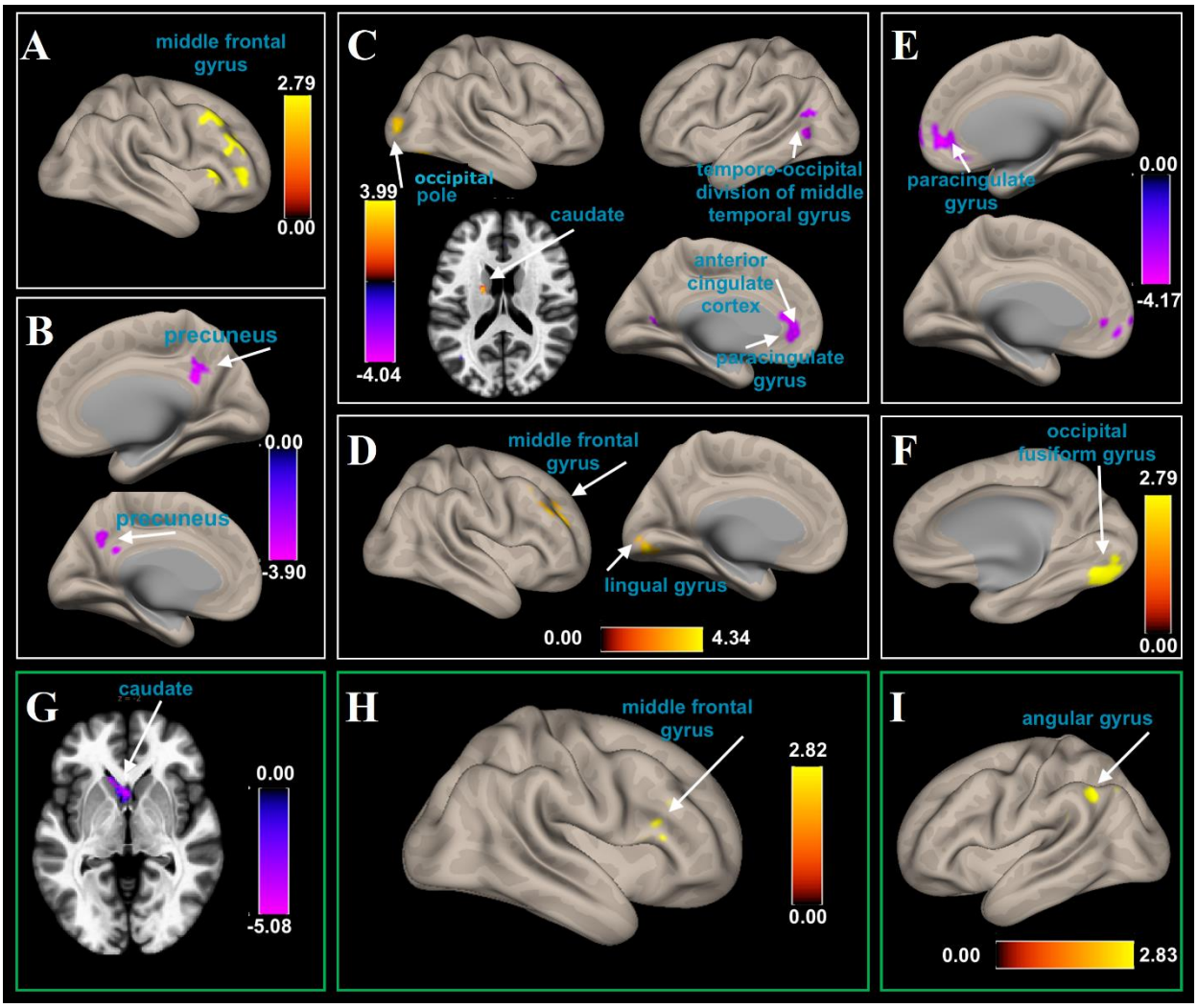

Figure 5. 12. The effects of SCR WM tract on the connectivity of the task-modulated FPN and DAN in younger (white boxes) and older (green box) subjects. A: SCR ~ FEF for aSC > NEU. B: SCR ~ IPS for aSC > NEU. C: SCR ~ PPC for aSC > NEU. D: SCR ~ FEF for eSC > NEU. E: SCR ~ IPS for eSC > NEU. F: SCR ~ PPC for eSC > NEU. G: SCR ~ FEF for aSC > NEU. H: SCR ~ LPFC for eSC > NEU. I: SCR ~ FEF for eSC > NEU. The connectivity blobs are thresholded and cluster level corrected using FDR for multiple comparison at p =.05.

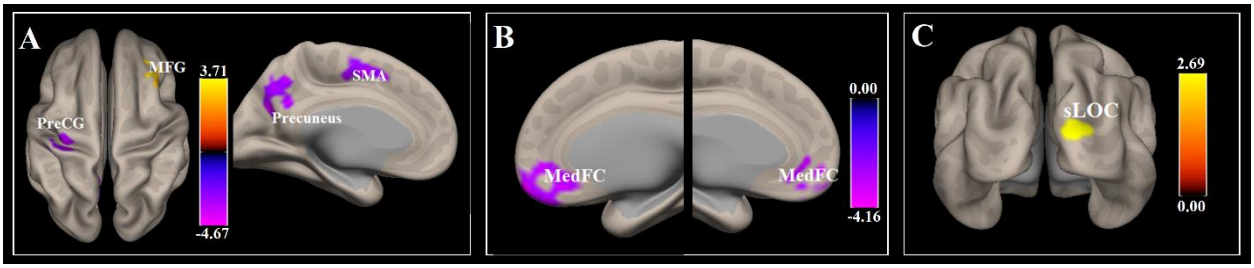

Figure 5. 13. Significant differences between the older and younger subjects in the effects of SCR WM tract on the connectivity of the task-modulated of DAN and FPN. A: Right FEF as seed for YOUNG_SCR > OLD_SCR as in-between subject contrast and aSC > NEU as in-between condition contrasts. B: Right IPS as seed for YOUNG_SCR > OLD_SCR as in-between subject contrast and eSC > NEU as in-between condition contrasts. C: Right PPC as seed for YOUNG_SCR > OLD_SCR as in-between subject contrast and eSC > NEU as in-between condition contrasts. The connectivity blobs are thresholded and cluster level corrected using FDR for multiple comparison at p = .05. PreCG: precentral gyrus. MFG: middle frontal gyrus. SMA: somatosensory association cortex. MedFC: medial frontal cortex. sLOC: superior division of lateral occipital cortex.

5.4. Discussion

There are three main findings in the fMRI-DTI study. First finding is the consistent pattern of the structure-function relationship of the PCR revealed for the aSC and eSC. In aSC condition, positive correlations of BOLD signals in precuneus and IPL with the FA values of PCR in older adults and negative correlation of BOLD signal in SOG (for aSC condition) and precuneus (for eSC condition) in younger adults were found. The PCR influence was on the SOG in aSC but precuneus in eSC. Second, WM of the PCR mainly influences aSC-modulated connectivity of the FEF with parieto-occipital circuits whereas SLF modulates FEF nodes to the parieto-frontal circuits and facilitates the integration of both dorsal and ventral streams at MFG carrying top-down contents of aSC signals. Third, significant age- and task-related modulations were revealed in the WM tracts on the functional connectivity involving the right FEF and IPS within the dorsal attention network (DAN) and involving the right LPFC and PPC within the fronto-parietal network (FPN). These findings supported the first hypothesis set for this study which is structural integrity (as indexed by FA) influences and dissociates the neural activities associated with allocentric and egocentric spatial coding. There were significant differences in the nature, magnitude, and extent of the task-related modulations between the younger and older subjects. The second hypothesis can only be partially supported as the results only showed age-related effects exerted on PCC and LPFC but not MT in the older group in aSC condition. The WM tracts involved were rather different from those anticipated. Instead of ILF, SLF, ACR and SPN, they were PCR, SCR, and SLF.

5.4.1. Differential structure-function relationships in aSC and eSC

The DTI-fMRI results revealed that the relationships between the WM tracts and functional ROIs in each of aSC and eSC were opposite to one another between the older and younger subjects. For older subjects, the eSC-related activations in the right IPL were positively correlated with the FA values of BCC and PCR. The eSC-related activations in the right precuneus and FEF were positively correlated with FA values in the SCR and PCR respectively; and activations of the right IPL's were positively correlated with FA values of the body and splenium of the corpus callosum. In contrast, besides the positive versus negative relationships, the FA-BOLD in younger subjects were less substantial than the older subjects. The aSC-related activations in the right SOG and eSC-related activations in the right precuneus showed significant negative correlations with the FA values of PCR. These results demonstrated the structure-function relationships tend to be modulated by both the nature of the spatial tasks, namely allocentric versus egocentric, and the degrees of white-matter tract integrity as in the younger versus older groups.

The right fronto-parietal regions have been reported to specialize in mediating both aSC- and eSC-related processes (Kravitz et al., 2011; Ptak, 2012). The superior longitudinal fasciculus (SLF) connects the key neural substrates and was found associated with visuospatial attention processes (Ptak, 2012; Ptak & Schnider, 2010; Vaessen et al., 2016). For example, the SLF connects the prefrontal cortex was associated with the reorienting attention when unexpected stimuli appeared; while the inferior longitudinal fasciculus (ILF) connects the PPC was associated with orienting attention to relevant stimuli (Bennett et al., 2012; Grady, 2012). Orienting and reorienting processes are key elements in top-down attention allocation (Corbetta et al., 2005; Corbetta et al., 2008; Corbetta & Shulman, 2002; Derbie et al., 2021; Geng & Vossel, 2013;

Kravitz et al., 2013). In our study, no significant relationship was observed between the SLF, ILF and other longitudinal tracts with any of the designated ROIs in either aSC or eSC conditions. Instead, the results revealed that the aSC- and eSC-related functional ROIs were correlated with the region-specific and non-longitudinal fibre bundles including the posterior and superior corona radiata, and body and splenium of the corpus callosum. The findings of the region-specific task-relevant FA-BOLD relationships are consistent with those reported in previous studies (Madden et al., 2010; Madden et al., 2007; Tuch et al., 2005). These studies have also shown a correlation between RT on a visual attention task and FA in the SPN.

Previous studies revealed age-related changes in visuospatial attention such as executive control of attention was associated with changes in the myelinated fibre bundles, which affected the speed and actions of the signal propagation across different neural networks in respond to the incoming stimuli (Rosenzweig, Vukadinovic, Turner, & Catani, 2012; Tuch et al., 2005). According to the myelin hypothesis, the correlation between the task-related BOLD signals and the FA values of these bundle/tracts should be negative. On the other hand, the increase in myelin thickness, which increases FA values, was found to correlate with the increase in the speed of behavioral response (Rosenzweig et al., 2012; Tuch et al., 2005). Consistent to the myelin hypothesis, without adjusting for the age-related effects, the results of this study showed the reaction times in both the aSC and eSC conditions were negatively correlated with the FA values of the PCR, SPN, and SLF. The same patterns of correlations were observed in both the younger and older groups. The relationships between the reaction times and white matter integrity is a rather simple account of the uniqueness of the neural processes behind the spatial coding. The differences in the structure-function relationship across the younger and older subjects are also not considered. The results therefore should be interpreted with caution.

5.4.2. Influence of WM integrity on BOLD signals

The results of this study revealed region-specific and microstructure of the white matter tracts were important features influencing the unique functional ROIs for mediating spatial coding processes. For instance, the FA values of the posterior and superior corona radiata respectively accounted for the highest variances of the activations in the IPL and FEF during aSC condition. The correlations FA-BOLD correlations were positive in the older subjects but were negative in the younger subjects for both the aSC and eSC conditions. The findings on the region- and task specificity are consistent with those reported in other studies (for review: Warbrick, Rosenberg, & Shah, 2017). Negative FA-BOLD association has been interpreted as neural processing efficiency in that increases in FA values would reduce task-relevant activations resulted in increases in task processing efficiency (Burzynska et al., 2013; Zhu, Hakun, Johnson, & Gold, 2014; Zhu, Johnson, Kim, & Gold, 2015). An increase in FA suggests decrease in water diffusion of the fibre bundles suggesting better organization within the fibre bundles for facilitating transmission of functional signals along and across fibre tracts (Davis & Moayedi, 2013). In case of older subjects showed degraded performances in allocentric but not egocentric spatial coding (for review: Colombo et al., 2017), one would expect positive FA-BOLD relationship in older subjects for aSC condition. Consistent with this preposition, the results indicate that the effect of the posterior and superior corona radiata on the BOLD signal was positive in the aSC condition in older subjects. This effect was found in the frontoparietal regions suggesting that the aging effect tended to act on the FPAN (Andrews-Hanna et al., 2007). It is noteworthy that negative FA-BOLD relationships were revealed in the younger subjects. These were the PCR to the BOLD aSC BOLD signal in SOG and eSC BOLD signal in precuneus. When compared with the younger subjects, older subjects in this study showed extensive activations in the parietal regions for both the aSC and eSC conditions

(see Figure 4.6), with negative FA-BOLD. The findings in the occipitoparietal regions in younger subjects may suggest better performances in allocentric spatial coding would have attributed to the higher FA resulting in lower BOLD signals for producing the responses on task, which is analogous to the neural processing efficiency hypothesis applicable to younger adults (Burzynska et al., 2013). The neural efficiency hypothesis states that faster performance (in both speed and accuracy) in younger adults often accompanied by less extensive activation than the activation by slower performance in older adults (Haier et al., 1988).

5.4.3. Influence of PCR integrity on functional connectivity

The last part of the study is to explore how white matter integrity would influence the functional connectivity of neural substrates mediating aSC and eSC. The knowledge gained further informs the neural models of spatial coding adding to the findings revealed in the previous sections. In general, the results revealed from gPPI showed dissociable age-related structure-function relationships both in terms of magnitude and patterns of functional connectivity among neural substrates in the DAN and FPN for the aSC and eSC conditions.

Modulated with age-related PCR FA differences, there were significant increases in functional connectivity of FEF with other nodes in the parietooccipital regions including sLOC and OFusG in the eSC condition. The age-related PCR effect was found to mainly acted on the decrease in the FEF-sLOC connectivity. The age-related changes in the FEF connectivity within the DAN can be interpreted based on the neural processing efficiency which suggests that the increases in the functional connectivity older subjects might have required more neural resource for compensating the white matter degradation than their younger counterpart (Davis & Moayedi, 2013; Haier et al., 1988). For the FEF-sLOC, sLOC has been shown in an animal study to modulate

processing of object representation in visual-field (James, Humphrey, Gati, Menon, & Goodale, 2002).

Our findings on the FEF connectivity and eSC are consistent with those reported in other studies highlighting the role of FEF in top-down processing of visual contents relevant to egocentric spatial coding (Kravitz et al., 2011; Ptak, 2012; Vossel et al., 2014). It is plausible that, relative to younger subjects, the slower reaction times in the older subjects is likely to be attributed to the decreased in the functional connectivity of the right FEF with other nodes within the DAN. The implication of the decrease in the FEF-sLOC connectivity is that the impact might have been under the influence of the PCR and happened as early as when older subjects processed the visual stimuli in the egocentric spatial coding task. Different from eSC, findings in the aSC condition revealed, under the influence of the PCR, there were significant increases in the LPFC connectivity with sLOC within the FPN in the older subjects. As the LPFC was found to associate with top-down attention control and execution (Cieslik, Zilles, Grefkes, & Eickhoff, 2011; Zhu et al., 2014), the increase in the LPFC-sLOC connectivity in aSC indicates that older subjects would have intensified the attention control and executive for processing the visual representations during the allocentric spatial coding task.

The findings on the connectivity of LPFC and PPC within the FPN, under the influence of PCR, with the precuneus, AG and SFG suggest the plausible involvement of the default mode network (Fox et al., 2005) in the eSC condition among the younger subjects. The deceases in these connectivity reveal the possibility that near and far nodes within the FPN might have competed for mediating the task-related neural efficiency (Burzynska et al., 2013; Neubauer & Fink, 2009; Zhu et al., 2014). In contrast, the connectivity of LPFC and PCC with the SMG however was

increased in the eSC condition. SMG was found to mediate visual object recognition, particularly the when top-down competing objects appeared in the visual field (Rushworth & Taylor, 2006). The influence of PCR also covered the connectivity of IPS with the anterior division of superior temporal gyrus (aSTG) in the aSC condition suggesting the involvement of working memory when older subjects performed the task (Byrne et al., 2007; Chen et al., 2014; Milner & Goodale, 2008).

Age-related differences showed further dissociation in the functional connectivity under the influence of PCR between the two types of spatial coding. The age-related differences were unique in the FEF connectivity with the sLOC and OFusG for the eSC condition, and the IPS connectivity with the ICC for the aSC condition. Older subjects had decreases in the connectivity when compared with the younger subjects. Functionally, the OFusG, sLOC, and ICC were reported to feed object representation and recognition information to the FEF and IPS of DAN (Kravitz et al., 2011; Szczepanski et al., 2013). The results of this study further demonstrated that these neural substrates were under the influence of PCR, functionally connected with each of the FEF and IPS, as well as serving distinctive roles in each spatial coding type. The finding of the IPS-ICC is worth noting that the role of the ICC in allocentric spatial coding would have been to project visual signals involving the parieto-medial temporal pathway (Kravitz et al., 2011). The nature of the IPS connectivity for both aSC and eSC in younger subjects indicates that the visual signal projection would also have involved the parieto-occipital circuits. The connectivity of the IPS and LPFC with the caudate in the eSC condition suggests sensorimotor coordination might have involved when performing on the task (Grahn, Parkinson, & Owen, 2008).

5.4.4. Influence of SLF integrity on functional connectivity

The influences of the SLF on functional connectivity within the DAN were found to be different between the two types of spatial coding. In younger subjects, the SLF influence lowered the IPS connectivity in both the aSC and eSC conditions. The connectivity was between IPS and Forb (near node) and iLOC (far node) for the eSC condition, and MFG, STG, and ITG for the aSC condition. Younger subjects with shorter reaction times were associated with lower activations among the connected neural substrates. Other studies revealed higher task performance, i.e. fast and accurate responses, among young adults were commonly associated with lower brain activities than those of lower performance (Burzynska et al., 2013; Neubauer & Fink, 2009). This premises appeared to hold for IPS, but not for FEF. In younger subjects, the SLF influence mainly increased the FEF connectivity in both the aSC and eSC conditions. The connectivity was between FEF and MFG and iLOC for aSC condition and bilateral MFG, FP, and CO.

Two important implications could be drawn from the SLF influence to IPS and FEF that the two DAN areas modulate both aSC and eSC quite differently and while IPS rely on gray matter connectivity, the FEF might be critical node for feedforward and feedbackward loops in resource demanding aSC (involving iLOC, ITG, MFG, and SFG) and in eSC (involving MFG, FP, and CO) in way WM integrity facilitates the gray matter aSC/eSC function. In anyway, the DAN (IPS and FEF) appeared to be engaged and integrate aSC signals from the ventral stream as seen from the strong connection to temporal lobe and SLF facilitating the near and far nodes subserving spatial coding.

The between-group comparisons further signify the importance of the SLF on influencing the functional connectivity particularly in the DAN and for allocentric spatial coding. Similarly,

differences are observed between the FEF and IPS. First, aging effects appear to only act on the aSC-modulated connectivity but not on the eSC-modulated connectivity. Second, the increases in the connectivity of the IPS with MFG and pITG were found to be much stronger than that in the connectivity of the FEF and FP suggesting that age-related changes in allocentric spatial coding would have involved the SLF integrity for mediating priority mapping (Ptak, 2012). The priority mapping is to inhibit the influence of bottom-up signals within the PPC top-down processing between competing targets and distractors (Geng & Mangun, 2009). Besides visual mapping, IPS has been revealed playing a role in the visuospatial attention when maintaining images in working memory (Bray, Shimojo, & O'Doherty, 2007). The neural processes mentioned are critical during allocentric spatial coding. Apart from DAN, age-related differences were also revealed in the LPFC of FPN under the aSC condition. The SLF- and aSC-modulated connectivity showed an increase between the LPFC and pSMG among older adults. pSMG mediates visual object recognition and spatial updating, and efficient visual updating is a key element of top-down attention control (Burles, Slone, & Iaria, 2017). Together with the LPFC which plays a role in top-down attention control (Corbetta et al., 2008; Corbetta & Shulman, 2002), the impact on the LPFC-pSMG connectivity by the SLF perhaps can explain slower reaction times among the older subjects in the aSC task compared to younger subjects. Integrating the findings on the DAN and FPN, the integrity of the SLF is likely to exert its influence on the parieto-medial pathway in which the MFG serves as a "circuit-breaker" for passing top-down visuospatial information from the ventral stream (reorienting and VSTM components of aSC) and the DAN for spatial updating by the neural substrates in the parietal lobe and executive attention in the LPFC, while are critical in allocentric spatial coding.

5.4.5. Influence of SCR integrity on functional connectivity

The findings on the influence of SCR revealed comparable results of those in SLF that its integrity modulated IPS and FEF within the DAN rather differently in the aSC and eSC conditions. One interesting finding revealed is the connectivity of IPS with the precuneus, which further confirm visual working memory is crucial in the processing of the visuospatial images in allocentric spatial coding (Bray et al., 2007). On the contrary, under the SCR's influence, the results on the connectivity of the FEF with the MFG indicated that it did not differentiate between aSC and eSC, of which is different from the results in the SLF. The FEF-MFG connectivity was found significantly modulated by the SCR integrity in both the aSC and eSC conditions when compared with the significantly modulated by the SLF integrity only in the aSC condition. The most noticeable SCR influence was observed on the increases in connectivity of the PPC with the toMTG, ACC, OP, and caudate in the aSC condition. This was compared with the increase in the connectivity of the PPC with the OFusG in the eSC condition.

The main observation on the between-group comparisons revealed, under the influence of the SCR integrity and aSC task condition, older subjects tended to show relative increase in connectivity of the FEF with the precuneus, SMA and PreCG but a decrease in connectivity between FEF and MFG. The opposite patterns of connectivity from the FEF are consistent with those described as the age-related posterior to anterior shift unique to aging effects (Brosnan et al., 2018; Grady, 2012; Zhang, Lee, & Qiu, 2017). These two regions are thought to engage in memory-guided visuospatial attention tasks (Goldfarb, Chun, & Phelps, 2016) suggesting the unique neural processes involved in allocentric spatial coding.

5.4.6. Conclusion

The most significant structure-function relationships associated with aSC were between PCR and BOLD signal IPL, precuneus, and SOG and SCR with BOLD signal in FEF. Compared to aSC, very few FA-BOLD relationships were observed for the eSC. The right IPL was the most brain area that its aSC and eSC BOLD signals heavily associated to WM tracts. The main structure-function interaction was observed between PCR and FEF, SLF and FEF including regions in parieto-frontal areas, and SCR and PPC. While the PCR facilitates aSC-modulated connectivity of FEF mainly to parieto-occipital circuits, SLF appeared to hold the key nodes for FEF and parieto-frontal circuits (involving precuneus, aSMG, and SMA) and far reaching influence to both dorsal and ventral streams (STG, ITG) that top-down visual aSC signals integrated mainly at MFG. Disregarding of ageing, effect modulation of spatial coding in FEF requires structure-function interaction and connected to dorsal and ventral attention systems equally. The additional knowledge added to the model of spatial coding was that there is links between age-related allocentric declines in neural efficiency along the FPN, expressed in a stronger functional connectivity of key areas of the parieto-medial temporal pathways. The allocentric functional efficiency are linked to the function-structure interaction mediated by WM tract in PCR for parieto-occipital GM functions and SLF for near and far neural areas along the fronto-parietal attention network. WM integrity scaffolds neural areas subserving aSC in older adults, and less important for processing spatial coding in younger adults in-line with neural efficiency hypothesis.

CHAPTER 6

6. Integrated Model of Spatial Coding and General Conclusion

6.1. The Integrated Model of Spatial Coding

In Chapter 4, based on the ALE and fNIRS studies, an enhanced model of spatial coding was drawn. In the model, it was suggested that the two spatial coding types involves top-down attention, encoding visual representation, and response-mapping processes, which is sub-served by neural substrates in the parieto-frontal regions, whereas functional dissociation of the two spatial coding types were observed in parieto-occipital circuits (see Figure 4.1 in Chapter 4). Chapter 5 was aimed to test the enhanced spatial coding model and the robustness of the model in ageing, by using combined diffusion tensor imaging (DTI) and functional magnetic resonance imaging (fMRI) data from 27 younger adults and 24 older adults. Chapter results suggested that there is links between age-related allocentric declines in neural efficiency along the FPAN, expressed higher FA resulting in lower BOLD signals (negative relationship of BOLD signal and FA) analogous to the neural processing efficiency hypothesis (Haier et al., 1988; Neubauer & Fink, 2009). The allocentric functional efficiency were linked to the function-structure interaction mediated by WM tract in PCR for parieto-occipital GM functions and SLF for near and far neural areas along the fronto-parietal attention network, and SCR for PPC GM functions. Generally, WM integrity scaffolds neural areas subserving aSC in older adults, and less important for processing spatial coding in younger adults consistent with neural efficiency hypothesis. Based on the series of studies and results in this thesis, the following integrated model of spatial coding is deliberated.

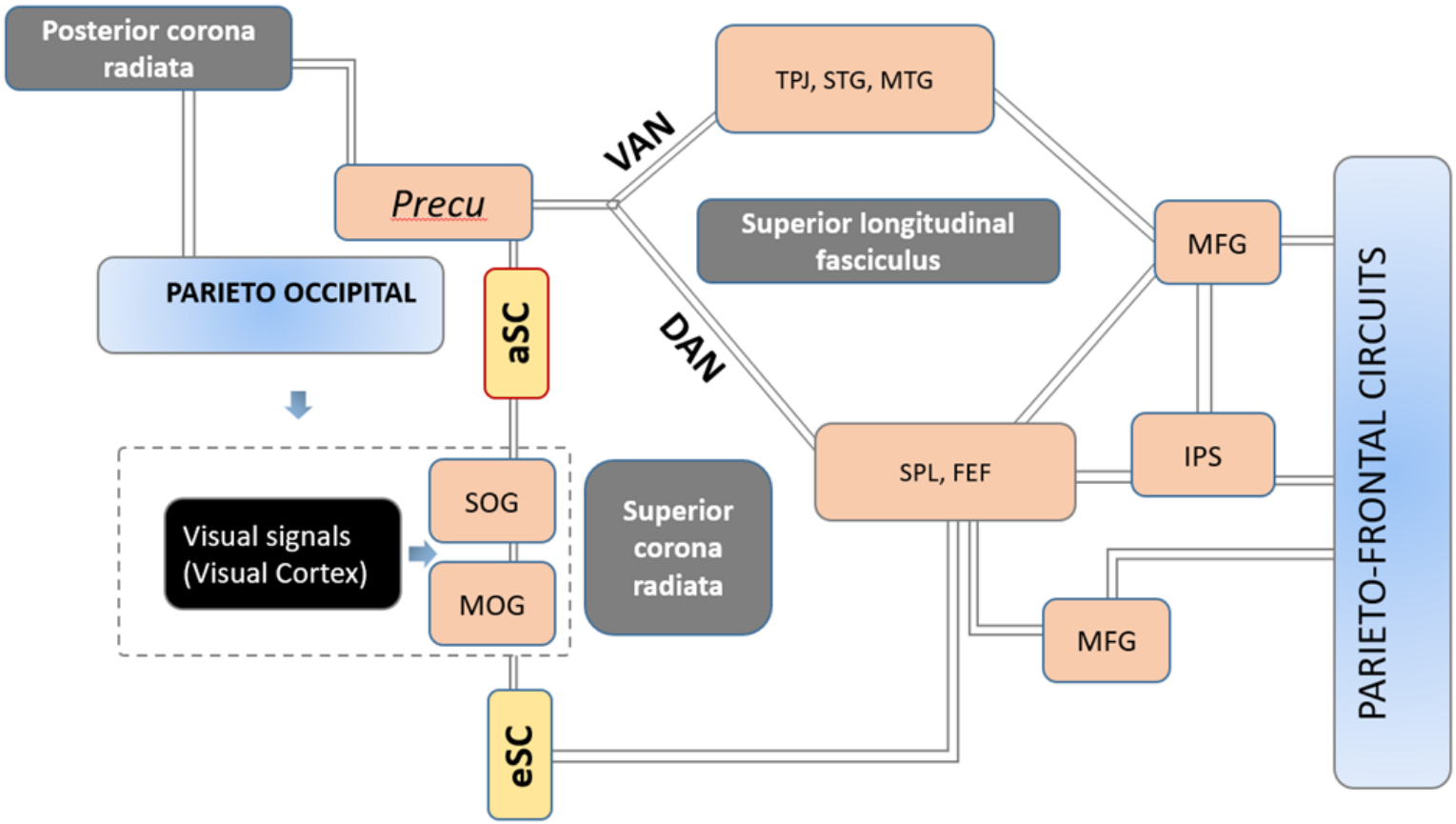
Posterior corona radiata
TPJ, STG, MTG
VAN
Precu
Superior longitudinal fasciculus
MFG
PARIETO OCCIPITAL
aSC
DAN
PARIETO-FRONTAL CIRCUITS
SPL, FEF
IPS
SOG
Visual signals (Visual Cortex)
Superior corona radiata
MOG
MFG
eSC

Figure 6. 1. The integrated model of spatial coding. Both spatial coding types differentiate in the parieto-occipital circuit and share the parieto-frontal circuit which subserve attention execution and response mapping. For aSC, visual signals projected from visual cortex are carried forward via the SOG to the caudal parts of inferior parietal lobule. The caudal parts of inferior parietal lobule feedforward the aSC signals to the precuneus and project them further to both the VAN and DAN. The VAN mainly subserves the visual short-term working memory while the DAN mainly subserves the spatial relationships of objects including attention shift, updating, and switching involved in aSC. The information flows from the VAN and DAN reaches the MFG for further processing. MFG serves as a control gate for both attention streams while IPS mainly feedforwards the DAN signals to the MFG. Further processing of the integrated aSC signals is subserved by the parieto-frontal circuits including DLPFC involving attention control and re-orientation. For eSC, visual signals from visual cortex are feedforward via the MOG to the caudal parts of the inferior parietal lobule. These signals can also flow directly to the precuneus from ?? depending on the nature of the visuospatial task. Different from aSC, eSC signals mainly are processes within the DAN. The processed eSC signals are projected to MFG which serves as a feedforward control mechanism to the parieto-frontal circuits subserving attentional control and response mapping. Both the aSC and eSC-modulated connectivity within the parieto-occipital circuits are facilitated by white-matter tract of the posterior corona radiata. The sub-regions within the superior parietal cortex which subserve both aSC and eSC are mainly interconnected by white-matter tract of the superior corona radiata. The SLF facilitates the near and far brain areas for both aSC and eSC-modulated connectivity's within the DAN. These includes parieto-occipital circuits and parieto-

frontal regions. On the other hand, SLF facilities for near and far brain areas only to aSC-modulated connectivity's within the VAN.

6.2. General Conclusion

In this thesis, using multimodal imaging methods, series of studies aimed at enhancing and integrating the model of spatial representations in human were carried out. Based on the evidence of neural underpinnings revealed sub-serving both aSC and eSC, the following conclusions can be drawn:

- The two spatial coding types are dissociated in the parieto-occipital circuits and share the parieto-frontal circuits. The parieto-frontal circuits are mainly involved in top-down attention, encoding visual representation, and response-mapping processes.
- When compared with eSC, aSC demands more orienting attention and updating of spatial information.
- Allocentric spatial coding recruit's different neural areas based on the nature and demand of the paradigm-specific processes which is not the case for egocentric spatial coding.
- The white-matter tract of the PCR facilitates aSC- and eSC-modulated connectivity of FEF mainly to parieto-occipital circuits.
- The white-matter tract of SLF holds the key nodes for FEF and parieto-frontal circuits (involving precuneus, aSMG, and SMA) and far-reaching influence to both dorsal and ventral streams (STG, ITG) that top-down visual aSC signals integrated mainly at MFG.
- The white-matter tract of SCR facilitates mainly aSC and eSC-modulated connectivity of the sub-regions within the PPC.

- Regardless of ageing, effect modulation of spatial coding in FEF requires structure-function interaction and connected to dorsal and ventral attention systems equally.
- Allocentric functional efficiency are associated with the function-structure interaction mediated by the white matter tract of PCR for parieto-occipital grey matter functions, SLF for near and far neural areas along the fronto-parietal attention network, and SCR for PPC grey matter functions.
- The MFG sub-serves as a control gate mechanism for signals projected from the DAN and FPN during aSC but only from the DAN during eSC.

References

Amso, D., & Scerif, G. (2015). The attentive brain: insights from developmental cognitive neuroscience. *Nat Rev Neurosci, 16*(10), 606-619. doi:10.1038/nrn4025

Andersson, J. L., Jenkinson, M., & Smith, S. (2007). Non-linear optimisation. FMRIB technical report TR07JA1. *Practice. 2007a Jun*.

Andrews-Hanna, J. R., Snyder, A. Z., Vincent, J. L., Lustig, C., Head, D., Raichle, Marcus E., & Buckner, R. L. (2007). Disruption of Large-Scale Brain Systems in Advanced Aging. *Neuron, 56*(5), 924-935. doi:10.1016/j.neuron.2007.10.038

Awh, E., & Jonides, J. (2001). Overlapping mechanisms of attention and spatial working memory. *Trends Cogn Sci, 5*(3), 119-126.

Barra, J., Laou, L., Poline, J.-B., Lebihan, D., & Berthoz, A. (2012). Does an oblique/slanted perspective during virtual navigation engage both egocentric and allocentric brain strategies? *PloS one, 7*(11), e49537.

Barrett, D. J., Bradshaw, M. F., Rose, D., Everatt, J., & Simpson, P. J. (2001). Reflexive shifts of covert attention operate in an egocentric coordinate frame. *Perception, 30*(9), 1083-1091.

Bennett, I. J., Motes, M. A., Rao, N. K., & Rypma, B. (2012). White matter tract integrity predicts visual search performance in young and older adults. *Neurobiology of aging, 33*(2), 433. e421-433. e431.

Bernier, P. M., & Grafton, S. T. (2010). Human posterior parietal cortex flexibly determines reference frames for reaching based on sensory context. *Neuron, 68*(4), 776-788. doi:10.1016/j.neuron.2010.11.002

Boccia, M., Nemmi, F., & Guariglia, C. (2014). Neuropsychology of Environmental Navigation in Humans: Review and Meta-Analysis of fMRI Studies in Healthy Participants. *Neuropsychology Review, 24*(2), 236-251. doi:10.1007/s11065-014-9247-8

Boccia, M., Sulpizio, V., Nemmi, F., Guariglia, C., & Galati, G. (2017). Direct and indirect parieto-medial temporal pathways for spatial navigation in humans: evidence from resting-state functional connectivity. *Brain Struct Funct, 222*(4), 1945-1957.

Botta, F., Santangelo, V., Raffone, A., Lupianez, J., & Belardinelli, M. O. (2010). Exogenous and endogenous spatial attention effects on visuospatial working memory. *Q J Exp Psychol (Hove), 63*(8), 1590-1602. doi:10.1080/17470210903443836

Bray, S., Shimojo, S., & O'Doherty, J. P. (2007). Direct instrumental conditioning of neural activity using functional magnetic resonance imaging-derived reward feedback. *J Neurosci, 27*(28), 7498-7507. doi:10.1523/Jneurosci.2118-07.2007

Brian, A. K. (2014). *Aging effect on egocentric and allocentric frames of reference in visual attention: an event-related potential (ERP) study.* (PhD dissertation). The Hong Kong Polytechnic University, Hong Kong.

Brosnan, M. B., Demaria, G., Petersen, A., Dockree, P. M., Robertson, I. H., & Wiegand, I. (2018). Plasticity of the Right-Lateralized Cognitive Reserve Network in Ageing. *Cereb Cortex, 28*(5), 1749-1759. doi:10.1093/cercor/bhx085

Burgess, N. (2006). Spatial memory: how egocentric and allocentric combine. *Trends Cogn Sci, 10*(12), 551-557. doi:10.1016/j.tics.2006.10.005

Burgess, N. (2008). Spatial cognition and the brain. *Ann N Y Acad Sci, 1124*(1), 77-97. doi:10.1196/annals.1440.002

Burles, F., Slone, E., & Iaria, G. (2017). Dorso-medial and ventro-lateral functional specialization of the human retrosplenial complex in spatial updating and orienting. *Brain Struct Funct, 222*(3), 1481-1493. doi:10.1007/s00429-016-1288-8

Burzynska, A. Z., Garrett, D. D., Preuschhof, C., Nagel, I. E., Li, S. C., Backman, L., . . . Lindenberger, U. (2013). A scaffold for efficiency in the human brain. *J. Neurosci., 33*(43), 17150-17159. doi:10.1523/jneurosci.1426-13.2013

Buschman, T. J., & Miller, E. K. (2007). Top-down versus bottom-up control of attention in the prefrontal and posterior parietal cortices. *Science, 315*(5820), 1860-1862. doi:10.1126/science.1138071

Byrne, P., Becker, S., & Burgess, N. (2007). Remembering the past and imagining the future: a neural model of spatial memory and imagery. *Psychol Rev, 114*(2), 340-375. doi:10.1037/0033-295X.114.2.340

Castiello, U. (2005). The neuroscience of grasping. *Nat Rev Neurosci, 6*(9), 726-736. doi:10.1038/nrn1744

Chafee, M. V., Averbeck, B. B., & Crowe, D. A. (2007). Representing spatial relationships in posterior parietal cortex: single neurons code object-referenced position. *Cereb Cortex, 17*(12), 2914-2932. doi:10.1093/cercor/bhm017

Chechlacz, M., Gillebert, C. R., Vangkilde, S. A., Petersen, A., & Humphreys, G. W. (2015). Structural Variability within Frontoparietal Networks and Individual Differences in Attentional Functions: An Approach Using the Theory of Visual Attention. *J. Neurosci., 35*(30), 10647-10658. doi:10.1523/jneurosci.0210-15.2015

Chechlacz, M., Humphreys, G. W., Sotiropoulos, S. N., Kennard, C., & Cazzoli, D. (2015). Structural organization of the corpus callosum predicts attentional shifts after continuous theta burst stimulation. *J Neurosci, 35*(46), 15353-15368.

Chechlacz, M., Rotshtein, P., Bickerton, W.-L., Hansen, P. C., Deb, S., & Humphreys, G. W. (2010). Separating neural correlates of allocentric and egocentric neglect: distinct cortical sites and common white matter disconnections. *Cogn. Neuropsychol., 27*(3), 277-303.

Chen, Q., Weidner, R., Weiss, P. H., Marshall, J. C., & Fink, G. R. (2012). Neural interaction between spatial domain and spatial reference frame in parietal-occipital junction. *J Cogn Neurosci, 24*(11), 2223-2236. doi:10.1162/jocn_a_00260

Chen, Y., Monaco, S., Byrne, P., Yan, X., Henriques, D. Y., & Crawford, J. D. (2014). Allocentric versus egocentric representation of remembered reach targets in human cortex. *J. Neurosci., 34*(37), 12515-12526. doi:10.1523/JNEUROSCI.1445-14.2014

Chica, A. B., Bartolomeo, P., & Lupianez, J. (2013). Two cognitive and neural systems for endogenous and exogenous spatial attention. *Behav Brain Res, 237*, 107-123. doi:10.1016/j.bbr.2012.09.027

Chun, M. M., Golomb, J. D., & Turk-Browne, N. B. (2011). A taxonomy of external and internal attention. *Annu Rev Psychol, 62*, 73-101. doi:10.1146/annurev.psych.093008.100427

Cieslik, E. C., Zilles, K., Grefkes, C., & Eickhoff, S. B. (2011). Dynamic interactions in the fronto-parietal network during a manual stimulus–response compatibility task. *NeuroImage*, *58*(3), 860-869. doi:https://doi.org/10.1016/j.neuroimage.2011.05.089

Clark, K., Squire, R. F., Merrikhi, Y., & Noudoost, B. (2015). Visual attention: linking prefrontal sources to neuronal and behavioral correlates. *Progress in neurobiology, 132*, 59-80.

Colby, C. L. (1998). Action-oriented spatial reference frames in cortex. *Neuron, 20*(1), 15-24.

Colombo, D., Serino, S., Tuena, C., Pedroli, E., Dakanalis, A., Cipresso, P., & Riva, G. (2017). Egocentric and allocentric spatial reference frames in aging: A systematic review. *Neuroscience & Biobehavioral Reviews, 80*, 605-621. doi:https://doi.org/10.1016/j.neubiorev.2017.07.012

Committeri, G., Galati, G., Paradis, A. L., Pizzamiglio, L., Berthoz, A., & LeBihan, D. (2004). Reference frames for spatial cognition: different brain areas are involved in viewer-, object-, and landmark-centered judgments about object location. *J Cogn Neurosci, 16*(9), 1517-1535. doi:10.1162/0898929042568550

Cooper, A. C. G., & Humphreys, G. W. (2000). Coding space within but not between objects: evidence from Balint's syndrome. *Neuropsychologia, 38*(6), 723-733. doi:10.1016/s0028-3932(99)00150-5

Cope, M., & Delpy, D. T. (1988). System for long-term measurement of cerebral blood and tissue oxygenation on newborn infants by near infra-red transillumination. *Med Biol Eng Comput, 26*(3), 289-294. doi:10.1007/BF02447083

Corbetta, M., Kincade, M. J., Lewis, C., Snyder, A. Z., & Sapir, A. (2005). Neural basis and recovery of spatial attention deficits in spatial neglect. *Nat Neurosci, 8*(11), 1603-1610. doi:10.1038/nn1574

Corbetta, M., Patel, G., & Shulman, G. L. (2008). The reorienting system of the human brain: from environment to theory of mind. *Neuron, 58*(3), 306-324. doi:10.1016/j.neuron.2008.04.017

Corbetta, M., & Shulman, G. L. (2002). Control of goal-directed and stimulus-driven attention in the brain. *Nat Rev Neurosci, 3*(3), 201-215. doi:10.1038/nrn755

Creem-Regehr, S. H., Neil, J. A., & Yeh, H. J. (2007). Neural correlates of two imagined egocentric transformations. *Neuroimage, 35*(2), 916-927. doi:10.1016/j.neuroimage.2006.11.057

Creem, S. H., Downs, T. H., Snyder, A., Downs III, J. H., & Proffitt, D. R. (2001). *Egocentric Versus Object-Relative Spatial Judgment Tasks Elicit Differences in Brain Activity.* Paper presented at the Annual meeting of the Cognitive Neuroscience Society.

Crowe, D. A., Averbeck, B. B., & Chafee, M. V. (2008). Neural ensemble decoding reveals a correlate of viewer-to object-centered spatial transformation in monkey parietal cortex. *J. Neurosci., 28*(20), 5218-5228.

Culham, J. C., & Valyear, K. F. (2006). Human parietal cortex in action. *Curr. Opin. Neurobiol., 16*(2), 205-212. doi:10.1016/j.conb.2006.03.005

Davis, K. D., & Moayedi, M. (2013). Central mechanisms of pain revealed through functional and structural MRI. *Journal of Neuroimmune Pharmacology, 8*(3), 518-534.

De Schotten, M. T., Dell'Acqua, F., Forkel, S. J., Simmons, A., Vergani, F., Murphy, D. G., & Catani, M. (2011). A lateralized brain network for visuospatial attention. *Nature neuroscience, 14*(10), 1245.

Dean, H. L., & Platt, M. L. (2006). Allocentric spatial referencing of neuronal activity in macaque posterior cingulate cortex. *J Neurosci, 26*(4), 1117-1127.

Derbie, A. Y., Chau, B., Lam, B., Fang, Y. H., Ting, K. H., Wong, C. Y. H., . . . Chan, C. C. H. (2021). Cortical Hemodynamic Response Associated with Spatial Coding: A Near-Infrared Spectroscopy Study. *Brain Topogr, 34*(2), 207-220. https://doi.org/10.1007/s10548-021-00821-9

Desikan, R. S., Segonne, F., Fischl, B., Quinn, B. T., Dickerson, B. C., Blacker, D., . . . Killiany, R. J. (2006). An automated labeling system for subdividing the human cerebral cortex on MRI scans into gyral based regions of interest. *Neuroimage, 31*(3), 968-980. doi:10.1016/j.neuroimage.2006.01.021

Desimone, R., & Duncan, J. (1995). Neural mechanisms of selective visual attention. *Annu Rev Neurosci, 18*(1), 193-222. doi:10.1146/annurev.ne.18.030195.001205

Eickhoff, S. B., Bzdok, D., Laird, A. R., Kurth, F., & Fox, P. T. (2012). Activation likelihood estimation meta-analysis revisited. *Neuroimage, 59*(3), 2349-2361. doi:10.1016/j.neuroimage.2011.09.017

Eickhoff, S. B., Laird, A. R., Grefkes, C., Wang, L. E., Zilles, K., & Fox, P. T. (2009). Coordinate-based activation likelihood estimation meta-analysis of neuroimaging data: a random-effects approach based on empirical estimates of spatial uncertainty. *Hum Brain Mapp, 30*(9), 2907-2926. doi:10.1002/hbm.20718

Eickhoff, S. B., Nichols, T. E., Laird, A. R., Hoffstaedter, F., Amunts, K., Fox, P. T., . . . Eickhoff, C. R. (2016). Behavior, sensitivity, and power of activation likelihood estimation characterized by massive empirical simulation. *Neuroimage, 137*, 70-85. doi:10.1016/j.neuroimage.2016.04.072

Eickhoff, S. B., Stephan, K. E., Mohlberg, H., Grefkes, C., Fink, G. R., Amunts, K., & Zilles, K. (2005). A new SPM toolbox for combining probabilistic cytoarchitectonic maps and functional imaging data. *Neuroimage, 25*(4), 1325-1335. doi:10.1016/j.neuroimage.2004.12.034

Ekstrom, A. D., Arnold, A. E., & Iaria, G. (2014). A critical review of the allocentric spatial representation and its neural underpinnings: toward a network-based perspective. *Front Hum Neurosci, 8*, 803. doi:10.3389/fnhum.2014.00803

Epstein, R. A. (2008). Parahippocampal and retrosplenial contributions to human spatial navigation. *Trends Cogn Sci, 12*(10), 388-396. doi:10.1016/j.tics.2008.07.004

Erel, H., & Levy, D. A. (2016). Orienting of visual attention in aging. *Neuroscience & Biobehavioral Reviews, 69*, 357-380. doi:https://doi.org/10.1016/j.neubiorev.2016.08.010

Fattori, P., Raos, V., Breveglieri, R., Bosco, A., Marzocchi, N., & Galletti, C. (2010). The dorsomedial pathway is not just for reaching: grasping neurons in the medial parieto-occipital cortex of the macaque monkey. *J Neurosci, 30*(1), 342-349.

Ferber, S., Humphrey, G. K., & Vilis, T. (2003). The lateral occipital complex subserves the perceptual persistence of motion-defined groupings. *Cerebral Cortex, 13*(7), 716-721.

Filimon, F. (2015). Are All Spatial Reference Frames Egocentric? Reinterpreting Evidence for Allocentric, Object-Centered, or World-Centered Reference Frames. *Front Hum Neurosci, 9*, 648. doi:10.3389/fnhum.2015.00648

Fink, G. R., Marshall, J. C., Weiss, P. H., Stephan, T., Grefkes, C., Shah, N. J., . . . Dieterich, M. (2003). Performing allocentric visuospatial judgments with induced distortion of the egocentric reference frame: an fMRI study with clinical implications. *Neuroimage, 20*(3), 1505-1517. doi:10.1016/j.neuroimage.2003.07.006

Fjell, A. M., Sneve, M. H., Storsve, A. B., Grydeland, H., Yendiki, A., & Walhovd, K. B. (2016). Brain Events Underlying Episodic Memory Changes in Aging: A Longitudinal Investigation of Structural and Functional Connectivity. *Cereb Cortex, 26*(3), 1272-1286. doi:10.1093/cercor/bhv102

Foley, R. T., Whitwell, R. L., & Goodale, M. A. (2015). The two-visual-systems hypothesis and the perspectival features of visual experience. *Conscious. Cogn., 35*, 225-233. doi:10.1016/j.concog.2015.03.005

Fox, M. D., Corbetta, M., Snyder, A. Z., Vincent, J. L., & Raichle, M. E. (2006). Spontaneous neuronal activity distinguishes human dorsal and ventral attention systems. *Proc. Natl. Acad. Sci. U. S. A., 103*(26), 10046-10051. doi:10.1073/pnas.0604187103

Fox, M. D., Snyder, A. Z., Vincent, J. L., Corbetta, M., Van Essen, D. C., & Raichle, M. E. (2005). The human brain is intrinsically organized into dynamic, anticorrelated functional networks. *Proc. Natl. Acad. Sci. U. S. A., 102*(27), 9673-9678. doi:10.1073/pnas.0504136102

Frey, S., Campbell, J. S., Pike, G. B., & Petrides, M. (2008). Dissociating the human language pathways with high angular resolution diffusion fiber tractography. *J. Neurosci., 28*(45), 11435-11444. doi:10.1523/jneurosci.2388-08.2008

Friedman, J., Hastie, T., & Tibshirani, R. (2009). glmnet: Lasso and elastic-net regularized generalized linear models. *R package version, 1*(4).

Frings, L., Wagner, K., Quiske, A., Schwarzwald, R., Spreer, J., Halsband, U., & Schulze-Bonhage, A. (2006). Precuneus is involved in allocentric spatial location encoding and recognition. *Exp. Brain Res., 173*(4), 661-672. doi:10.1007/s00221-006-0408-8

Galati, G., Committeri, G., Sanes, J. N., & Pizzamiglio, L. (2001). Spatial coding of visual and somatic sensory information in body-centred coordinates. *Eur J Neurosci, 14*(4), 737-746. doi:10.1046/j.0953-816x.2001.01674.x

Galati, G., Lobel, E., Vallar, G., Berthoz, A., Pizzamiglio, L., & Le Bihan, D. (2000). The neural basis of egocentric and allocentric coding of space in humans: a functional magnetic resonance study. *Exp. Brain Res., 133*(2), 156-164. doi:10.1007/s002210000375

Galletti, C., Gamberini, M., Kutz, D. F., Fattori, P., Luppino, G., & Matelli, M. (2001). The cortical connections of area V6: an occipito-parietal network processing visual information. *Eur. J. Neurosci., 13*(8), 1572-1588. doi:10.1046/j.0953-816x.2001.01538.x

Gamboz, N., Zamarian, S., & Cavallero, C. (2010). Age-related differences in the attention network test (ANT). *Experimental aging research, 36*(3), 287-305.

Ganesh, S., van Schie, H. T., Cross, E. S., de Lange, F. P., & Wigboldus, D. H. (2015). Disentangling neural processes of egocentric and allocentric mental spatial transformations using whole-body photos of self and other. *Neuroimage, 116*, 30-39. doi:10.1016/j.neuroimage.2015.05.003

Geng, J. J., & Mangun, G. R. (2009). Anterior intraparietal sulcus is sensitive to bottom-up attention driven by stimulus salience. *J. Cogn. Neurosci., 21*(8), 1584-1601. doi:10.1162/jocn.2009.21103

Geng, J. J., & Vossel, S. (2013). Re-evaluating the role of TPJ in attentional control: contextual updating? *Neurosci Biobehav Rev, 37*(10 Pt 2), 2608-2620. doi:10.1016/j.neubiorev.2013.08.010

Gola, M., Kamiński, J., Brzezicka, A., & Wróbel, A. (2012). Beta band oscillations as a correlate of alertness—changes in aging. *International Journal of Psychophysiology, 85*(1), 62-67.

Goldfarb, E. V., Chun, M. M., & Phelps, E. A. (2016). Memory-guided attention: independent contributions of the hippocampus and striatum. *Neuron, 89*(2), 317-324.

Gomez, A., Cerles, M., Rousset, S., Le Bas, J. F., & Baciu, M. (2013). Ongoing egocentric spatial processing during learning of non-spatial information results in temporal-parietal activity during retrieval. *Front Psychol, 4*, 366. doi:10.3389/fpsyg.2013.00366

Gomez, A., Cerles, M., Rousset, S., Remy, C., & Baciu, M. (2014). Differential hippocampal and retrosplenial involvement in egocentric-updating, rotation, and allocentric processing during online spatial encoding: an fMRI study. *Front Hum Neurosci, 8*, 150. doi:10.3389/fnhum.2014.00150

Gomez, A., Rousset, S., & Baciu, M. (2009). Egocentric-updating during navigation facilitates episodic memory retrieval. *Acta Psychol (Amst), 132*(3), 221-227. doi:10.1016/j.actpsy.2009.07.003

Goodale, M. A. (2014). How (and why) the visual control of action differs from visual perception. *Proc. R. Soc. B, 281*(1785), 20140337. Retrieved from https://www.ncbi.nlm.nih.gov/pmc/articles/PMC4024294/pdf/rspb20140337.pdf

Goodale, M. A., & Milner, A. D. (1992). Separate visual pathways for perception and action. *Trends Neurosci, 15*(1), 20-25. doi:10.1016/0166-2236(92)90344-8

Grady, C. (2012). The cognitive neuroscience of ageing. *Nat Rev Neurosci, 13*(7), 491-505. doi:10.1038/nrn3256

Grahn, J. A., Parkinson, J. A., & Owen, A. M. (2008). The cognitive functions of the caudate nucleus. *Progress in Neurobiology, 86*(3), 141-155. doi:https://doi.org/10.1016/j.pneurobio.2008.09.004

Gramann, K., Muller, H. J., Schonebeck, B., & Debus, G. (2006). The neural basis of ego- and allocentric reference frames in spatial navigation: evidence from spatio-temporal coupled

current density reconstruction. *Brain Res, 1118*(1), 116-129. doi:10.1016/j.brainres.2006.08.005

Greve, D. N., & Fischl, B. (2009). Accurate and Robust Brain Image Alignment using Boundary-based Registration. *NeuroImage, 48*(1), 63-72. doi:10.1016/j.neuroimage.2009.06.060

Haier, R. J., Siegel, B. V., Nuechterlein, K. H., Hazlett, E., Wu, J. C., Paek, J., . . . Buchsbaum, M. S. (1988). Cortical glucose metabolic rate correlates of abstract reasoning and attention studied with positron emission tomography. *Intelligence, 12*(2), 199-217. doi:https://doi.org/10.1016/0160-2896(88)90016-5

Harris, M. A., & Wolbers, T. (2014). How age-related strategy switching deficits affect wayfinding in complex environments. *Neurobiology of aging, 35*(5), 1095-1102.

Hashimoto, R., Tanaka, Y., & Nakano, I. (2010). Heading disorientation: a new test and a possible underlying mechanism. *Eur Neurol, 63*(2), 87-93. doi:10.1159/000276398

Heinzel, S., Haeussinger, F. B., Hahn, T., Ehlis, A. C., Plichta, M. M., & Fallgatter, A. J. (2013). Variability of (functional) hemodynamics as measured with simultaneous fNIRS and fMRI during intertemporal choice. *Neuroimage, 71*, 125-134. doi:10.1016/j.neuroimage.2012.12.074

Hopfinger, J. B., Buonocore, M. H., & Mangun, G. R. (2000). The neural mechanisms of top-down attentional control. *Nat. Neurosci., 3*(3), 284-291. doi:10.1038/72999

Husain, M., & Nachev, P. (2007). Space and the parietal cortex. *Trends in cognitive sciences, 11*(1), 30-36.

Iaria, G., Chen, J. K., Guariglia, C., Ptito, A., & Petrides, M. (2007). Retrosplenial and hippocampal brain regions in human navigation: complementary functional contributions

to the formation and use of cognitive maps. *Eur J Neurosci, 25*(3), 890-899. doi:10.1111/j.1460-9568.2007.05371.x

James, T. W., Humphrey, G. K., Gati, J. S., Menon, R. S., & Goodale, M. A. (2002). Differential effects of viewpoint on object-driven activation in dorsal and ventral streams. *Neuron, 35*(4), 793-801.

Jang, K. E., Tak, S., Jung, J., Jang, J., Jeong, Y., & Ye, J. C. (2009). Wavelet minimum description length detrending for near-infrared spectroscopy. *J Biomed Opt, 14*(3), 034004. doi:10.1117/1.3127204

Jenkinson, M., Bannister, P., Brady, M., & Smith, S. (2002). Improved optimization for the robust and accurate linear registration and motion correction of brain images. *Neuroimage, 17*(2), 825-841.

Kanwisher, N., & Wojciulik, E. (2000). Visual attention: insights from brain imaging. *Nat Rev Neurosci, 1*(2), 91-100. doi:10.1038/35039043

Kastner, S., & Ungerleider, L. G. (2000). Mechanisms of visual attention in the human cortex. *Annual review of neuroscience, 23*(1), 315-341.

Kocsis, L., Herman, P., & Eke, A. (2006). The modified Beer–Lambert law revisited. *Physics in Medicine & Biology, 51*(5), N91. doi:10.1088/0031-9155/51/5/N02

Kozhevnikov, M., Motes, M. A., Rasch, B., & Blajenkova, O. (2006). Perspective-taking vs. mental rotation transformations and how they predict spatial navigation performance. *Applied Cognitive Psychology, 20*(3), 397-417.

Krall, S., Rottschy, C., Oberwelland, E., Bzdok, D., Fox, P., Eickhoff, S., . . . Konrad, K. (2015). The role of the right temporoparietal junction in attention and social interaction as

revealed by ALE meta-analysis. *Brain Struct Funct, 220*(2), 587-604. doi:10.1007/s00429-014-0803-z

Kravitz, D. J., Saleem, K. S., Baker, C. I., & Mishkin, M. (2011). A new neural framework for visuospatial processing. *Nat Rev Neurosci, 12*(4), 217-230. doi:10.1038/nrn3008

Kravitz, D. J., Saleem, K. S., Baker, C. I., Ungerleider, L. G., & Mishkin, M. (2013). The ventral visual pathway: an expanded neural framework for the processing of object quality. *Trends Cogn Sci, 17*(1), 26-49. doi:10.1016/j.tics.2012.10.011

Lambrey, S., Doeller, C., Berthoz, A., & Burgess, N. (2012). Imagining Being Somewhere Else: Neural Basis of Changing Perspective in Space. *Cerebral Cortex, 22*(1), 166-174. doi:10.1093/cercor/bhr101

Lithfous, S., Dufour, A., Blanc, F., & Després, O. (2014). Allocentric but not egocentric orientation is impaired during normal aging: An ERP study. *Neuropsychology*, *28*(5), 761.

Liu, N., Li, H., Su, W., & Chen, Q. (2017). Common and specific neural correlates underlying the spatial congruency effect induced by the egocentric and allocentric reference frame. *Hum Brain Mapp, 38*(4), 2112-2127. doi:10.1002/hbm.23508

Lu, J., Li, D., Li, F., Zhou, A., Wang, F., Zuo, X., . . . Jia, J. (2011). Montreal cognitive assessment in detecting cognitive impairment in Chinese elderly individuals: a population-based study. *Journal of geriatric psychiatry and neurology*, *24*(4), 184-190.

Madden, D. J., Costello, M. C., Dennis, N. A., Davis, S. W., Shepler, A. M., Spaniol, J., . . . Cabeza, R. (2010). Adult age differences in functional connectivity during executive control. *Neuroimage, 52*(2), 643-657.

Madden, D. J., Spaniol, J., Whiting, W. L., Bucur, B., Provenzale, J. M., Cabeza, R., . . . Huettel, S. A. (2007). Adult age differences in the functional neuroanatomy of visual attention: a combined fMRI and DTI study. *Neurobiology of aging, 28*(3), 459-476. doi:10.1016/j.neurobiolaging.2006.01.005

Makris, N., Kennedy, D. N., McInerney, S., Sorensen, A. G., Wang, R., Caviness, V. S., Jr., & Pandya, D. N. (2005). Segmentation of subcomponents within the superior longitudinal fascicle in humans: a quantitative, in vivo, DT-MRI study. *Cereb Cortex, 15*(6), 854-869. doi:10.1093/cercor/bhh186

Makris, N., Papadimitriou, G. M., Sorg, S., Kennedy, D. N., Caviness, V. S., & Pandya, D. N. (2007). The occipitofrontal fascicle in humans: a quantitative, in vivo, DT-MRI study. *Neuroimage, 37*(4), 1100-1111. doi:10.1016/j.neuroimage.2007.05.042

Maniega, S. M., Valdes Hernandez, M. C., Clayden, J. D., Royle, N. A., Murray, C., Morris, Z., . . . Wardlaw, J. M. (2015). White matter hyperintensities and normal-appearing white matter integrity in the aging brain. *Neurobiology of aging, 36*(2), 909-918. doi:10.1016/j.neurobiolaging.2014.07.048

McLaren, D. G., Ries, M. L., Xu, G., & Johnson, S. C. (2012). A generalized form of context-dependent psychophysiological interactions (gPPI): A comparison to standard approaches. *NeuroImage, 61*(4), 1277-1286. doi:https://doi.org/10.1016/j.neuroimage.2012.03.068

McNab, F., Zeidman, P., Rutledge, R. B., Smittenaar, P., Brown, H. R., Adams, R. A., & Dolan, R. J. (2015). Age-related changes in working memory and the ability to ignore distraction. *Proc. Natl. Acad. Sci. U. S. A., 112*(20), 6515-6518. doi:10.1073/pnas.1504162112

Milner, A. (2017). How do the two visual streams interact with each other? *Experimental Brain Research*, 1-12.

Milner, A. D., & Goodale, M. A. (2008). Two visual systems re-viewed. *Neuropsychologia, 46*(3), 774-785. doi:10.1016/j.neuropsychologia.2007.10.005

Mitchell, J. F., Sundberg, K. A., & Reynolds, J. H. (2009). Spatial attention decorrelates intrinsic activity fluctuations in macaque area V4. *Neuron, 63*(6), 879-888.

Moher, D., Liberati, A., Tetzlaff, J., Altman, D. G., & Group, P. (2009). Preferred reporting items for systematic reviews and meta-analyses: the PRISMA statement. *PLoS medicine, 6*(7), e1000097. Retrieved from https://www.ncbi.nlm.nih.gov/pmc/articles/PMC2707599/pdf/pmed.1000097.pdf

Montefinese, M., Sulpizio, V., Galati, G., & Committeri, G. (2015). Age-related effects on spatial memory across viewpoint changes relative to different reference frames. *Psychological research, 79*(4), 687-697.

Moore, T., & Fallah, M. (2004). Microstimulation of the frontal eye field and its effects on covert spatial attention. *J Neurophysiol, 91*(1), 152-162. doi:10.1152/jn.00741.2002

Mori, S., Oishi, K., Jiang, H., Jiang, L., Li, X., Akhter, K., . . . Woods, R. (2008). Stereotaxic white matter atlas based on diffusion tensor imaging in an ICBM template. *Neuroimage, 40*(2), 570-582.

Mou, W., McNamara, T. P., Valiquette, C. M., & Rump, B. (2004). Allocentric and egocentric updating of spatial memories. *Journal of experimental psychology: Learning, Memory, and Cognition, 30*(1), 142. doi:10.1037/0278-7393.30.1.142

Muller, V. I., Cieslik, E. C., Laird, A. R., Fox, P. T., Radua, J., Mataix-Cols, D., . . . Eickhoff, S. B. (2018). Ten simple rules for neuroimaging meta-analysis. *Neurosci Biobehav Rev, 84*, 151-161. doi:10.1016/j.neubiorev.2017.11.012

Murtagh, F. (1985). Multidimensional clustering algorithms. In *Compstat Lectures, Vienna: Physika Verlag, 1985*.

Nachev, P., Kennard, C., & Husain, M. (2008). Functional role of the supplementary and pre-supplementary motor areas. *Nature Reviews Neuroscience, 9*, 856. doi:10.1038/nrn2478

Neggers, S. F., Van der Lubbe, R. H., Ramsey, N. F., & Postma, A. (2006). Interactions between ego- and allocentric neuronal representations of space. *Neuroimage, 31*(1), 320-331. doi:10.1016/j.neuroimage.2005.12.028

Neubauer, A. C., & Fink, A. (2009). Intelligence and neural efficiency. *Neuroscience & Biobehavioral Reviews, 33*(7), 1004-1023. doi:https://doi.org/10.1016/j.neubiorev.2009.04.001

Niogi, S. N., Mukherjee, P., Ghajar, J., Johnson, C. E., Kolster, R., Lee, H., . . . McCandliss, B. D. (2008). Structural dissociation of attentional control and memory in adults with and without mild traumatic brain injury. *Brain, 131*(12), 3209-3221. doi:10.1093/brain/awn247

Niogi, S. N., Mukherjee, P., Ghajar, J., & McCandliss, B. D. (2010). Individual differences in distinct components of attention are linked to anatomical variations in distinct white matter tracts. *Frontiers in neuroanatomy, 4*, 2.

Noudoost, B., Chang, M. H., Steinmetz, N. A., & Moore, T. (2010). Top-down control of visual attention. *Curr. Opin. Neurobiol., 20*(2), 183-190. doi:10.1016/j.conb.2010.02.003

Park, H. J., Kim, J. J., Lee, S. K., Seok, J. H., Chun, J., Kim, D. I., & Lee, J. D. (2008). Corpus callosal connection mapping using cortical gray matter parcellation and DT-MRI. *Hum Brain Mapp, 29*(5), 503-516. doi:10.1002/hbm.20314

Parslow, D. M., Rose, D., Brooks, B., Fleminger, S., Gray, J. A., Giampietro, V., . . . Morris, R. G. (2004). Allocentric spatial memory activation of the hippocampal formation measured with fMRI. *Neuropsychology, 18*(3), 450-461. doi:10.1037/0894-4105.18.3.450

Pertzov, Y., Avidan, G., & Zohary, E. (2011). Multiple reference frames for saccadic planning in the human parietal cortex. *J. Neurosci., 31*(3), 1059-1068. doi:10.1523/JNEUROSCI.3721-10.2011

Posner, M. I. (1980). Orienting of attention. *Q J Exp Psychol, 32*(1), 3-25. doi:10.1080/00335558008248231

Prado, J., Carp, J., & Weissman, D. H. (2011). Variations of response time in a selective attention task are linked to variations of functional connectivity in the attentional network. *NeuroImage, 54*(1), 541-549. doi:10.1016/j.neuroimage.2010.08.022

Ptak, R. (2012). The frontoparietal attention network of the human brain: action, saliency, and a priority map of the environment. *Neuroscientist, 18*(5), 502-515. doi:10.1177/1073858411409051

Ptak, R., & Schnider, A. (2010). The dorsal attention network mediates orienting toward behaviorally relevant stimuli in spatial neglect. *J Neurosci, 30*(38), 12557-12565.

R Core Team. (2017). R: A language and environment for statistical computing. Retrieved from http://www.R-project.org/

Rodgers, M. K., Sindone III, J. A., & Moffat, S. D. (2012). Effects of age on navigation strategy. *Neurobiology of aging, 33*(1), 202. e215-202. e222.

Rosenzweig, I., Vukadinovic, Z., Turner, A. J., & Catani, M. (2012). Neuroconnectivity and valproic acid: The myelin hypothesis. *Neuroscience & Biobehavioral Reviews, 36*(8), 1848-1856. doi:https://doi.org/10.1016/j.neubiorev.2012.05.006

Rushworth, M., & Taylor, P. (2006). TMS in the parietal cortex: updating representations for attention and action. *Neuropsychologia, 44*(13), 2700-2716.

Ryali, S., Chen, T., Supekar, K., & Menon, V. (2012). Estimation of functional connectivity in fMRI data using stability selection-based sparse partial correlation with elastic net penalty. *Neuroimage, 59*(4), 3852-3861. doi:10.1016/j.neuroimage.2011.11.054

Saj, A., Cojan, Y., Musel, B., Honore, J., Borel, L., & Vuilleumier, P. (2014). Functional neuro-anatomy of egocentric versus allocentric space representation. *Neurophysiol Clin, 44*(1), 33-40. doi:10.1016/j.neucli.2013.10.135

Schindler, A., & Bartels, A. (2013). Parietal cortex codes for egocentric space beyond the field of view. *Curr. Biol., 23*(2), 177-182. doi:10.1016/j.cub.2012.11.060

Seghier, M. L. (2013). The angular gyrus: multiple functions and multiple subdivisions. *The Neuroscientist, 19*(1), 43-61. doi:10.1177/1073858412440596

Shibata, H., & Inui, T. (2011). Brain activity associated with recognition of appropriate action selection based on allocentric perspectives. *Neurosci Lett, 491*(3), 187-191. doi:10.1016/j.neulet.2011.01.033

Singh, A. K., Okamoto, M., Dan, H., Jurcak, V., & Dan, I. (2005). Spatial registration of multichannel multi-subject fNIRS data to MNI space without MRI. *Neuroimage, 27*(4), 842-851. doi:10.1016/j.neuroimage.2005.05.019

Smith, S. M. (2002). Fast robust automated brain extraction. *Hum Brain Mapp, 17*(3), 143-155. doi:10.1002/hbm.10062

Smith, S. M., Jenkinson, M., Johansen-Berg, H., Rueckert, D., Nichols, T. E., Mackay, C. E., . . . Behrens, T. E. (2006). Tract-based spatial statistics: voxelwise analysis of multi-subject diffusion data. *Neuroimage, 31*(4), 1487-1505. doi:10.1016/j.neuroimage.2006.02.024

Smith, S. M., Jenkinson, M., Woolrich, M. W., Beckmann, C. F., Behrens, T. E., Johansen-Berg, H., . . . Matthews, P. M. (2004). Advances in functional and structural MR image analysis and implementation as FSL. *Neuroimage, 23 Suppl 1*, S208-219. doi:10.1016/j.neuroimage.2004.07.051

Smith, S. M., & Nichols, T. E. (2009). Threshold-free cluster enhancement: addressing problems of smoothing, threshold dependence and localisation in cluster inference. *Neuroimage, 44*(1), 83-98. doi:10.1016/j.neuroimage.2008.03.061

Stein, J. F. (1992). The representation of egocentric space in the posterior parietal cortex. *Behav Brain Sci, 15 Spec No 4*(4), 691-700. doi:10.1017/S0140525X00072605

Sullivan, E. V., Rohlfing, T., & Pfefferbaum, A. (2010). Quantitative fiber tracking of lateral and interhemispheric white matter systems in normal aging: relations to timed performance. *Neurobiology of aging, 31*(3), 464-481. doi:10.1016/j.neurobiolaging.2008.04.007

Szczepanski, S. M., Pinsk, M. A., Douglas, M. M., Kastner, S., & Saalmann, Y. B. (2013). Functional and structural architecture of the human dorsal frontoparietal attention network. *Proc. Natl. Acad. Sci. U. S. A., 110*(39), 15806-15811. doi:10.1073/pnas.1313903110

Tak, S., Yoon, S. J., Jang, J., Yoo, K., Jeong, Y., & Ye, J. C. (2011). Quantitative analysis of hemodynamic and metabolic changes in subcortical vascular dementia using simultaneous near-infrared spectroscopy and fMRI measurements. *Neuroimage, 55*(1), 176-184. doi:10.1016/j.neuroimage.2010.11.046

Thaler, L., & Goodale, M. A. (2011). Neural substrates of visual spatial coding and visual feedback control for hand movements in allocentric and target-directed tasks. *Front Hum Neurosci, 5*, 92. doi:10.3389/fnhum.2011.00092

Thompson, K. G., Biscoe, K. L., & Sato, T. R. (2005). Neuronal basis of covert spatial attention in the frontal eye field. *J. Neurosci., 25*(41), 9479-9487. doi:10.1523/JNEUROSCI.0741-05.2005

Toronov, V., Webb, A., Choi, J. H., Wolf, M., Michalos, A., Gratton, E., & Hueber, D. (2001). Investigation of human brain hemodynamics by simultaneous near-infrared spectroscopy and functional magnetic resonance imaging. *Med Phys, 28*(4), 521-527. doi:10.1118/1.1354627

Tuch, D. S., Salat, D. H., Wisco, J. J., Zaleta, A. K., Hevelone, N. D., & Rosas, H. D. (2005). Choice reaction time performance correlates with diffusion anisotropy in white matter pathways supporting visuospatial attention. *Proc. Natl. Acad. Sci. U. S. A., 102*(34), 12212-12217. doi:10.1073/pnas.0407259102

Turkeltaub, P. E., Eickhoff, S. B., Laird, A. R., Fox, M., Wiener, M., & Fox, P. (2012). Minimizing within-experiment and within-group effects in Activation Likelihood Estimation meta-analyses. *Hum Brain Mapp, 33*(1), 1-13. doi:10.1002/hbm.21186

Turner, G. R., & Spreng, R. N. (2012). Executive functions and neurocognitive aging: dissociable patterns of brain activity. *Neurobiology of aging, 33*(4), 826. e821-826. e813.

Uddin, L. Q., Supekar, K., Amin, H., Rykhlevskaia, E., Nguyen, D. A., Greicius, M. D., & Menon, V. (2010). Dissociable Connectivity within Human Angular Gyrus and Intraparietal Sulcus: Evidence from Functional and Structural Connectivity. *Cerebral Cortex, 20*(11), 2636-2646. doi:10.1093/cercor/bhq011

Ungerleider. (1982). Two cortical visual systems. *Analysis of visual behavior*, 549-586.

Ungerleider, L. (1994). 'What' and 'where' in the human brain. *Current Opinion in Neurobiology, 4*(2), 157-165. doi:10.1016/0959-4388(94)90066-3

Vaessen, M. J., Saj, A., Lovblad, K.-O., Gschwind, M., & Vuilleumier, P. (2016). Structural white-matter connections mediating distinct behavioral components of spatial neglect in right brain-damaged patients. *Cortex, 77*, 54-68. doi:https://doi.org/10.1016/j.cortex.2015.12.008

Vallar, G., Lobel, E., Galati, G., Berthoz, A., Pizzamiglio, L., & Le Bihan, D. (1999). A fronto-parietal system for computing the egocentric spatial frame of reference in humans. *Exp. Brain Res., 124*(3), 281-286. doi:10.1007/s002210050624

van Asselen, M., Kessels, R. P., Kappelle, L. J., & Postma, A. (2008). Categorical and coordinate spatial representations within object-location memory. *Cortex, 44*(3), 249-256.

van der Stoep, N., Postma, A., & Nijboer, T. C. W. (2017). Multisensory Perception and the Coding of Space. In A. Postma & I. J. M. van der Ham (Eds.), *Neuropsychology of Space* (pp. 123-158). San Diego: Academic Press.

Van Essen, D., Anderson, C., & Felleman, D. (1992). Information processing in the primate visual system: an integrated systems perspective. *Science, 255*(5043), 419-423. doi:10.1126/science.1734518

Vann, S. D., Aggleton, J. P., & Maguire, E. A. (2009). What does the retrosplenial cortex do? *Nature Reviews Neuroscience, 10*, 792. doi:10.1038/nrn2733

Voineskos, A. N., Rajji, T. K., Lobaugh, N. J., Miranda, D., Shenton, M. E., Kennedy, J. L., . . . Mulsant, B. H. (2012). Age-related decline in white matter tract integrity and cognitive

performance: a DTI tractography and structural equation modeling study. *Neurobiology of aging, 33*(1), 21-34.

Vossel, S., Geng, J. J., & Fink, G. R. (2014). Dorsal and ventral attention systems: distinct neural circuits but collaborative roles. *Neuroscientist, 20*(2), 150-159. doi:10.1177/1073858413494269

Walter, E., & Dassonville, P. (2008). Visuospatial contextual processing in the parietal cortex: an fMRI investigation of the induced Roelofs effect. *Neuroimage, 42*(4), 1686-1697. doi:10.1016/j.neuroimage.2008.06.016

Wang, R., & Spelke, E. (2002). Human spatial representation: insights from animals. *Trends Cogn Sci, 6*(9), 376. doi:10.1016/S1364-6613(02)01961-7

Wang, R. F., & Spelke, E. S. (2000). Updating egocentric representations in human navigation. *Cognition, 77*(3), 215-250.

Warbrick, T., Rosenberg, J., & Shah, N. J. (2017). The relationship between BOLD fMRI response and the underlying white matter as measured by fractional anisotropy (FA): A systematic review. *NeuroImage, 153*, 369-381. doi:https://doi.org/10.1016/j.neuroimage.2016.12.075

Wegman, J., Tyborowska, A., & Janzen, G. (2014). Encoding and retrieval of landmark-related spatial cues during navigation: an fMRI study. *Hippocampus, 24*(7), 853-868. doi:10.1002/hipo.22275

Weiner, K. S., & Zilles, K. (2016). The anatomical and functional specialization of the fusiform gyrus. *Neuropsychologia, 83*, 48-62. doi:10.1016/j.neuropsychologia.2015.06.033

Weniger, G., Siemerkus, J., Schmidt-Samoa, C., Mehlitz, M., Baudewig, J., Dechent, P., & Irle, E. (2010). The human parahippocampal cortex subserves egocentric spatial learning

during navigation in a virtual maze. *Neurobiol Learn Mem, 93*(1), 46-55. doi:10.1016/j.nlm.2009.08.003

Werner, S. (2005). *Allocentric spatial judgements by re-mapping egocentric coordinates: a fMRI study.* (MSc Thesis). Eberhard-Karls-Universität Tübingen, Tübingen, Germany.

Westlye, L. T., Grydeland, H., Walhovd, K. B., & Fjell, A. M. (2011). Associations between regional cortical thickness and attentional networks as measured by the attention network test. *Cereb Cortex, 21*(2), 345-356. doi:10.1093/cercor/bhq101

Whitfield-Gabrieli, S., & Nieto-Castanon, A. (2012). Conn: a functional connectivity toolbox for correlated and anticorrelated brain networks. *Brain connectivity, 2*(3), 125-141.

Wilson, K. D., Woldorff, M. G., & Mangun, G. R. (2005). Control networks and hemispheric asymmetries in parietal cortex during attentional orienting in different spatial reference frames. *Neuroimage, 25*(3), 668-683. doi:10.1016/j.neuroimage.2004.07.075

Wolbers, T., Hegarty, M., Büchel, C., & Loomis, J. M. (2008). Spatial updating: how the brain keeps track of changing object locations during observer motion. *Nature neuroscience, 11*(10), 1223. Retrieved from https://www.nature.com/articles/nn.2189.pdf

Woolrich, M. W., Ripley, B. D., Brady, M., & Smith, S. M. (2001). Temporal Autocorrelation in Univariate Linear Modeling of FMRI Data. *NeuroImage, 14*(6), 1370-1386. doi:https://doi.org/10.1006/nimg.2001.0931

Worsley, K. (2001). Statistical analysis of activation images. *Functional MRI: An introduction to methods, 14*(1), 251-270.

Yin, H. H., Mulcare, S. P., Hilario, M. R., Clouse, E., Holloway, T., Davis, M. I., . . . Costa, R. M. (2009). Dynamic reorganization of striatal circuits during the acquisition and consolidation of a skill. *Nat Neurosci, 12*(3), 333-341. doi:10.1038/nn.2261

Yin, X., Han, Y., Ge, H., Xu, W., Huang, R., Zhang, D., . . . Liu, S. (2013). Inferior frontal white matter asymmetry correlates with executive control of attention. *Human brain mapping, 34*(4), 796-813.

Zaehle, T., Jordan, K., Wustenberg, T., Baudewig, J., Dechent, P., & Mast, F. W. (2007). The neural basis of the egocentric and allocentric spatial frame of reference. *Brain Res., 1137*(1), 92-103. doi:10.1016/j.brainres.2006.12.044

Zanto, T. P., & Gazzaley, A. (2013). Fronto-parietal network: flexible hub of cognitive control. *Trends Cogn Sci, 17*(12), 602-603. doi:10.1016/j.tics.2013.10.001

Zhang, H., & Ekstrom, A. (2013). Human neural systems underlying rigid and flexible forms of allocentric spatial representation. *Hum Brain Mapp, 34*(5), 1070-1087. doi:10.1002/hbm.21494

Zhang, H., Lee, A., & Qiu, A. (2017). A posterior-to-anterior shift of brain functional dynamics in aging. *Brain Struct Funct, 222*(8), 3665-3676.

Zhu, Z., Hakun, J. G., Johnson, N. F., & Gold, B. T. (2014). Age-related increases in right frontal activation during task switching are mediated by reaction time and white matter microstructure. *Neuroscience, 278*, 51-61. doi:10.1016/j.neuroscience.2014.07.076

Zhu, Z., Johnson, N. F., Kim, C., & Gold, B. T. (2015). Reduced frontal cortex efficiency is associated with lower white matter integrity in aging. *Cereb Cortex, 25*(1), 138-146. doi:10.1093/cercor/bht212